AN EXPERIMENTAL INVESTIGATION OF FORCED CONVECTIVE BOILING AT HIGH QUALITIES INSIDE TUBES PRECEDED BY 180 DEGREE BENDS

By

M. NAYEEM FARUKHI

Bachelor of Science
Oklahoma State University
Stillwater, Oklahoma
1965

Master of Science
Oklahoma State University
Stillwater, Oklahoma
1967

Submitted to the Faculty of the Graduate College
of the Oklahoma State University
in partial fulfillment of the requirements
for the Degree of
DOCTOR OF PHILOSOPHY
December, 1973

AN EXPERIMENTAL INVESTIGATION OF FORCED CONVECTIVE BOILING AT HIGH QUALITIES INSIDE TUBES PRECEDED BY 180 DEGREE BENDS

Thesis Approved:

Thesis Adviser

Dean of the Graduate College

ACKNOWLEDGMENTS

I am deeply indebted to my adviser, Dr. Jerald D. Parker, for his many helpful and thought-provoking suggestions during the writing of this dissertation, for his help during the course of my M.S. and Ph.D. degrees, and for being a friend in times of need.

The helpful suggestions made by the members of the Advisory Committee, Drs. Kenneth J. Bell, F. C. McQuiston, and W. G. Tiederman, during various stages of the Ph.D. program are also acknowledged.

I wish to express my appreciation to my former boss at Westinghouse, Mr. W. M. Byerley, for furnishing the test sections and for financial assistance in the form of consulting fees from 1969 through 1972.

Thanks are due to the School of Chemical Engineering and especially to Dr. Kenneth J. Bell for allowing me to use their heat transfer test facilities, to the School of Mechanical and Aerospace Engineering for financial assistance throughout my graduate work, and to the National Science Foundation for funding the heat transfer tests for one year.

I am very grateful to my wife, Suraiya, for tolerating my many moods during these sometimes trying four years, for her encouragement during times of crises, and for bearing the hardships resulting from my involvement in pursuing a Ph.D. degree.

This work is dedicated to my mother, Noorie Zainab, and my late father, Himayathullah, whose personal sacrifices during my undergraduate years made this work possible.

TABLE OF CONTENTS

LIST OF TABLES

LIST OF FIGURES

NOMENCLATURE

A	area, ft^2
d	tube diameter, inches
$d\phi$	arc length, radians
dz	incremental length, ft
G	mass velocity, lbm/(hr.-ft^2)
h	heat transfer coefficient, Btu/(hr.-ft^2-°F)
K	thermal conductivity, Btu/(hr.-ft-°F)
L	length, feet
Q, q	heat flow, Btu/hour
R	bend radius, feet
r	tube radius, feet
T	wall thickness, feet
t	temperature, °F
V	velocity, ft/sec
W	mass flow rate, lbm/hour

Subscripts

c	center line
cs	cross-section
e	exit
f	flooding
G	gas
g	generated

i	inside
in	inlet
L	liquid, loss
l	loss
o	outside
out	outlet
S	steam, superficial
sat	saturated
t	total
tp	two phase
w	water

Greek Letters

Δr	incremental radius, feet
Λ	$(\rho_L \rho_G)^{\frac{1}{2}}$, lbm/ft^3
μ	viscosity, lbm/(hr.-ft.)
ρ	electrical resistivity, $(ohms\text{-}in^2)/in.$, or density, lbm/ft^3
σ	surface tension, dynes/cm
Ψ	$\mu_L^{1/3}/(\sigma\rho_L^{2/3})$ - $(cm)(ft)^{5/3}/(dynes)(hr)^{1/3}(lbm)^{1/3}$

CHAPTER I

INTRODUCTION

Fluids flow boiling in conduits are characterized by various distributions of the liquid and vapor phase at any given cross section of the flow. The classification of these phase distributions, although somewhat arbitrary, is of fundamental importance since it is often a necessary tool in effectively predicting thermal and hydraulic characteristics of heat transfer equipment. Furthermore, successful design and operation of boiling systems depend to a large extent on the boiling process, and boiling in bends is of practical importance since bends are often employed in shell and tube type heat exchangers, steam generators and refrigeration equipment.

A single phase fluid flowing axially in a curved conduit is known to have an induced secondary flow superimposed on it as shown in Figure 1(a). However, researchers working with annular two phase flow in helically coiled tubes hypothesized that induced centrifugal forces should force the liquid onto the outside wall, as shown in Figure 1(b), rather than allowing it to flow in an annular fashion. The investigation of Carver et al. (3)*, Miropolskiy et al. (2), and Owhadi et al. (3) revealed that this hypothesis was inaccurate since they obtained higher dryout qualities with the coiled tubes than those normally found

---

*Numbers in parentheses denote references cited in the Bibliography.

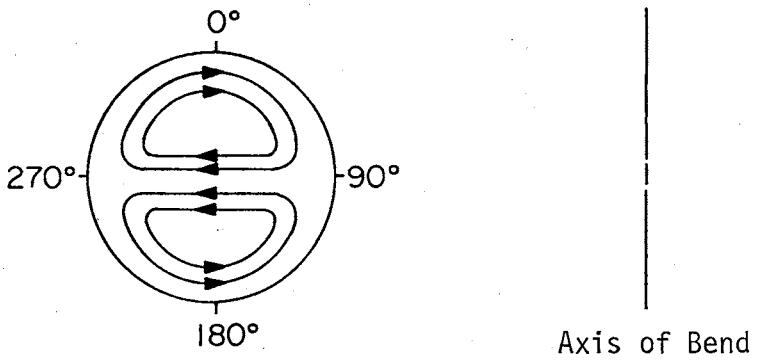

(a) Secondary Flow in Single Phase Fluid Flow

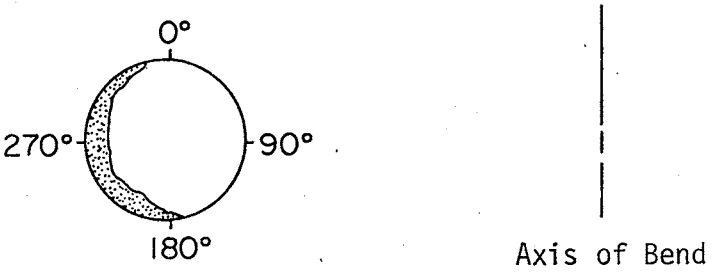

(b) Liquid Centrifuging in Two Phase Fluid Flow

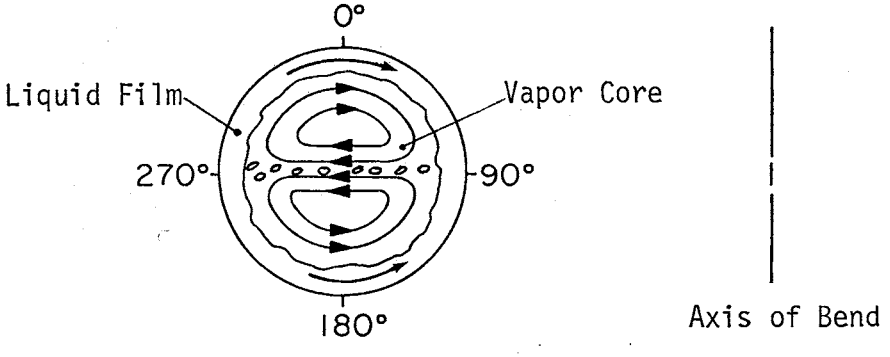

(c) Secondary Flow in Two Phase Annular Flow

Figure 1. Secondary Flow in Curved Tubes

in straight tubes. Based on these findings Owhadi et al. (3), Banerjee et al. (4), and Crain (5) hypothesized that secondary flow similar to the one shown in Figure 1(c) should exist in the vapor core of two phase mixtures flowing annularly inside helically coiled tubes.

Banerjee et al. (4) also observed that for high qualities the liquid travelled at the 90° position instead of the 270° position. They called this phenomenon "film inversion" and attributed it to the fact that the centrifugal force on the gas phase is much greater than the liquid phase, due to the high gas velocity. Crain (5) and other investigators, however, have noted that the bend-induced secondary flow in the vapor core also helps in shearing the liquid from the 270° position to the 90° position.

Based on the information given above, it was believed that the boiling process would be quite different not only in a 180° bend but also in the straight horizontal tube downstream of the bend. It was also believed that since the residence time of a fluid particle in the bend would be considerably less than that in a helically coiled tube, the bend should disrupt the incoming two phase flow pattern rather than establish it.

The purpose of this study was to investigate experimentally the thermal and hydrodynamic behavior of forced convective boiling of water inside horizontal serpentine tubes with vertically oriented bends. The objectives were achieved in two phases. The first phase was involved with visual observations of flow patterns inside two clear, serpentine tube test sections incorporated in an air-water loop while the second phase dealt with obtaining local heat transfer coefficients for steam-water mixtures flow boiling inside two INCONEL 600 serpentine tube test

sections incorporated in a heat transfer loop. The heat transfer coefficients were utilized in determining flow patterns, i.e., phase distributions.

CHAPTER II

LITERATURE SURVEY

At the time this program was initiated there was only meager information concerning two phase flow inside 180° tube bends. In recent years, however, some more work done by British researchers has been reported in the open literature but experimental data for these studies has been extremely difficult to obtain.

Single Phase Flow

Lis and Thelwell (6) investigated in some detail the heat transfer phenomena to water flowing, in the turbulent regime, in a straight vertical tube preceded by a 180° bend. They determined that the local heat transfer coefficients were nonuniform up to twelve diameters downstream of the bend and the variation of local heat transfer at any cross section decreased with either an increase in Reynolds number or as the ratio of bend to tube radii decreased.

Ede (7) also investigated the effect of a 180° bend on the heat transfer coefficients for the laminar, transition, and the turbulent regimes in a horizontal serpentine tube test section. Generally, he found the phenomena quite complex to analyze in the laminar and transition regions. For the turbulent region, he found that the variation in the local heat transfer coefficient generally disappeared within ten to twenty diameters downstream of the bend.

Adiabatic Two Phase Flow

Alves (8) observed two phase flow patterns of air-water and oil-air mixtures flowing in a one-inch pipe with a 180° return bend. He described various flow patterns observed in the straight sections as well as in the bend and presented a flow regime map as function of superficial gas and liquid velocities.

Baker (9), after reviewing the literature, presented the data of Alves (8) and other investigators in the form of a horizontal, two phase, flow regime map.

Diabatic Two Phase Flow

Very little work on two phase diabatic flow in horizontal serpentine tubes has been reported in the U.S.A. Zahn (10) is apparently the only researcher who investigated the effects of 180° bends on the boiling process in the straight upstream and downstream section of the bends. His tests were conducted with Refrigerant R22 flow boiling inside a test section made from a 0.46 inch ID horizontal serpentine coil with a 22 inch span and 1.08 inch radius bends. Zahn reported that a dry patch was generally observed at the top of the tube downstream of the bend for qualities up to 30 percent. He attributed this phenomenon to the evaporation of the thin liquid film that generally covered the upper tube surface. Zahn also reported that there was no appreciable difference between upflow and downflow in the test section and that, in general, the flow was thoroughly mixed after exiting from the bend. Finally, he presented his observations on Baker's (9) map and demonstrated the

similarity between foiling flow patterns and adiabatic flow patterns. However,he modified some of the flow pattern descriptions given by Baker.

In the U.K. several investigations have been conducted with two phase flow boiling in serpentine tubes. Rounthwaite (11) experimented with steam/water mixtures flow boiling inside a 1.6-inch ID, serpentine tube at pressures up to 950 PSIA and heat fluxes up to 25,000 Btu/(hr-sq. ft.). He found that at low qualities flow stratification occurred and this caused large variations in the local heat transfer coefficients at any given cross section of the tube. For the high quality runs he found that dryout generally occurred at the top first and at a quality between 94 percent and 98 percent. However, some more heating was necessary before total dryout occurred. The instrumentation near the bend exit and in the bend was inadequate and consequently the effect of the bend on the boiling process was not reported in detail.

Following the initiation of the author's experimental work, two more British studies were reported. The interest stemmed from the fact that numerous tube failures were encountered in the steam evaporators of the Trawsfyndd power plant that incorporated horizontal serpentine tubes (12). Lis and Strickland (13) investigated the boiling process with steam-water mixtures in a 1.6-inch ID, horizontal serpentine tube. They found that under certain conditions in the annular flow regime a dry patch would form at the top of the tube downstream of the bend and that this dry patch was surrounded by zones of fluctuating wall temperatures. They also found that when the bend was placed in a horizontal plane the amplitudes of the fluctuating temperatures were attenuated considerably. Lis and Strickland showed that the distance between the disturbance patch and the bend exit increased with quality but in

general the dry patches started at an L/D_i of about 14 and extended to almost the end of the tube. The experiments were carried out at heat fluxes up to 25,000 Btu/hr/sq. ft., pressures between 220 and 950 PSIA, qualities between 0 percent and 65 percent, and mass velocities from 70,000 to 810,000 lbm/hr/sq. ft.

Recently, Robertson (14) investigated the dryout phenomenon for steam-water mixtures in a 0.746-inch ID, horizontal serpentine tube and showed that the phenomenon is quite different for horizontal tubes as compared to vertical tubes. The experiments were conducted for pressures between 500 and 1000 psi , heat fluxes between 200,000 and 250,000 Btu/hr/sq. ft., mass velocity of 500,000 lbm/hr/sq. ft., and qualities between 20 percent and 50 percent. He found that in the annular flow regime dry patches occurred downstream of the bend but at higher heat fluxes than those reported by Lis and Strickland (13). He attributed this to the effect of tube diameter.

CHAPTER III

EXPERIMENTAL SYSTEM

The experimental program was divided into two phases. The first phase dealt with visual studies of air-water mixtures flowing inside clear TYGON tube test sections while the second phase was associated with forced convective boiling of steam-water mixtures flowing inside INCONEL test sections.

The experimental program for the heat transfer tests is explained below whereas the experimental program for the visual tests is discussed in Appendix A.

Loop Description

A schematic diagram of the loop is shown in Figure 2 and photographic views are shown in Figures 3 and 4.

Saturated steam at 50 psi was fed into the system from a 3/4-inch laboratory supply line. The steam injection system was made from 3/4-inch copper, brass, and stainless steel tubing and fittings. The main steam valve in the supply line was always throttled to allow part of the liquid to flash before being fed into the system. After flowing through this valve, steam was routed through an ANDERSON-IBEC in-line steam separator. The separator effectively dried the steam by centrifuging the moisture and scale from the main line. Dried steam was then sent to a NORGREN steam pressure regulator while the moisture and scale

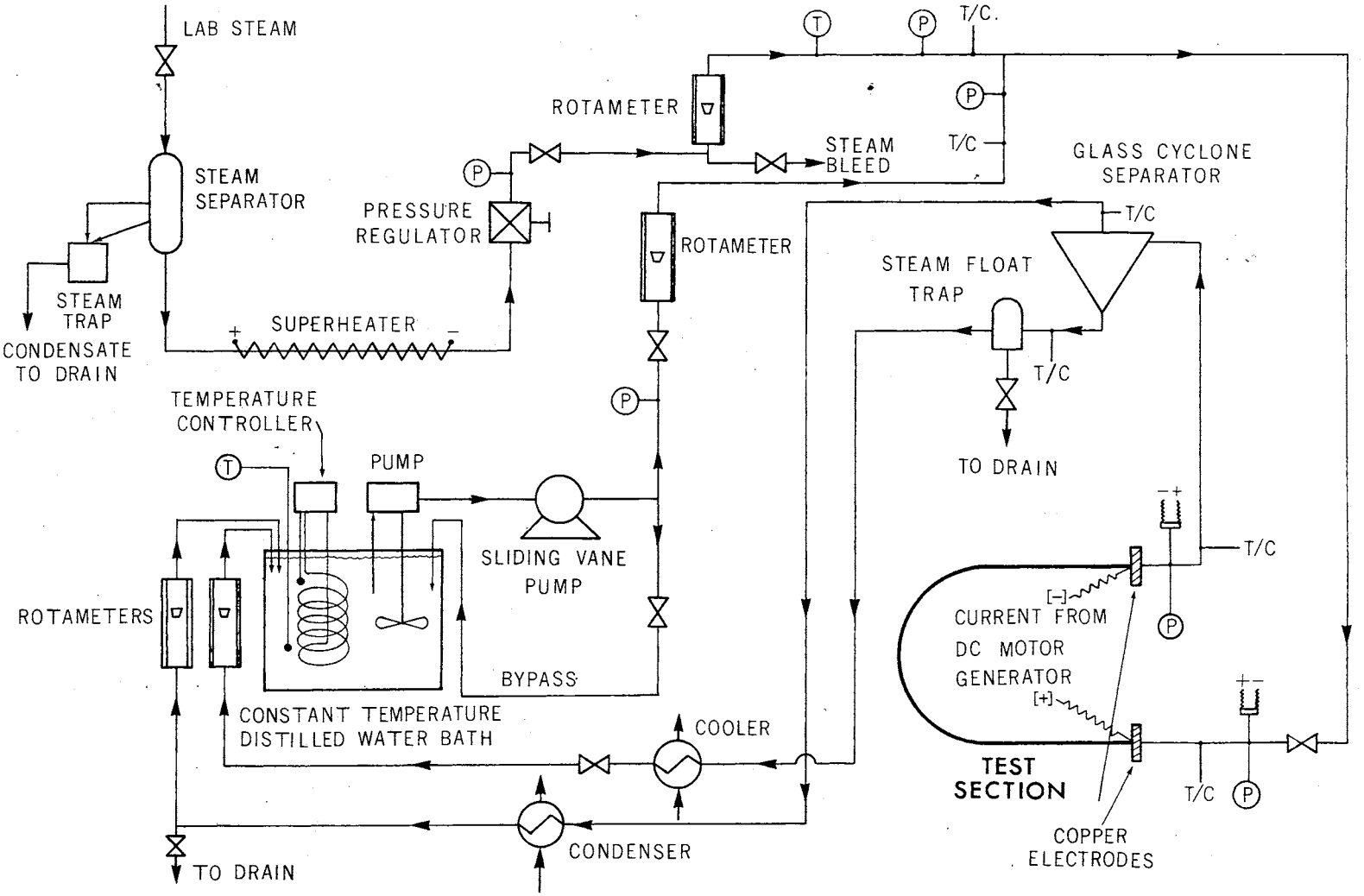

Figure 2. Heat Transfer Loop

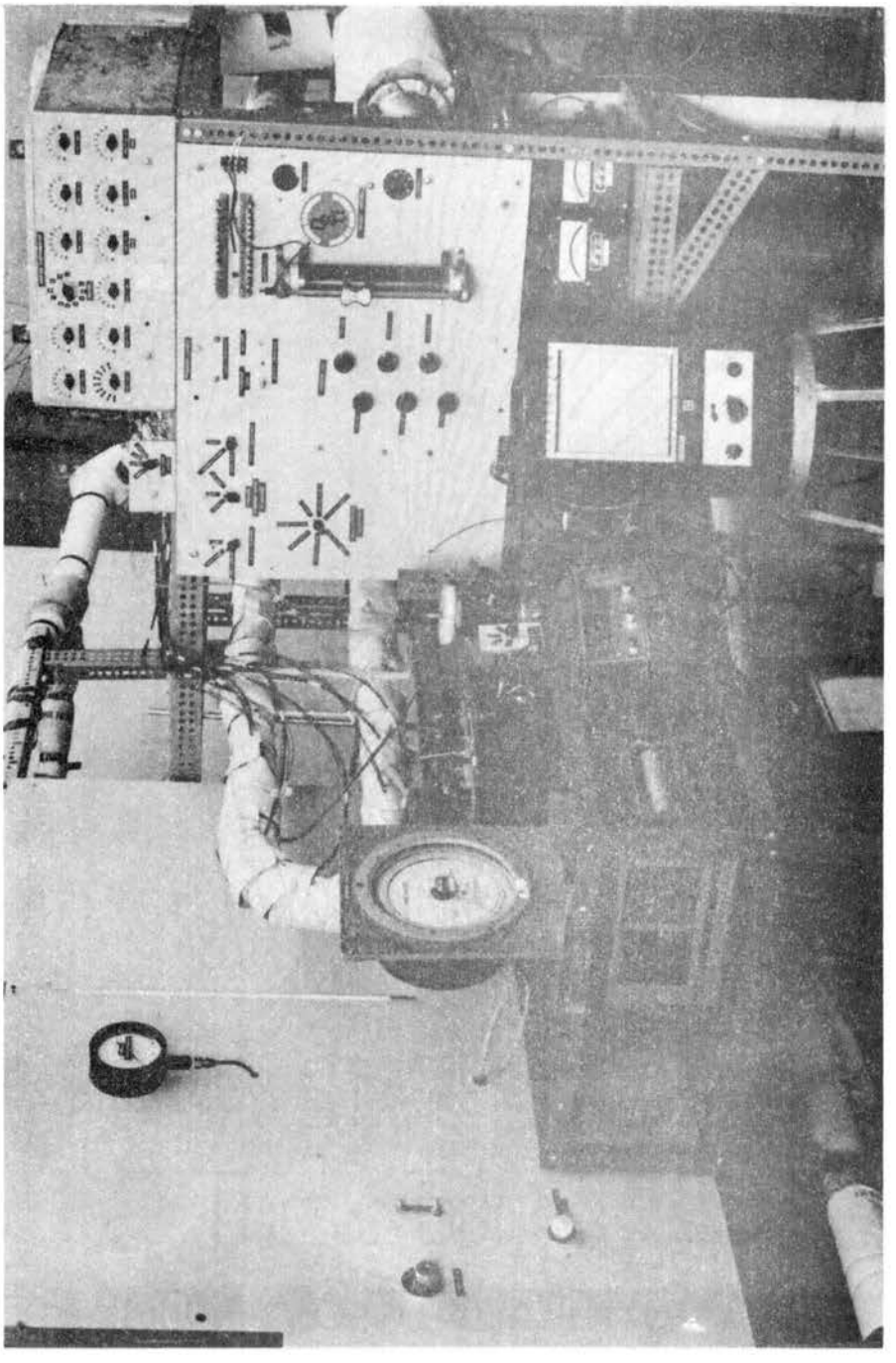

Figure 3. Photograph of the Heat Transfer Loop, Instrumentation and Test Section

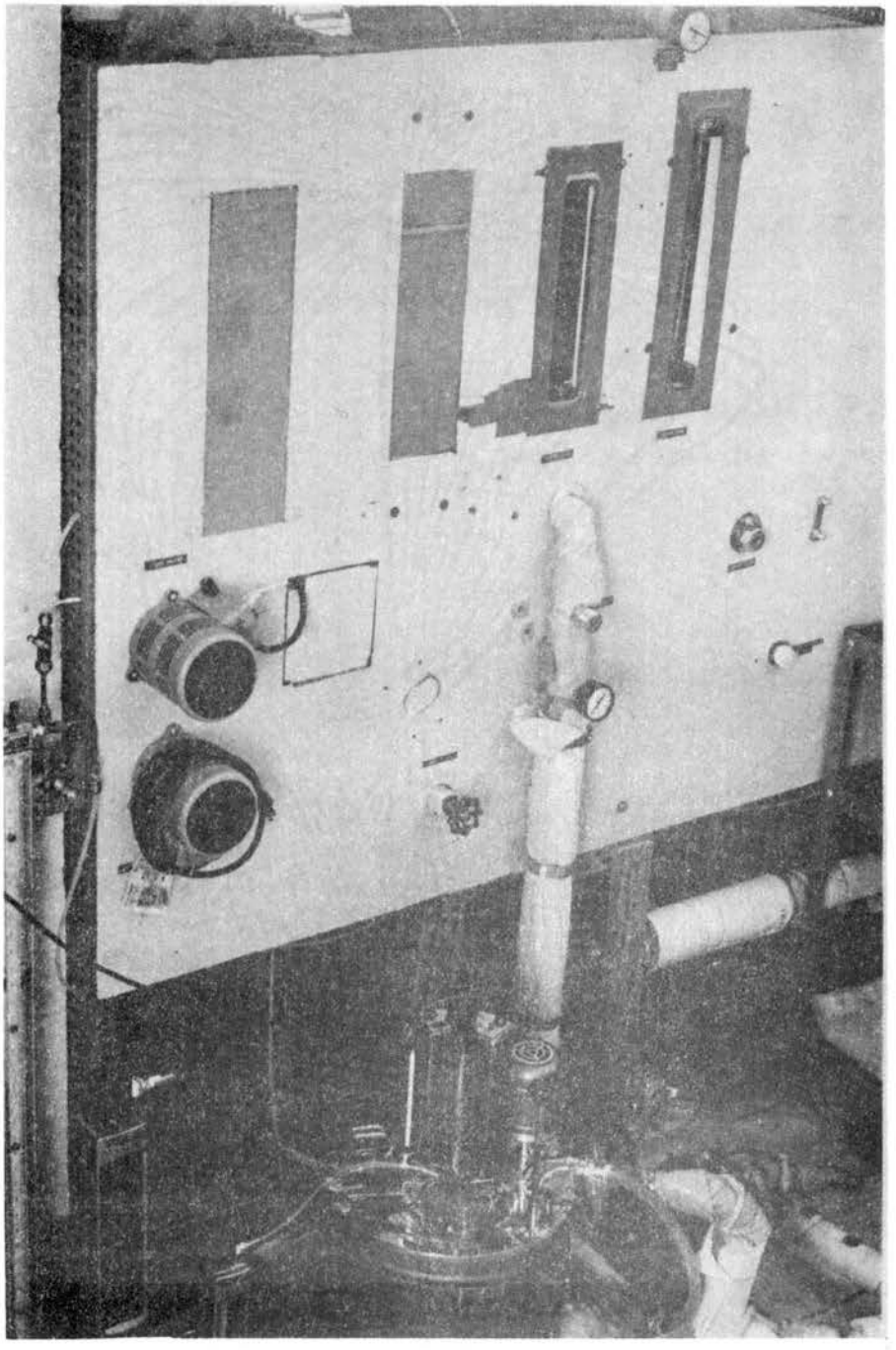

Figure 4. Photograph of the Heat Transfer Loop and Water Injection System

were removed from the system by means of a steam trap. An electric tape heater was also used in the line to superheat the steam feed so that dry conditions were realized for all runs. From the pressure regulator, steam was routed through a 3/4-inch MANATROL needle valve and a rotameter before being mixed with the water stream.

Distilled water was supplied to the system from a COLORA constant temperature bath which included a temperature controller, a mixer, and a small centrifugal pump. The water injection system was made from 1/2-inch copper, brass, and stainless steel tubing and fittings. Water, from the bath, was sent to an EASTERN sliding vane pump, a 1/2-inch MANATROL needle valve, and a BROOKS rotameter before being mixed with the steam feed. Part of the water feed from the pump was returned to the bath via a bypass line. The bypass flow rate was controlled by a 1/4-inch MANATROL needle valve.

The steam-water mixture flowed from the mixing tee to the test section after passing through a 3/4-inch MANATROL needle valve. The valve was used to raise the back pressure of the injection systems whenever there was an indication of possible flow oscillations. From the test section the mixture was sent to a glass cyclone separator where the steam was separated and sent to a condenser, while the water was first sent to a float-type steam trap and then to a heat exchanger. Both exchangers were open to the atmosphere in order to vent the non-condensibles from the system.

Part of the condensed steam was returned to the bath while the remaining portion was routed to a drain. When the flow rate was being measured, however, all of the flow was returned to the bath where a calibrated Fischer and Porter rotameter was used to measure the flow

rate. Volume samples of the condensate over a known time period were also taken to double check the rotameter reading.

Water from the heat exchanger was returned to the bath where another calibrated Fischer and Porter rotameter was used to measure the water flow rate. Timed volume samples of the flow were also taken to double check the flow rate indicated by the rotameter.

Test Section Description

Two test sections made from 7/8-inch OD X 0.052-inch wall INCONEL 600 seamless tubing were used for the experiments. One test section had a radius bend of 4.75 inches while the other had a 9.875-inch bend. Both test sections are shown with the appropriate dimensions in Figure 5. The test sections were annealed after bending so that stress relieving would be avoided during heating.

The test sections were thermally insulated by wrapping them with several layers of bonded fiberglass tape and 2 inches of fiberglass sheets. The outside surface of the insulation was then wrapped with aluminum foil so that radiation losses would be minimized.

The test sections were electrically isolated from the loop by connecting them with a short piece of neoprene tubing at both ends.

Four pressure taps with a 1/16-inch hole were silver-soldered to the test section. The taps were electrically isolated from the recording instruments by connecting them with silicone rubber tubing.

The test sections were heated by passing DC current obtained from a Lincolnweld SA-750 motor generator. Two 1/4-inch thick copper bars which were silver soldered to the test sections served as electrodes for connection to the motor generator.

Temperature Measurements

Each test section was fitted with 88 thermocouples and their locations on each test section is shown in Figure 5. The thermocouples for the small bend test section were initially made from 24AWG Iron-Constantan wire since they were easy to work with. However, when the thermocouples were mounted on the test section and the test section was heated, about 70 of them detached themselves from the test section. The reason for this failure was attributed to the fact that all of the thermocouples were prestressed into position and during heating they were stress relieved and the cement bond was not capable of withstanding the stresses. Subsequently, all the thermocouples, except for the eight at axial location 11 of the small test section, were made from 30AWG wire since the thinner wire was more flexible and had smaller induced stresses.

The thermocouples were glued and mounted to the test section by following the procedure outlined below.

1. A bead of SAUREISEN No. 33 cement was placed at each thermocouple location.

2. After the bead dried completely it was sanded flat to about 1/2 mm thickness.

3. The hot junction of the thermocouple wire was placed at the designated location and the wire was temporarily held in place with adhesive tape.

4. Another bead of cement was then placed on the hot junction so that the thermocouple was completely glued to the surface.

5. After the cement dried the thermocouple was placed flat on the tube surface and clamped. A three inch span was allowed between the hot junction and the clamp to minimize conduction errors.

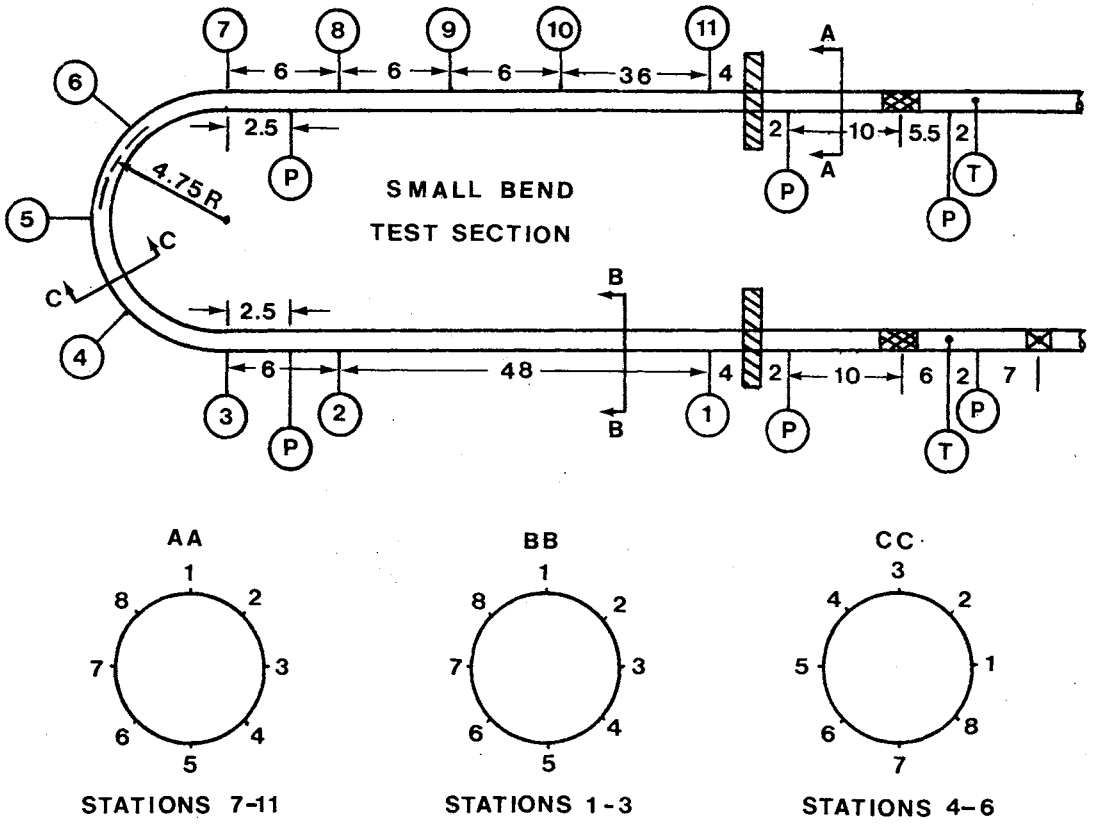

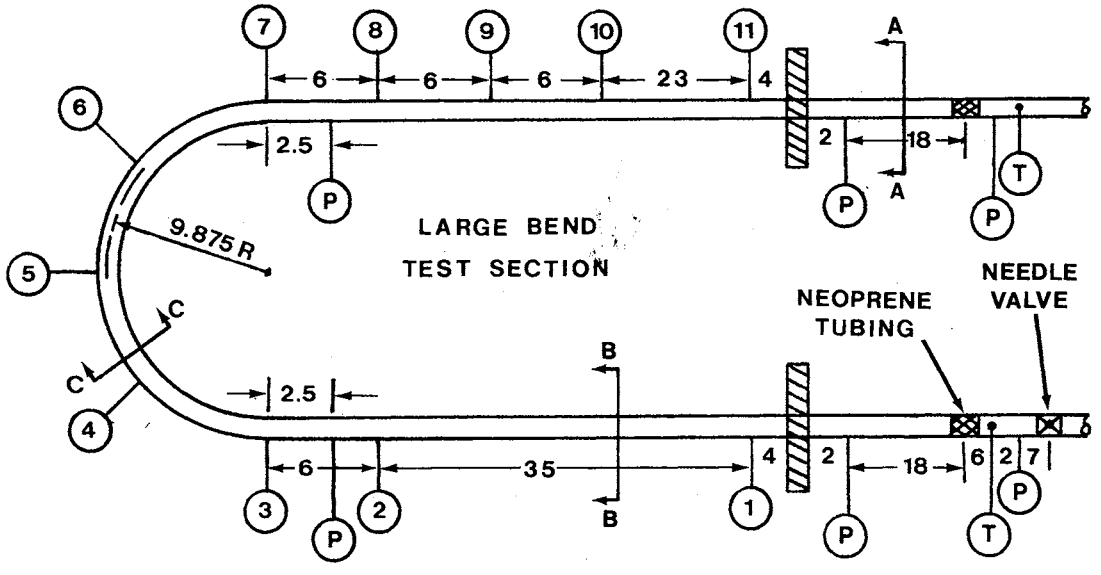

Figure 5. INCONEL Test Sections

The following fluid temperatures were also monitored for each experimental run (see Figure 2 for their locations in the loop).

1. Premix water temperature.
2. Premix steam temperature.
3. Mixture inlet temperature.
4. Mixture outlet temperature.
5. Steam temperature in the cyclone separator.
6. Water temperature in the cyclone separator.

The inlet and outlet mixture temperatures (items 3 and 4 above) were measured by ungrounded, sheathed thermocouples with the hot junctions exposed to the two phase mixture. The thermocouple assemblies were attached to the inlet and outlet lines by SWAGELOK fittings. The remaining fluid temperatures mentioned above were measured by thermocouples placed inside copper thermowells that were silver soldered to the lines.

All the surface thermocouples were connected to an array of barrier strips which in turn were connected to 11 rotary switches. The terminal lugs used on the barrier strips were made of either iron or constantan and this feature eliminated any problems associated with the creation of new thermocouples due to variation in room temperature. The rotary switches, however, were mounted on a panel and the connections were enclosed in a constant temperature box. The outputs from the rotary switches were brought to a master rotary switch which was hooked up to a Leeds and Northrup Numatron. The Numatron incorporated a reference junction compensator and the output was displayed in digital form in degrees Fahrenheit. The Numatron was calibrated prior to usage according to manufacturer's specifications.

An auxiliary rotary switch with six connections was used to record any six thermocouple outputs on two Leeds and Northrup Speedomaxes. The recorders had variable spans and range and were calibrated several times during each run against a Leeds and Northrup millivolt potentiometer.

Pressure Measurements

The inlet and outlet mixture pressures were monitored by two CEC pressure transducers. The output of the transducers was either read on the Numatron or recorded on a CEC Model 5-124 oscillograph. The transducers were only used to verify the existence of steady conditions. The electronic circuits necessary to drive the transducers were constructed according to manufacturer's specifications.

The six pressure taps (see Figure 5 for locations) were connected to one main line by a series of Whitey valves. The switching system was connected in such a manner that any one of the six taps could be activated and read on a calibrated Wallace and Tiernan pressure guage.

Flow Measurements

The following flow rates were measured by timing known volume samples as well as by reading the output on calibrated rotameters.

1. Condensed steam flow rate from cyclone.
2. Water flow rate from cyclone.

The premix steam rotameter was used only as a flow indicating device since it could not be calibrated. The premix water rotameter was mostly used as a flow indicating device also, since some of the water always flashed into steam during the mixing process. However, the

indicated reading was accurate since the rotameter was calibrated at 175°F and all two phase runs were made with the bath at this temperature.

Electrical Measurements

The current to the test section was measured by a Weston Model 931 ammeter in conjunction with a 50MV shunt. The voltage drop across the test section was measured by a Weston Model 931 voltmeter and also by the Numatron for potentials of less than 20 volts.

CHAPTER IV

EXPERIMENTAL PROCEDURE

Thermocouple Calibration

All surface thermocouples were calibrated in situ by using dry saturated steam as a reference temperature. The thermocouple outputs were recorded after a run time of approximately eight hours. The calibration runs were performed twice with each test section. The second calibration was done after a few trial runs were made and the data from this run was used for correcting surface temperatures for other runs since it was felt that any errors in thermocouple outputs due to incomplete drying of the SAUREISEN cement bead would have been eradicated after the trial runs. During the runs, the atmospheric pressure and room temperature were also recorded so that the surface temperatures could be compared with the saturated steam temperature.

The inlet and outlet mixture thermocouples were also calibrated during the calibration runs except that their outputs were recorded on a potentiometer with a saturated steam bath as a reference junction.

Thermocouple readings for all runs were corrected by assuming that the conduction losses were proportional to the difference between the reading and room temperature for each run as compared to the difference during the calibration. Table I shows an example of such a correction and it can be seen that the corrected surface temperatures are within $\pm 0.1°F$ of the median temperature.

TABLE I

THERMOCOUPLE CALIBRATION CHECK WITH STEAM WATER FLOW AND NO HEAT FLUX

THERMOCOUPLE CALIBRATION RUNS - SMALL BEND

UNCORRECTED OUTSIDE WALL TEMPERATURES - DEGREES F

AXIAL STATION LOCATIONS

	1	2	3	4	5	6	7	8	9	10	11
1	226.9	226.2	226.2	226.4	226.1	226.2	226.0	226.0	225.9	225.9	225.1
2	227.1	226.2	226.3	226.3	226.3	226.0	226.0	225.9	225.4	225.6	225.3
3	226.8	226.3	226.2	226.5	226.2	226.0	225.9	226.1	226.0	225.6	224.9
4	227.0	226.5	226.5	226.2	226.3	226.1	226.1	225.9	226.1	225.6	224.9
5	226.9	226.3	226.3	226.1	225.9	225.8	226.2	226.3	225.9	225.9	224.9
6	227.0	226.3	226.5	226.1	225.9	226.1	226.1	226.1	225.9	225.8	224.1
7	227.0	226.4	226.3	226.1	226.2	226.1	226.2	225.9	226.1	225.8	225.2
8	226.7	226.5	226.3	226.3	226.3	226.1	226.2	225.9	225.8	225.9	223.6

CORRECTED OUTSIDE WALL TEMPERATURES - DEGREES F

AXIAL STATION LOCATIONS

	1	2	3	4	5	6	7	8	9	10	11
1	227.2	226.7	226.6	226.6	226.5	226.5	226.3	226.3	226.2	226.1	225.6
2	227.3	226.8	226.6	226.6	226.5	226.4	226.3	226.3	226.4	226.1	225.6
3	227.3	226.7	226.6	226.7	226.6	226.4	226.3	226.2	226.2	226.1	225.7
4	227.2	226.7	226.8	226.6	226.6	226.4	226.2	226.2	226.2	226.0	225.6
5	227.4	226.8	226.7	226.6	226.5	226.4	226.4	226.3	226.3	226.2	225.8
6	227.4	226.6	226.8	226.6	226.7	226.5	226.3	226.2	226.2	226.0	225.8
7	227.3	226.6	226.5	226.5	226.5	226.4	226.3	226.2	226.1	226.0	225.7
8	227.2	226.7	226.6	226.5	226.5	226.4	226.4	226.3	226.2	226.0	225.8

Pressure Gauge Calibration

The Wallace and Tiernan gauge was calibrated against a 60-inch mercury manometer and the accuracy was within the readability errors associated with the manometer. All other pressure gauges used in the heat transfer loop as well as the air-water loop were calibrated against the Wallace and Tiernan gauge. The pressure readings were corrected for hydrostatic height wherever necessary.

Rotameter Calibration

The rotameters used for measuring liquid flow in the heat transfer loop as well as in the air-water loop were calibrated by taking known volume samples collected during a specified time interval at the operating conditions. The samples were collected at least five times for each reading.

The air flow rotameter was not calibrated due to lack of equipment and the factory-supplied curves were used for calculating the flow rate. However, since the factory-supplied curves for water flow rates for the same rotameter checked to within 1½ percent of the calibrated flow rates, it was assumed that similar accuracies were realized for air flow rate readings.

The steam flow rotameter was not calibrated, as mentioned earlier, and it was used only as a flow indicating device.

All rotameter readings were corrected for pressure and temperature deviations where necessary.

Heat Loss Calibration

Heat losses for the test sections and the loop (test section exit to cyclone separator) were measured by slowly bleeding dry saturated steam at atmospheric pressure through the system and collecting a known volume of condensate for a specified time interval. The samples were collected several times during the run and only after about twelve hours of run time. The samples were collected from the test section exit and then from the cyclone exit, respectively, so that the heat loss in each section could be calculated.

Heat losses for each run were calculated by assuming that the losses were proportional to the difference between the test section (or loop) temperature and the room temperature for each run as compared to the calibration run.

Loop Operating Procedure

The following step-by-step procedure was followed for each run.

1. The generator was turned on and left to warm up for about 1½ hours.

2. Water was pumped through the system and the pressure lines were bled to remove any trapped gases.

3. Water was shut off from the main line and steam was bled through the system for about thirty minutes by which time the steam flow usually stabilized to the desired rate.

4. Water was introduced to the system at the desired rate.

5. After about five minutes, heat was added to the test section at the prescribed rate.

6. After steady conditions had been established (usually twenty minutes) the temperatures, pressures, and other operating conditions were measured and recorded.

In all the runs the bath was maintained at 175°F.

CHAPTER V

EXPERIMENTAL RESULTS

The experimental results for the air-water flow pattern tests as well as the steam-water heat transfer tests are presented in this chapter. A discussion on stability for the heat transfer tests is also presented even though all tests were conducted under stable conditions. Results for the two single phase runs are presented in Appendix C.

Air-Water Visual Tests

Hydrodynamic behavior of air-water mixtures flowing inside 180° tube bends, with 10-inch and 22-inch diameter bends, was investigated. These configurations closely approximated the 9.5-inch and 19.75-inch diameter bend, INCONEL 600, test sections that were used for the flow boiling study. Although Zahn (10) concluded from his study with refrigerant R22 evaporating inside a serpentine coil that there was no effect of flow direction on the hydrodynamic behavior of two phase flow in the straight sections, air-water flow behavior in both upflow and downflow directions was investigated in this study.

The following parametric ranges and flow regimes, as described by Alves (8) and later adapted by Baker (9), were investigated:

Total Mass Velocities:	15,000 to 80,000 lbm/(hr-sq. ft.)
Gas Qualities:	0% to 88%
Flow Regimes:	stratified, wavy, slug, plug, and annular.

All raw data was reduced by means of a computer program in which fluid property data and rotameter calibration curves were incorporated in the form of polynomial curve fits.

Flow Visualization

It was somewhat difficult to distinguish the flow patterns without using colored water, especially when the fluid velocities were high. The addition of dye into the liquid phase alleviated this problem considerably and red dye gave a better contrast than the green dye.

Although the still pictures arrested the motion adequately for all flow rates, the movies were only effective for low liquid flow rates, i.e., low liquid flow rates. For high liquid flow rates (total flow > 1000 lbm/hr) it would have been beneficial if the movies could have been filmed at about 200fps instead of 64fps. However, for these high flow rates the two phase flow behavior could be adequately described by still pictures since the basic flow pattern was similar to the flow patterns recorded with total flow rates between 700 to 1000 lbm/hr. Minor difficulties were also experienced in filming color movies with back lighting since the tolerance on the f stop was $\pm\frac{1}{2}$ for over-exposing or under-exposing the film.

The flow patterns were established by observing the flow in the inlet leg of the test section and analyzing it on a mean basis after "steady" conditions had been achieved. In the slug dominated regimes, however, there were always minor oscillations in the liquid flow and the mixture pressure at the test section inlet. The flow oscillations coincided with the frequency of slug ejection from the system while the pressure fluctuation occurred when slugs passed over the pressure tap.

Neither pressure nor flow oscillations were noticed in the air line. Further explanation on the slug flow behavior is given in the discussion on flow reversal. None of the above mentioned phenomena were encountered in the annular type regimes.

Since an explanation of flow pattern descriptions by Baker's (9) method seemed inadequate, due to their generality, the flow pattern description recommended by Zahn (10), with some modifications, was developed. Typical characteristics of the flow patterns can be found in the sketches given in Figure 6 and in the photographs shown in Figures 7 through 13. A brief explanation of each pattern is given below. Note that low liquid flow generally implies that $G_L\Psi$ is less than 80 and high liquid flow generally implies that $G_L\Psi$ is between 200 and 2000.

Bubble. A flow pattern where small discrete bubbles of gas flow in the top part of the tube at approximately the same velocity as the liquid.

Plug. A flow pattern where bubbles have coalesced and flow as plugs of gas alternately with plugs of liquid. The interface in the gas plug has a foamy appearance due to surface tension effects and bubbles may be attached to the interface.

Stratified. A flow pattern where liquid stays at the bottom of the tube and generally wets less than half of it. The interface is always smooth.

Slug. A flow pattern where liquid flows at the bottom of the tube and slugs of liquid travel through the tube at a velocity higher than the average liquid velocity. For low gas flows the interface may have

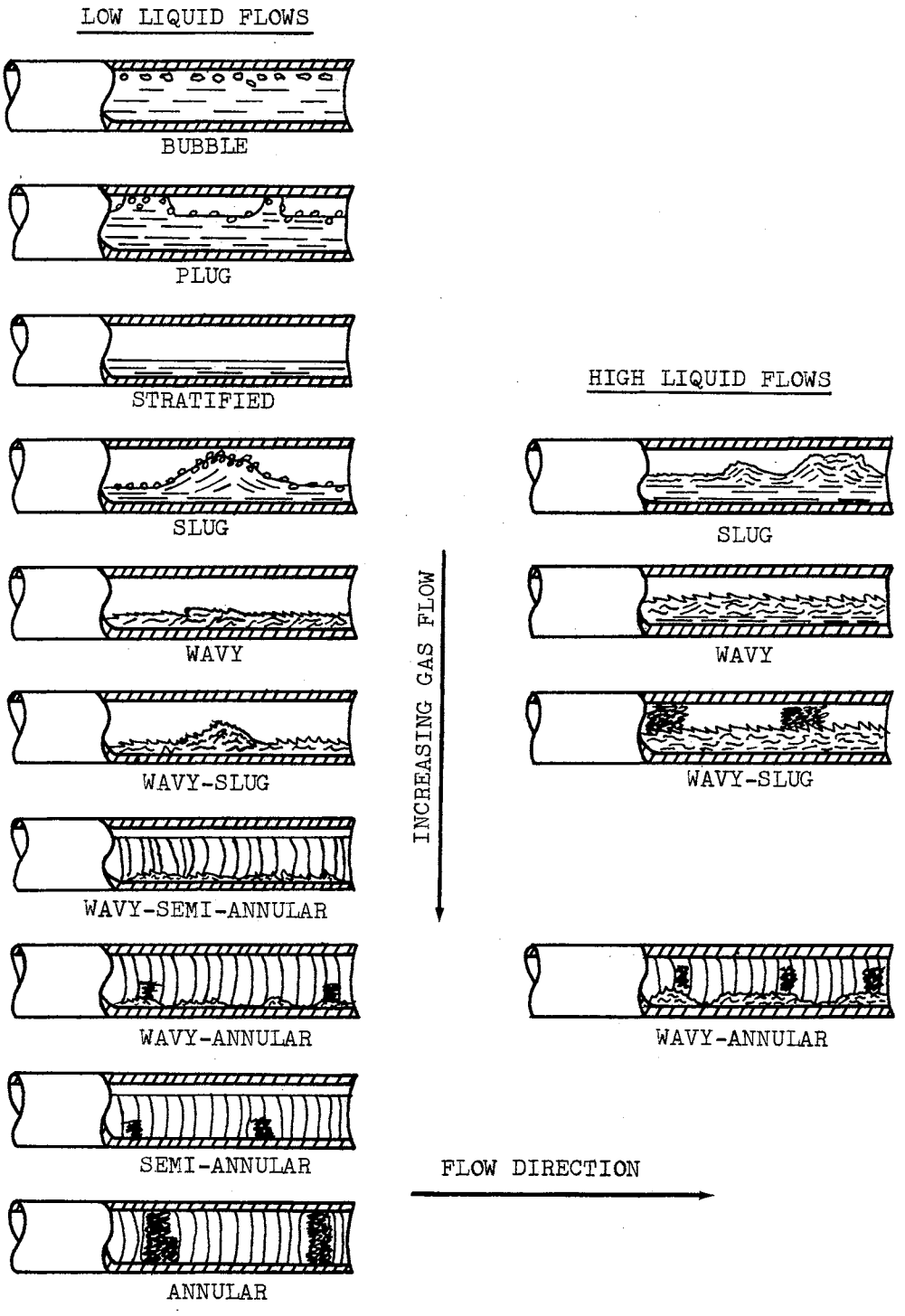

Figure 6. Typical Flow Patterns From Air-Water Tests

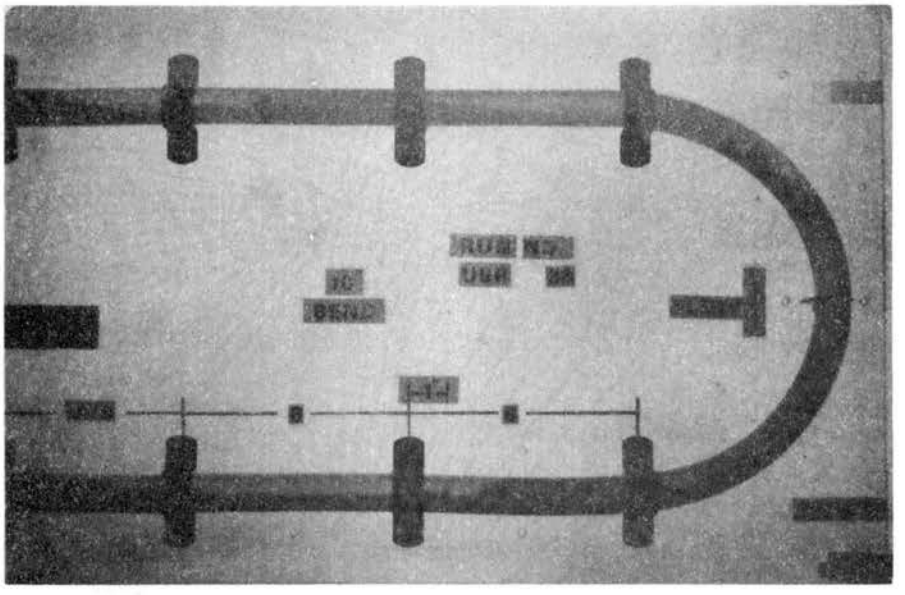

Figure 7. Plug Flow

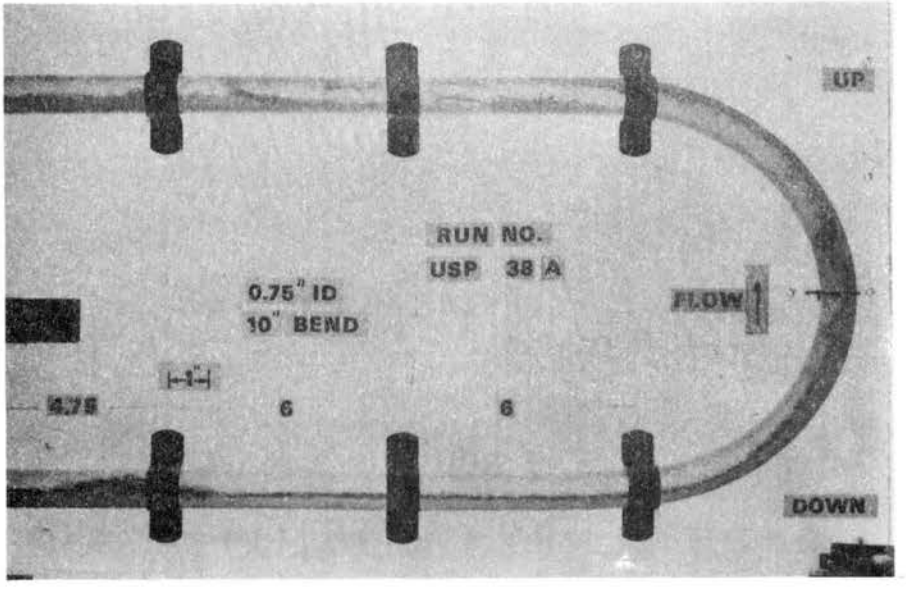

Figure 8. Slug Flow

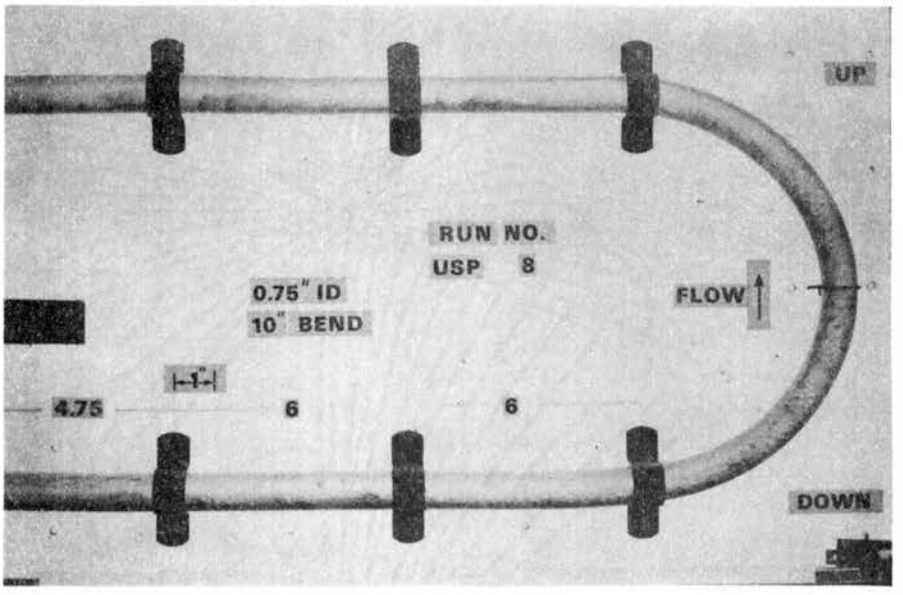

Figure 9. Wavy Flow

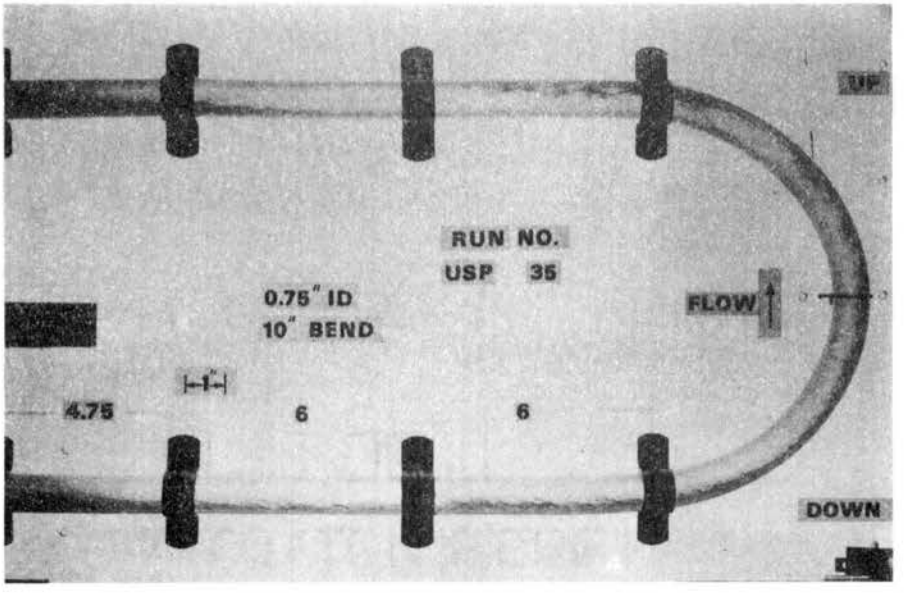

Figure 10. Wavy-Slug Flow

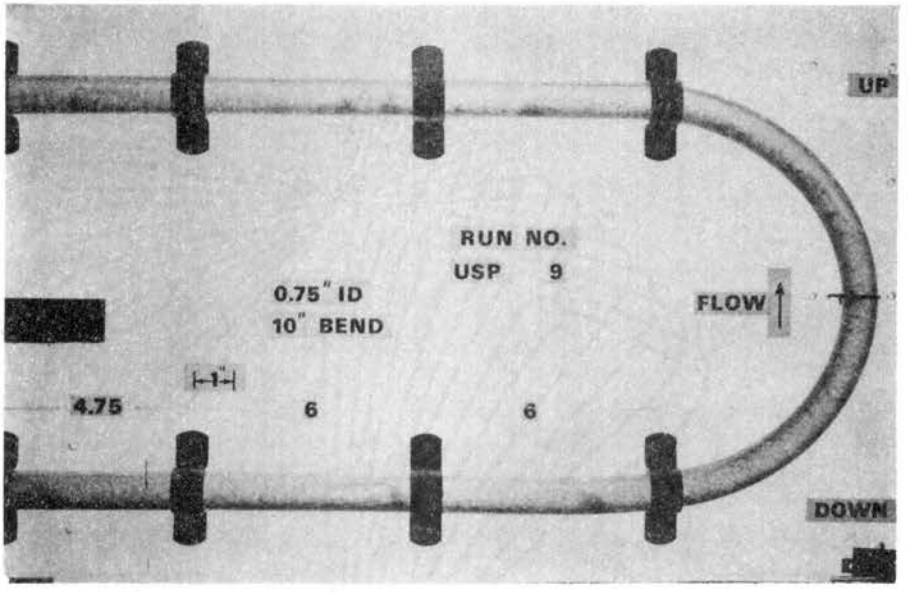

Figure 11. Wavy-Semi-Annular Flow

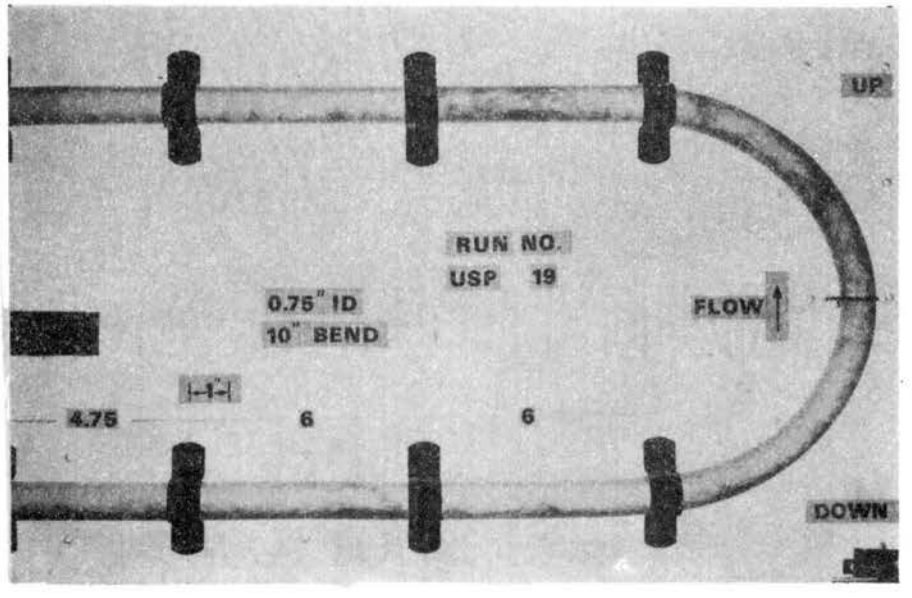

Figure 12. Wavy-Annular Flow

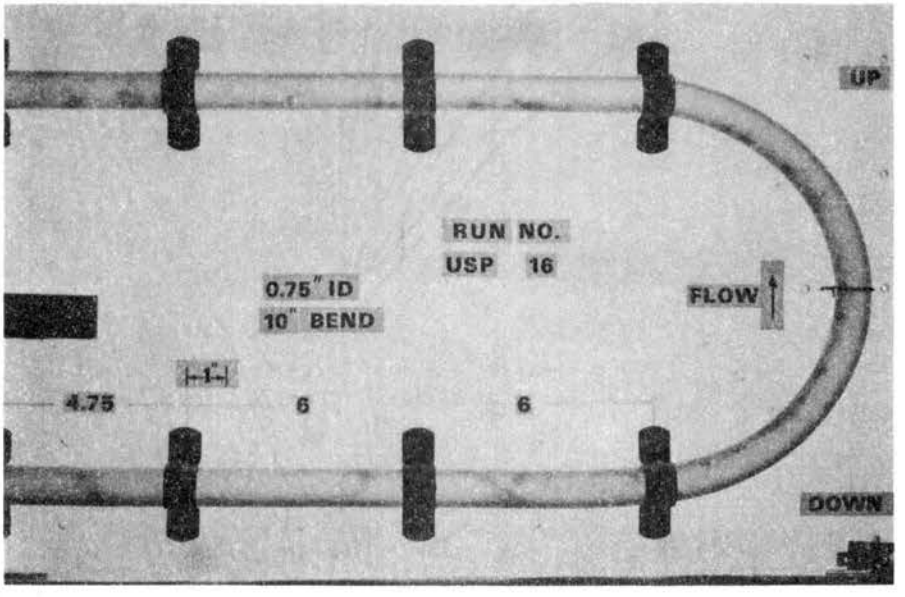

Figure 13. Annular Flow

bubbles attached to it whereas for high gas flows the interface will be rough.

Wavy. A flow pattern where liquid flows at the bottom and the interface is quite rough. For low liquid flows the liquid will wet less than half of the tube whereas for high liquid flows the liquid will wet about half of the tube.

Wavy-Slug. This regime is an extension of the wavy regime but the gas phase shears the liquid surface to form waves or slugs that intermittently wet the top part of the tube. The liquid slugs are generally thoroughly mixed with the gas.

Wavy-Semi-Annular. This is a transitory pattern that occurs only for very low liquid flows. A wavy liquid stream flows at the bottom while a rippled liquid stream flows on the side. The liquid wets only about 3/4 of the tube.

Wavy-Annular. This pattern is similar to the wavy-semi-annular pattern except that the rippled stream wets the whole tube. This is also an extension of the wavy-slug regime except that the slugs start to resemble disturbance waves.

Semi-Annular. This is basically an annular pattern except that the liquid only wets about 3/4 of the tube and occurs only for very low liquid flows. This pattern is also a transitory pattern.

Annular. A flow pattern where an evenly distributed liquid film travels on the wall in the form of ripples while fast travelling disturbance waves keep washing the ripples intermittently. The core is occupied by the gas phase.

Annular with Mist. A flow pattern where most of the liquid travels in the form of mist while a very thin liquid layer wets the tube. This pattern is generally difficult to observe visually.

Data Reduction

The data points were reduced and initially plotted on Baker's (9) map to check the agreement between the observed flow patterns and Baker's designations. In general, the comparisons were favorable. However, as numerous investigators have pointed out, Baker's map is somewhat inaccurate in that the regime boundaries are plotted as lines rather than bands. Although Scott (15) modified the map by incorporating these bands, the map was still inadequate since it did not include the subdivisions observed in this study. Furthermore, the coordinates on Baker's map are awkward to use as pointed out by Bell et al. (16). Using Bell's procedure, Baker's map was transformed and all the data points obtained in this study were plotted as shown in Figures 14, 15, 16, and 17. The transformed map was convenient to use for this study since all the points where liquid flow was held constant while gas flow was varied plotted on a vertical line.

A slight modification to the Baker map was incorporated in the transformation, viz. a log cycle was deleted from the abscissa and one was added to the ordinate. For further discussion on the transformation the reader is referred to Bell et al.'s paper (16).

During the course of the visual tests for runs near the annular-wavy regime border ($G_G/\Lambda = 1.5 \times 10^4$), it was observed that the liquid would invert from the outside to the inside in the bend. At slightly higher air flow rates annular flow was completely destroyed in the bend

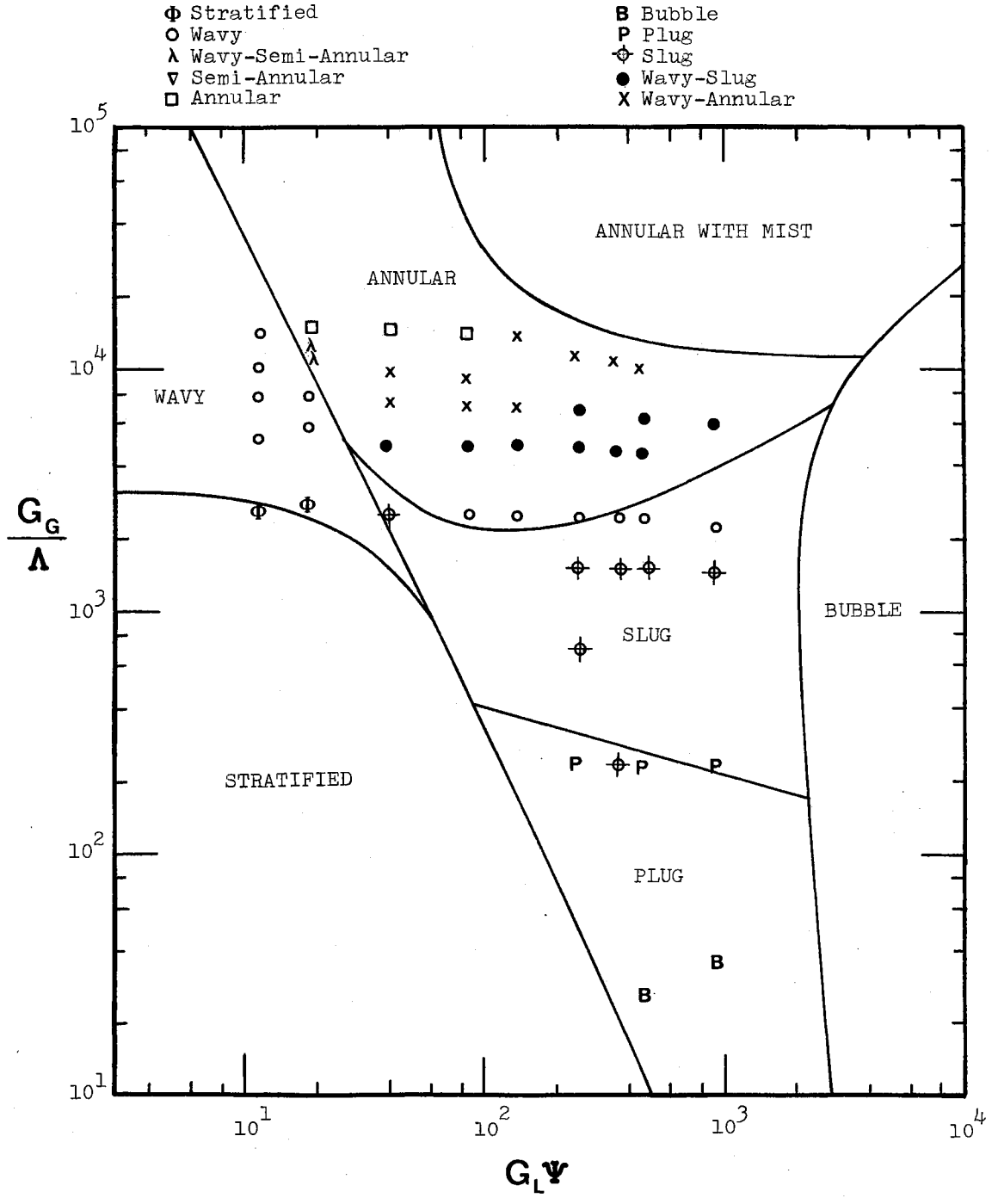

Figure 14. Air-Water Flow Pattern Data on Modified Baker's Map, Small Bend, Upflow

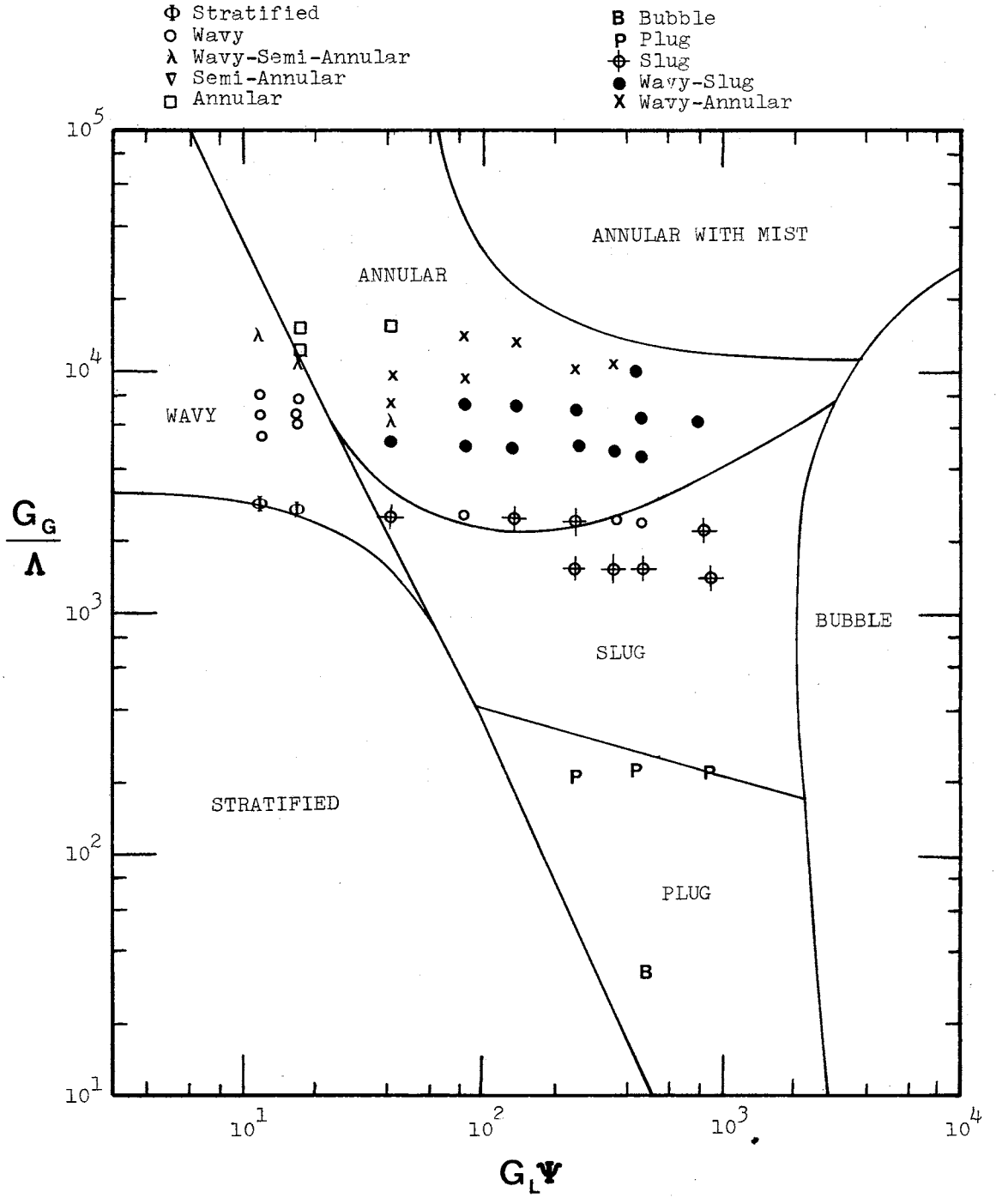

Figure 15. Air-Water Flow Pattern Data on Modified Baker's Map, Large Bend, Upflow

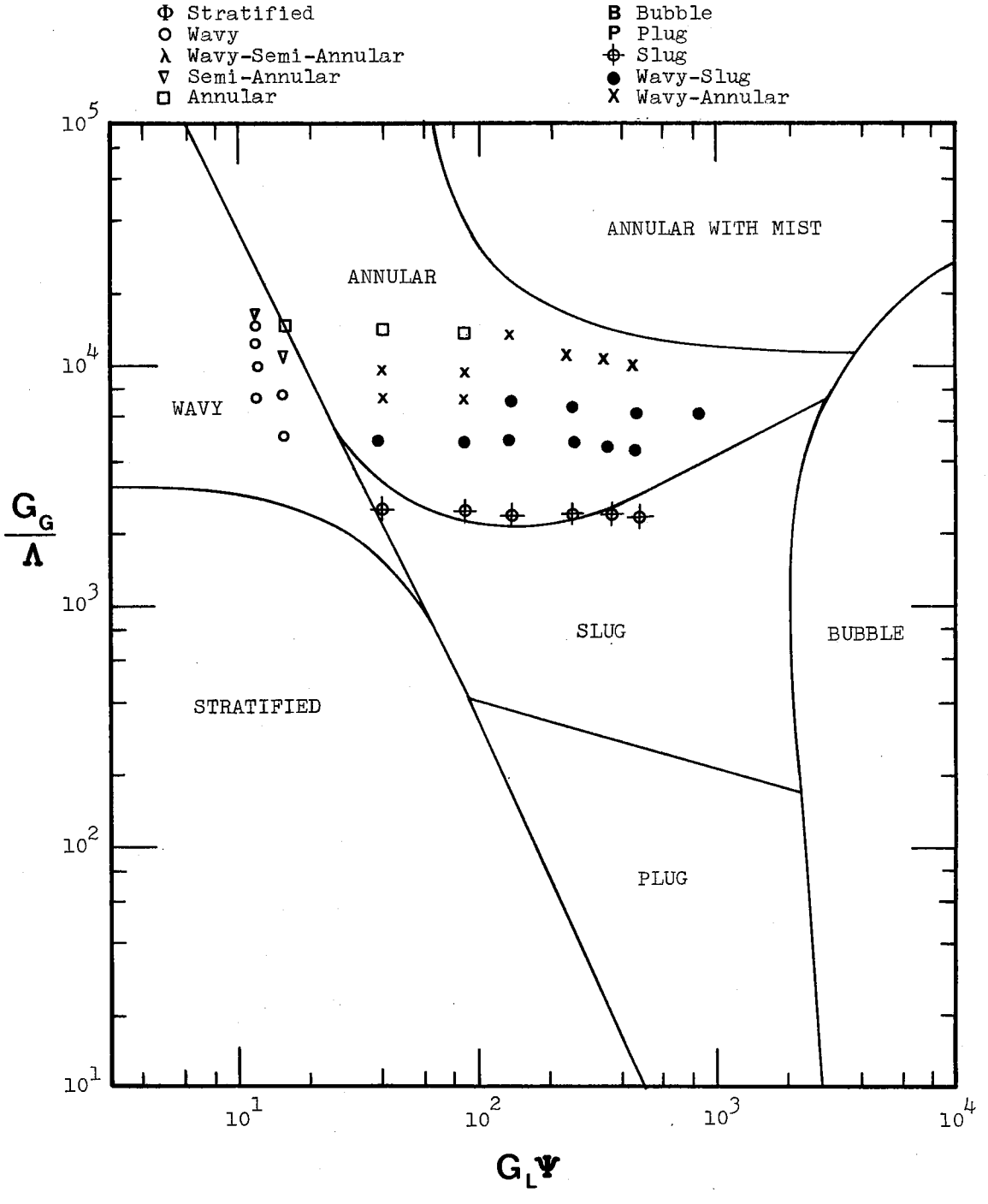

Figure 16. Air-Water Flow Pattern Data on Modified Baker's Map, Small Bend, Downflow

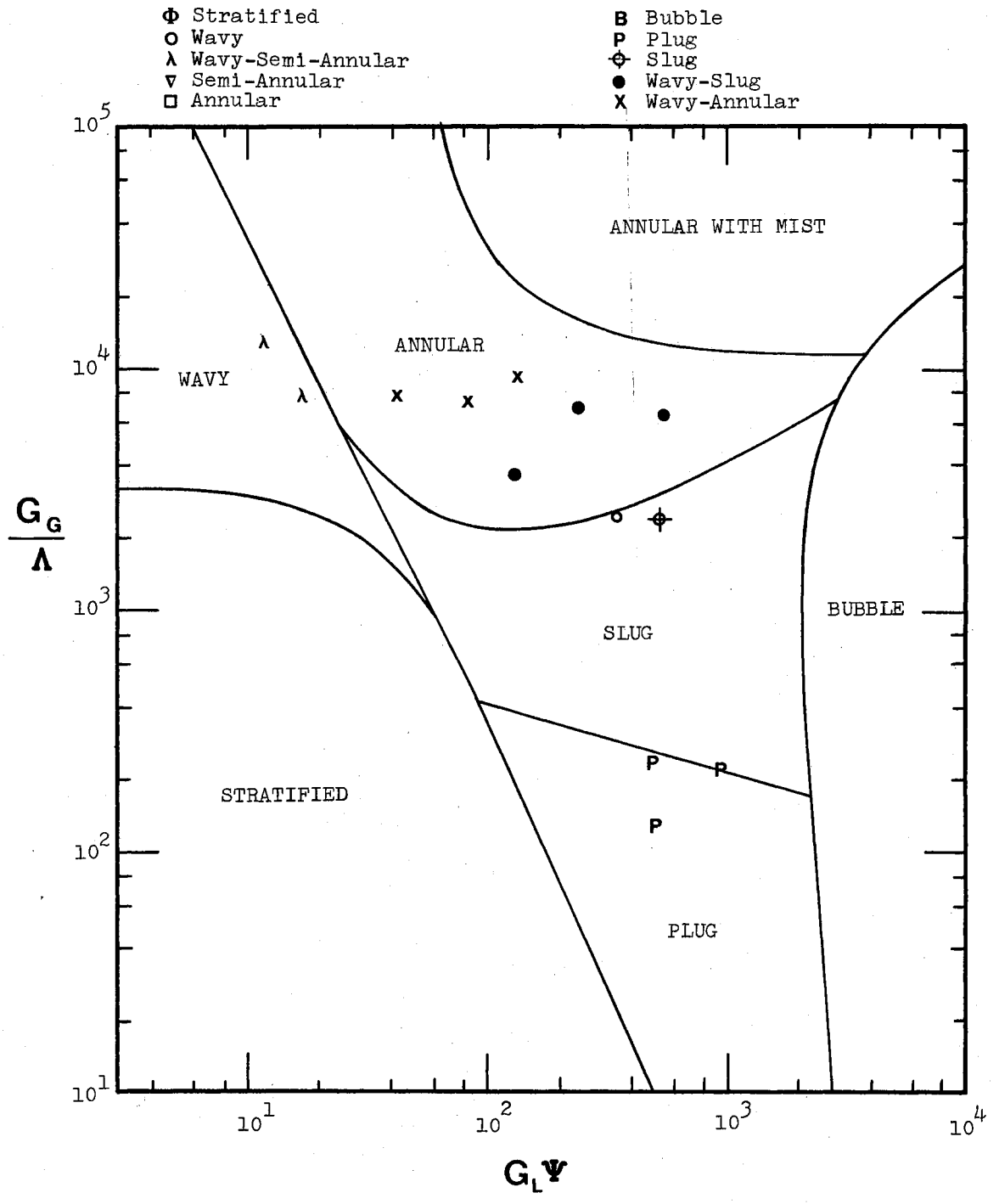

Figure 17. Air-Water Flow Pattern Data on Modified Baker's Map, Large Bend, Downflow

but re-established about 30 diameters downstream of the bend. This anomalous behavior can be seen in Figure 18(a) and (b) where secondary flow effects in the form of streaks are visible in Figure 18(a) but not in Figure 18(b).

The following table summarizes the flow patterns that are encountered as the gas flow is increased for constant liquid flow (see Figure 6). The flow patterns were identified by analyzing the conditions in the inlet leg of the test section.

TABLE II

FLOW PATTERNS FROM AIR-WATER TESTS

Low Liquid Flows	High Liquid Flows
Stratified	Bubble[2]
Wavy	Plug
Wavy-Semi-Annular[1]	Slug
Semi-Annular[1]	Wavy
Annular	Wavy-Slug
Annular with Mist	Wavy-Annular
	Annular
	Annular with Mist

[1] for $G_L\psi < 30$.

[2] May depend on inlet conditions.

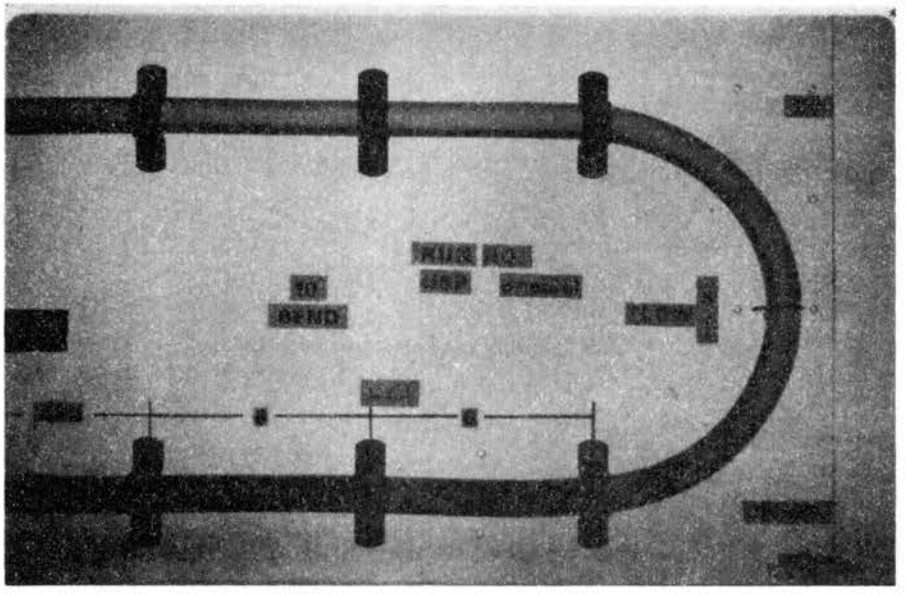

(a) Secondary Flow Visible

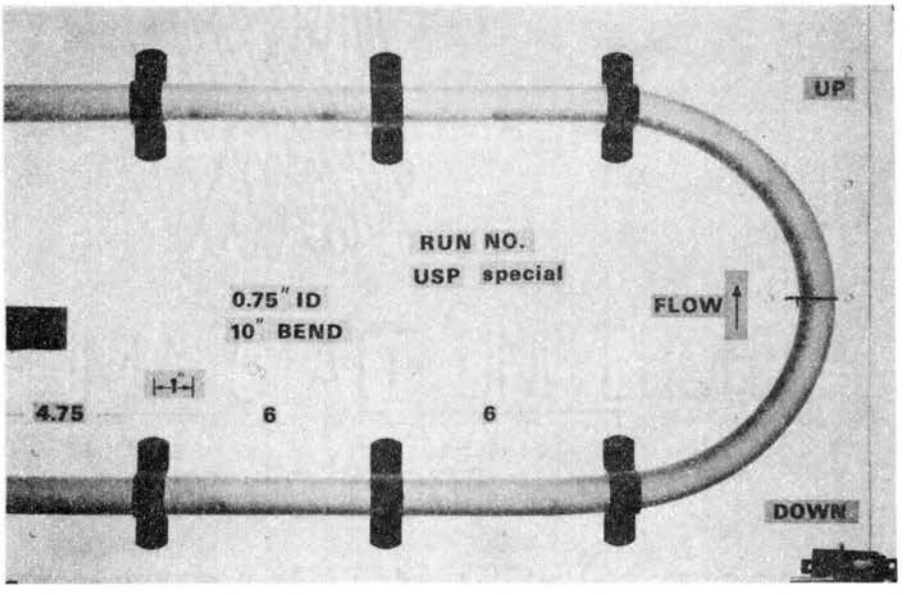

(b) Secondary Flow Invisible

Figure 18. Film Inversion

Steam-Water Heat Transfer Tests

The experiments with steam-water mixtures were conducted in the annular flow regime to see if the film inversion phenomenon encountered in the visual tests could be duplicated. The following parametric ranges were covered during the course of the study.

Total Mass Velocities: 28,000 to 61,000 lbm/(hr.-sq. ft.)

Steam Qualities: 60% to 98%

Average Heat Fluxes: 378 to 25,971 Btu/(hr.-sq. ft.)

Twenty three runs (Run 104 through Run 126) were made with the small bend test section and nine runs (Run 204 through Run 212) were made with the large bend test section. The procedure used for conducting Runs 104 through 126 was to perform a series of runs where the inlet quality and mass velocity were kept constant while the heat flux was changed in steps until a dry patch was observed either in the bend or in the outlet leg. However, this was not always possible since the steam supply rate was governed by the system operating pressure and it would change within a series. Consequently the mass velocity and the inlet quality were coupled variables and not independent variables as required.

Runs 204 through 212 were replicates of runs made with the small bend test section where a dry patch had been observed. Once again due to loop limitations, some runs with the large bend did not duplicate the small bend runs at all.

For all runs, the local heat transfer coefficients were calculated and plotted as a function of the heated length. The local heat transfer coefficient for saturated vapor was also plotted on the same graph and a dry patch on the tube surface was assumed when the two phase heat

transfer coefficient was approximately equal to the saturated vapor heat transfer coefficient. The heat transfer coefficient was calculated by the following equation.

$$h_{tp} = \frac{q/A}{T_{wi} - T_{sat}} \quad (1)$$

The inside wall temperature was calculated via the conduction equation outlined in Appendix B. The saturation temperature was obtained by interpolating the recorded data for pressure and temperature. The heat flux value was obtained by making a heat balance on the inside node as outlined in Appendix B.

The hydrodynamic data obtained from Runs 104 through 126 and Runs 204 through 212 was reduced and plotted as a cross-hatched area on Figures 19 and 20, respectively. It can be seen from these figures that the runs covered essentially the same area where film inversion was observed in the visual tests.

The heat transfer data obtained from Runs 104 through 126 and Runs 204 through 212 was reduced and plotted on Figures 21 through 46 and Figures 47 through 55, respectively. The curves for the heat transfer coefficients are numbered from 1 through 5. These numbers correspond to the peripheral thermocouple locations shown in Figure 5. The heat transfer coefficients values for curves numbered 2, 3, and 4 are actually arithmetic mean values of the coefficients for peripheral locations 2 and 8, 3 and 7, and 4 and 6, respectively.

Small Bend Tests

Figure 21 shows a semi-annular type flow pattern where half the tube downstream of the bend is dry. The liquid film inverts from the

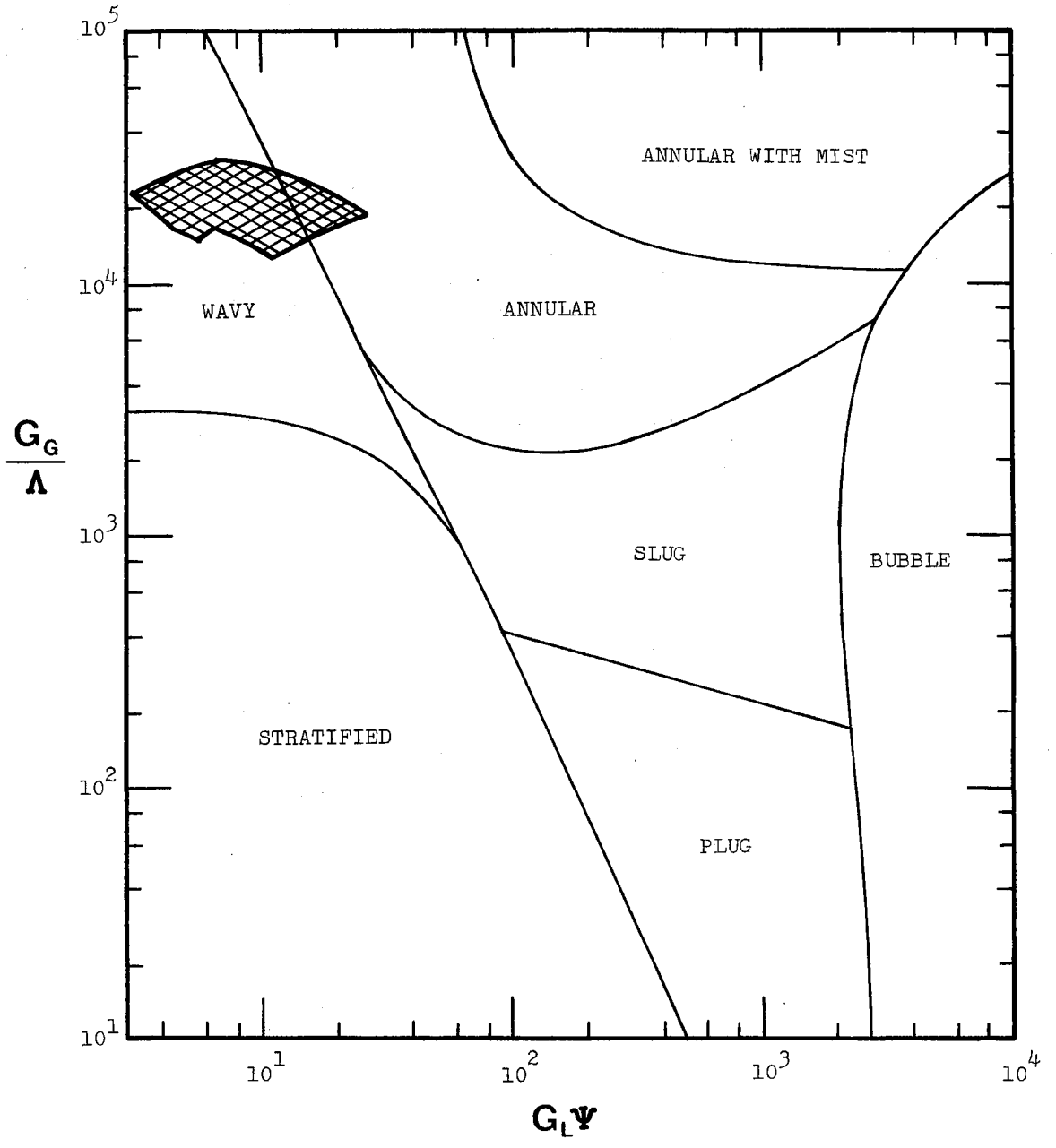

Figure 19. Steam-Water Runs on Modified Baker's Map, Small Bend

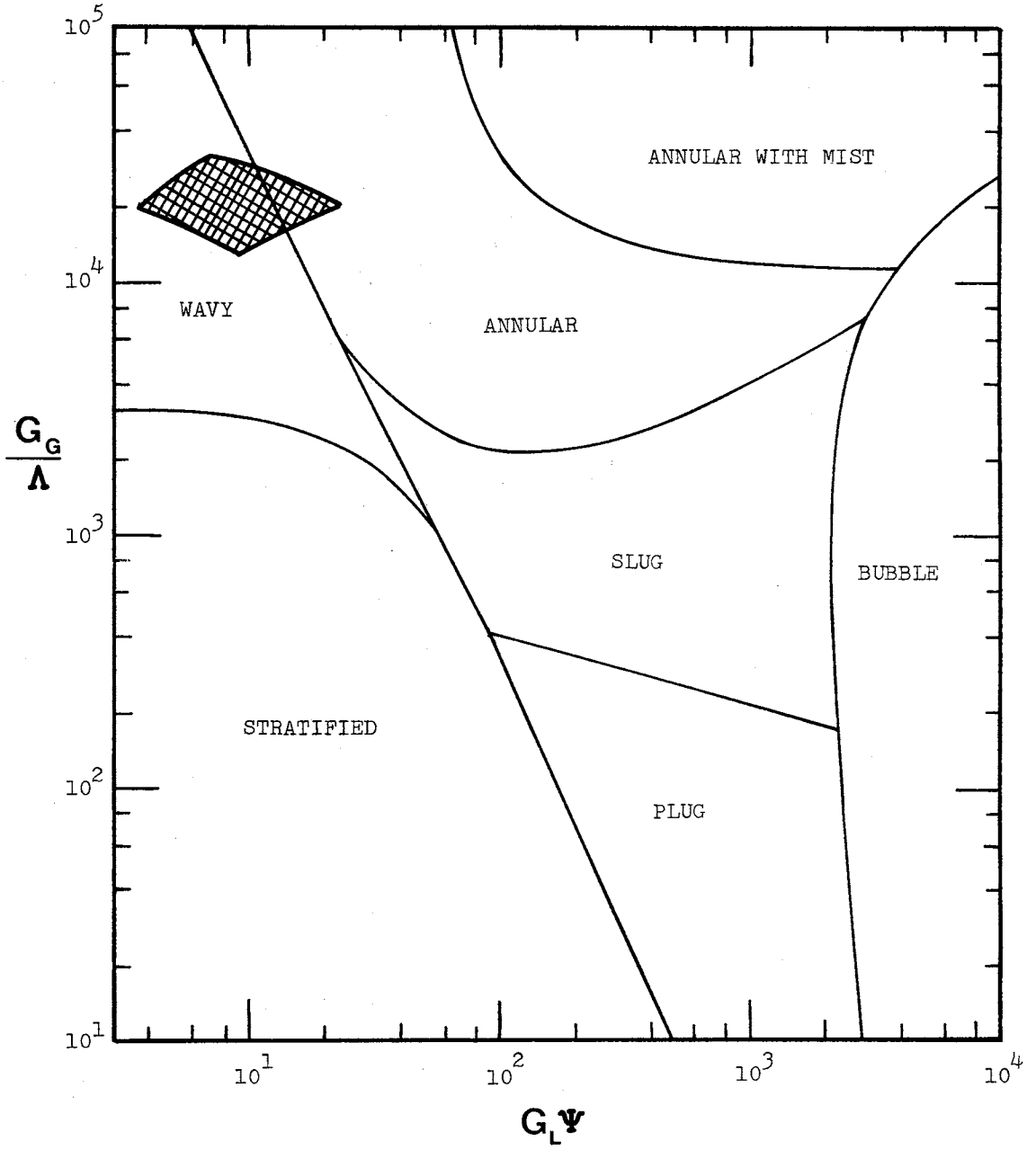

Figure 20. Steam-Water Runs on Modified Baker's Map, Large Bend

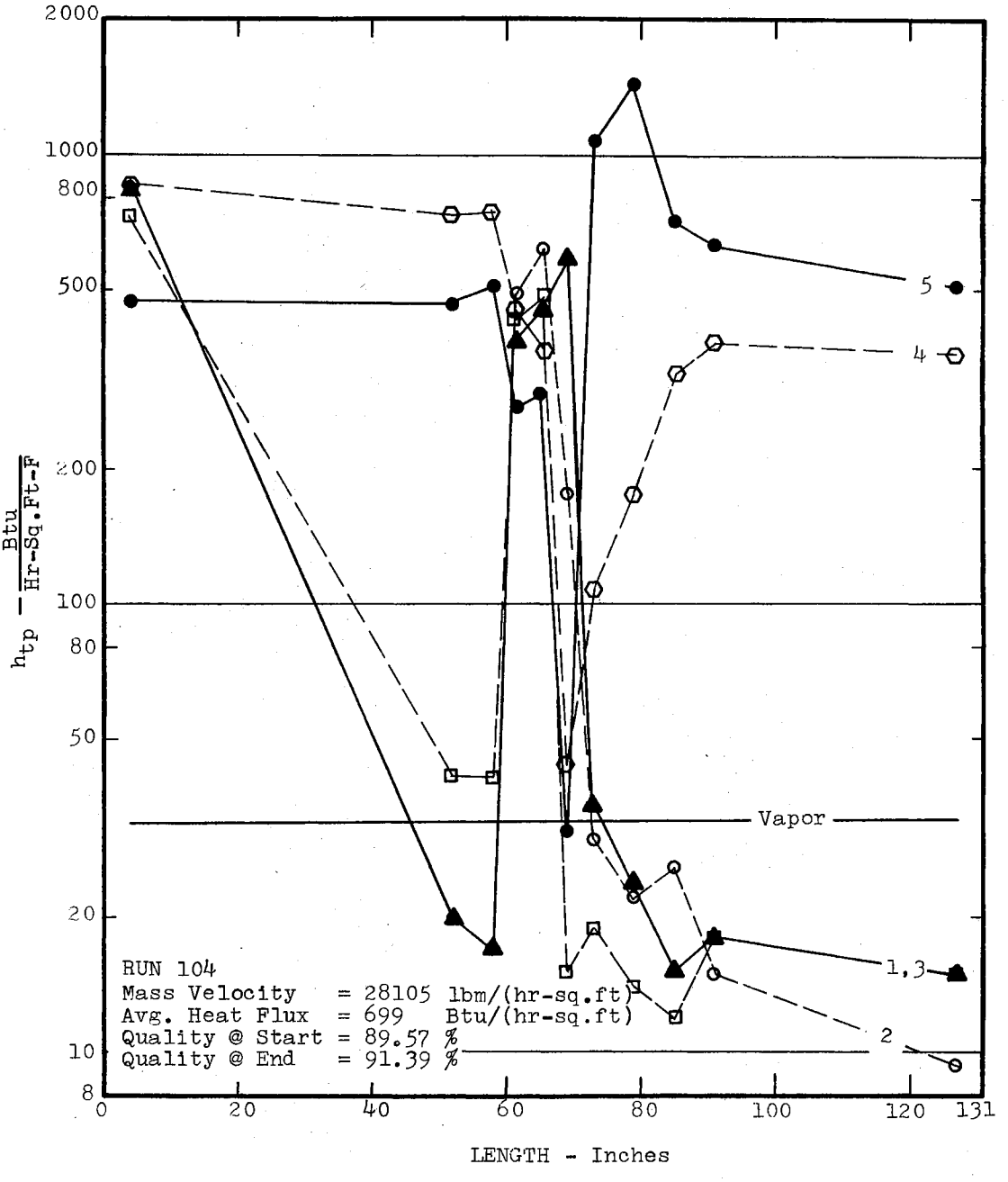

Figure 21. Heat Transfer Coefficients, Small Bend, Run 104

outside to the inside, midway in the bend. This is inferred by the fact that curve number 5 (outside wall) dips to the vapor curve at axial location 6 (L = 69.2 inches).

Data from Runs 105, 106 and 107 are plotted on Figures 22, 23 and 24, respectively. The heat transfer coefficient curves 3, 4, and 5 for Runs 105 and 106 exhibit a negative slope downstream of the bend whereas the curves for Run 107 exhibit a positive slope. The difference in slopes is probably due to the larger liquid inventory traveling at the bottom of the tube in Runs 105 and 106 than in 107. This observation can be substantiated by the fact that the heat transport mechanism across the laminar film is in the form of conduction heat transfer and the film temperature drop is directly proportional to the film thickness. Consequently, as the film thickness increases the heat transfer coefficient decreases.

Data from Run 108, shown in Figure 25, indicate the establishment of a dry patch, in the upper portion of the exit leg, that eventually disappears before the flow reaches the exit electrode.

Figure 26 reveals that a dry patch was established in the upper half of the tube downstream of the bend. Since the heat flux and the quality change were quite small, 378 Btu/(hr.-sq. ft.) and 0.8 percent, it is apparent that the dry patch was generated as an after-effect of the bend.

Figures 27 and 28 show data from Runs 110 and 111 where the inlet quality and mass velocity were kept constant while the heat flux was gradually increased. Figure 28 reveals the onset of a dry patch downstream of the bend and the re-establishment of wet conditions prior to end of heating.

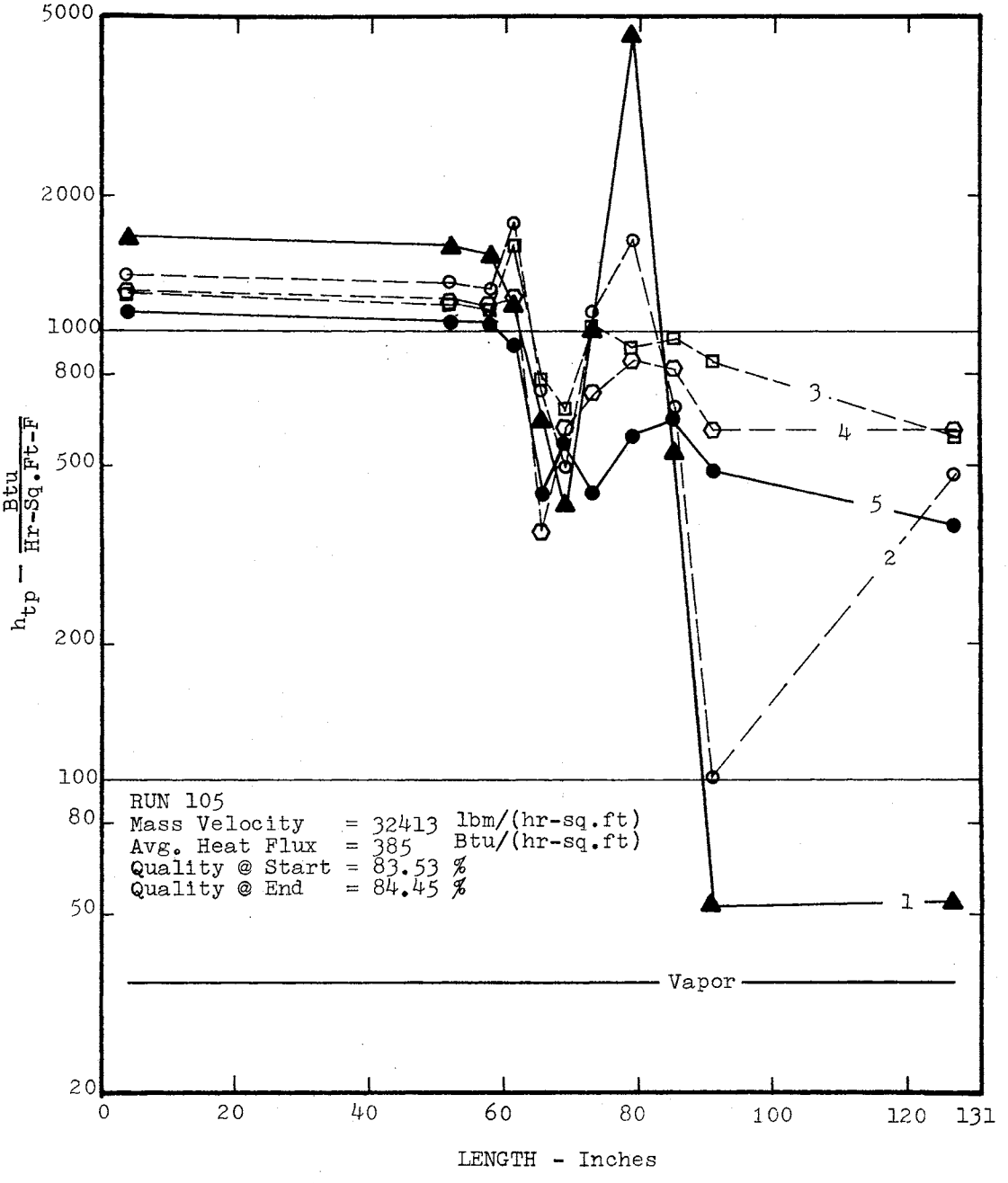

Figure 22. Heat Transfer Coefficients, Small Bend, Run 105

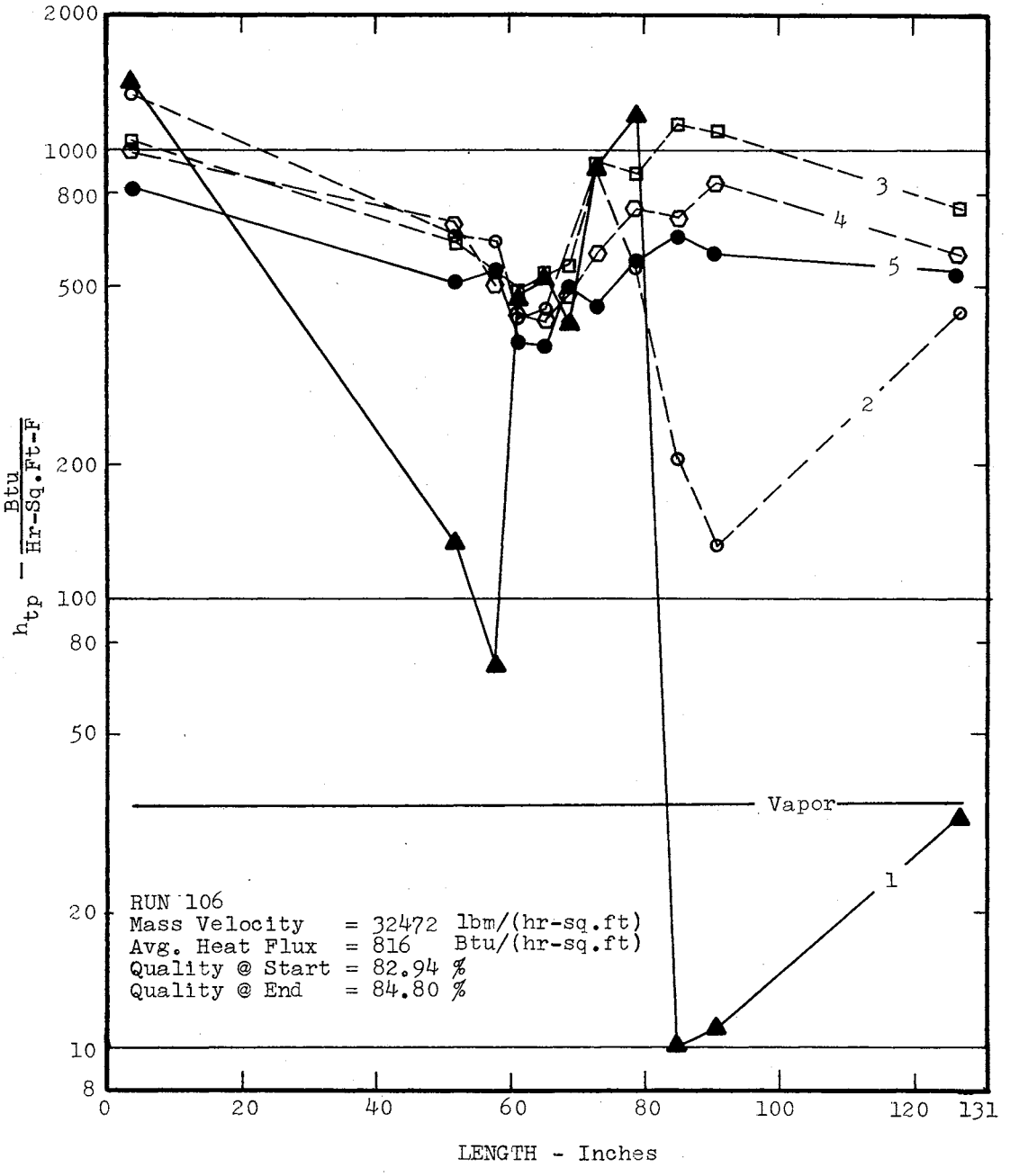

Figure 23. Heat Transfer Coefficients, Small Bend, Run 106

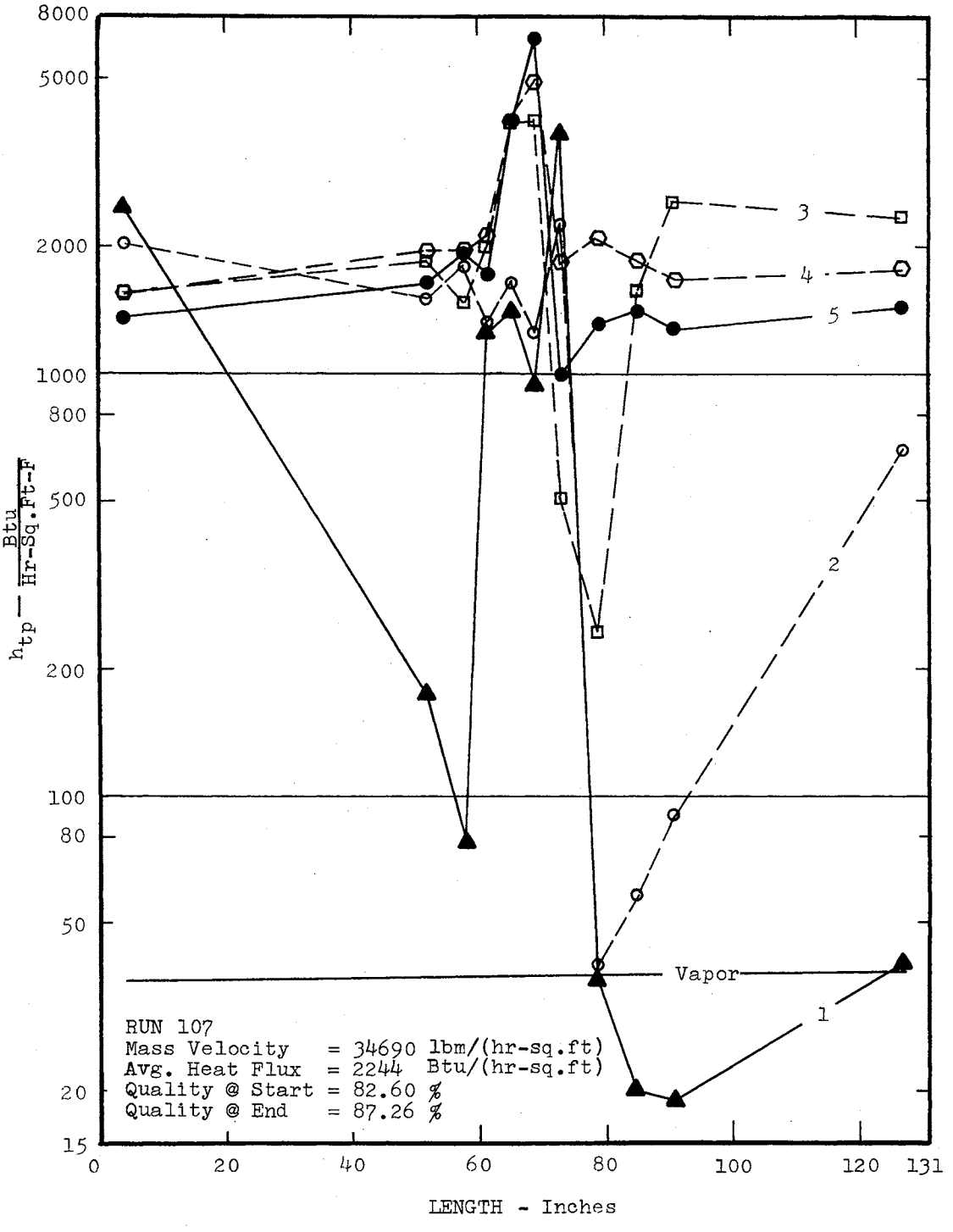

Figure 24. Heat Transfer Coefficients, Small Bend, Run 107

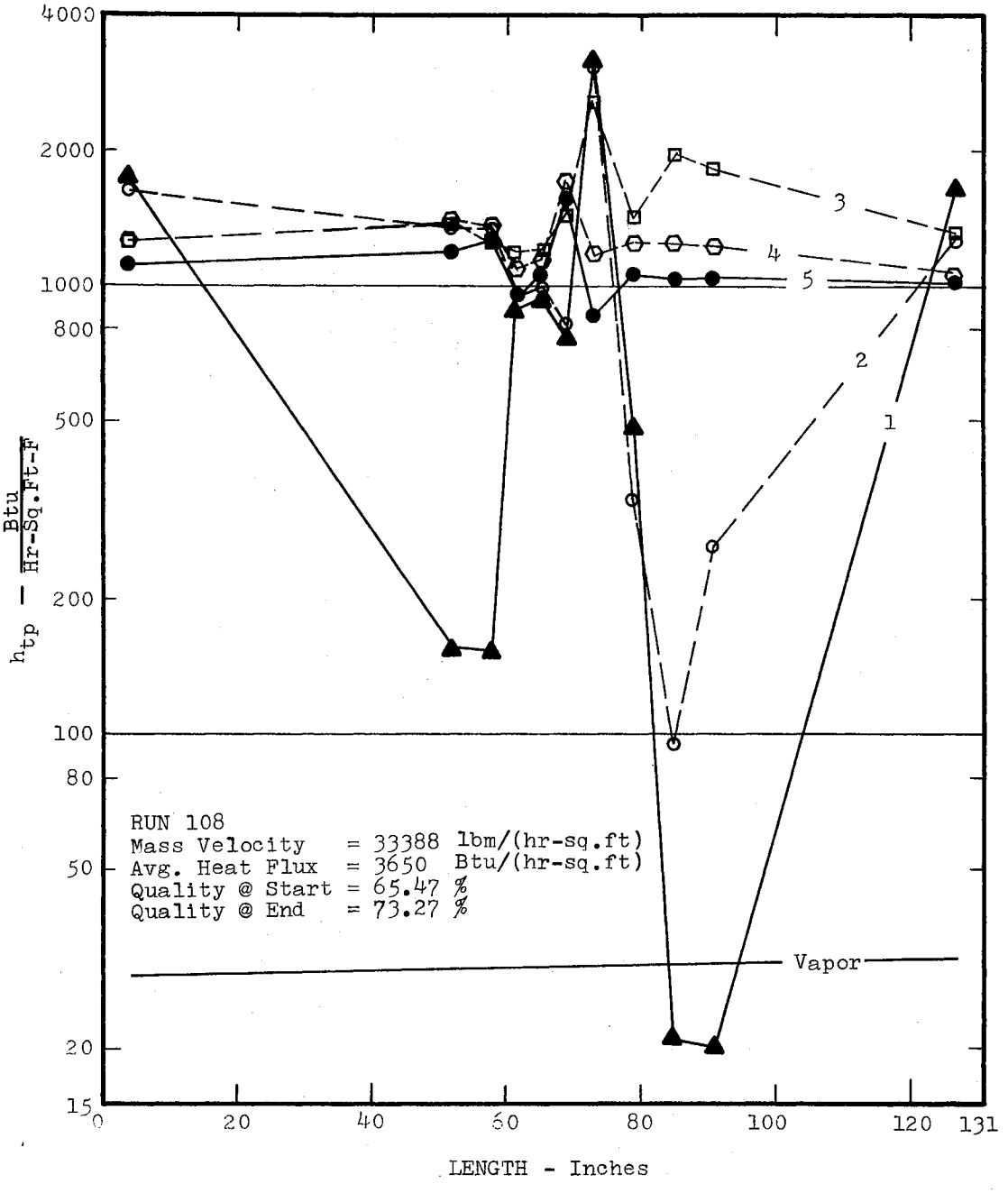

Figure 25. Heat Transfer Coefficients, Small Bend, Run 108

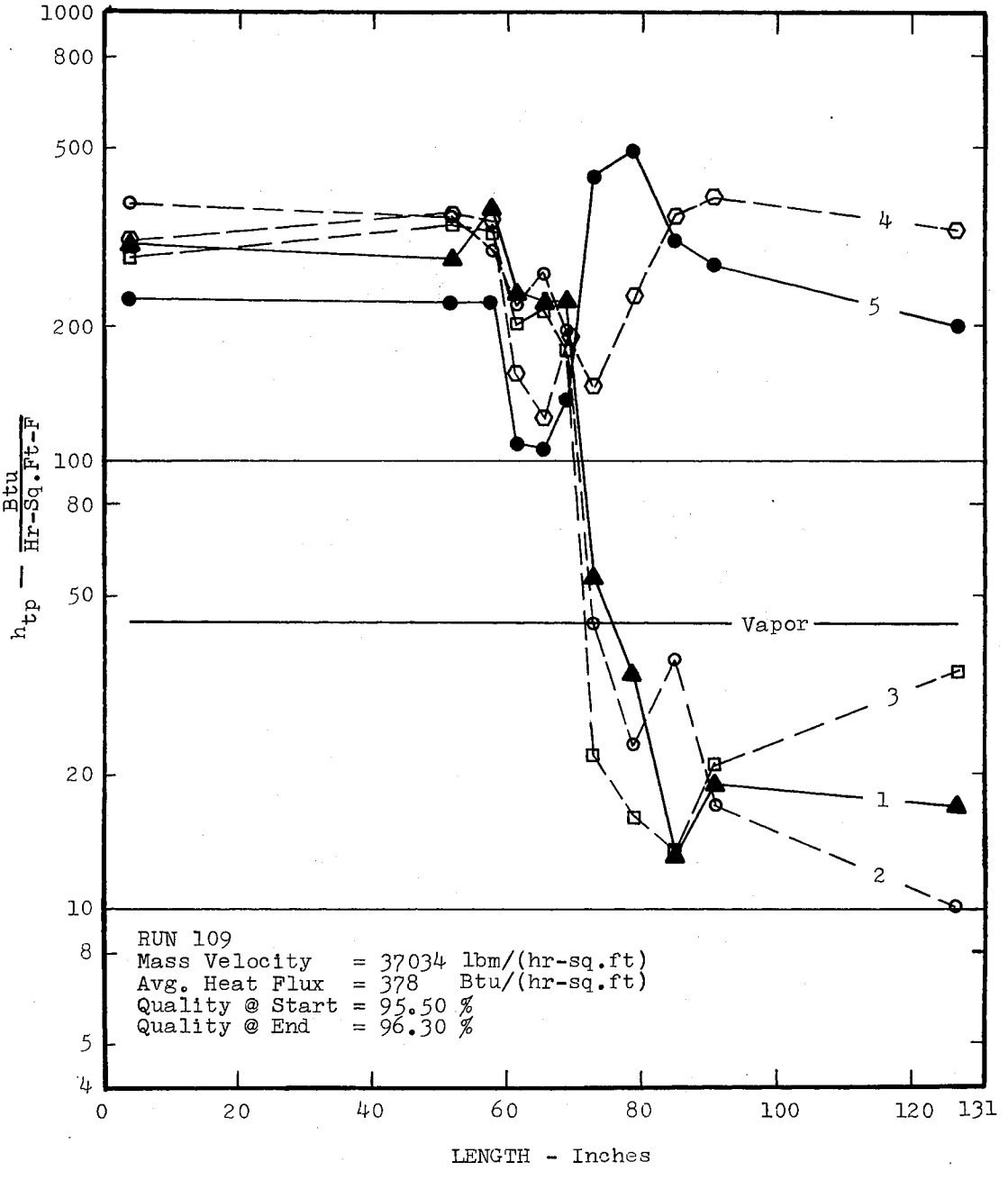

Figure 26. Heat Transfer Coefficients, Small Bend, Run 109

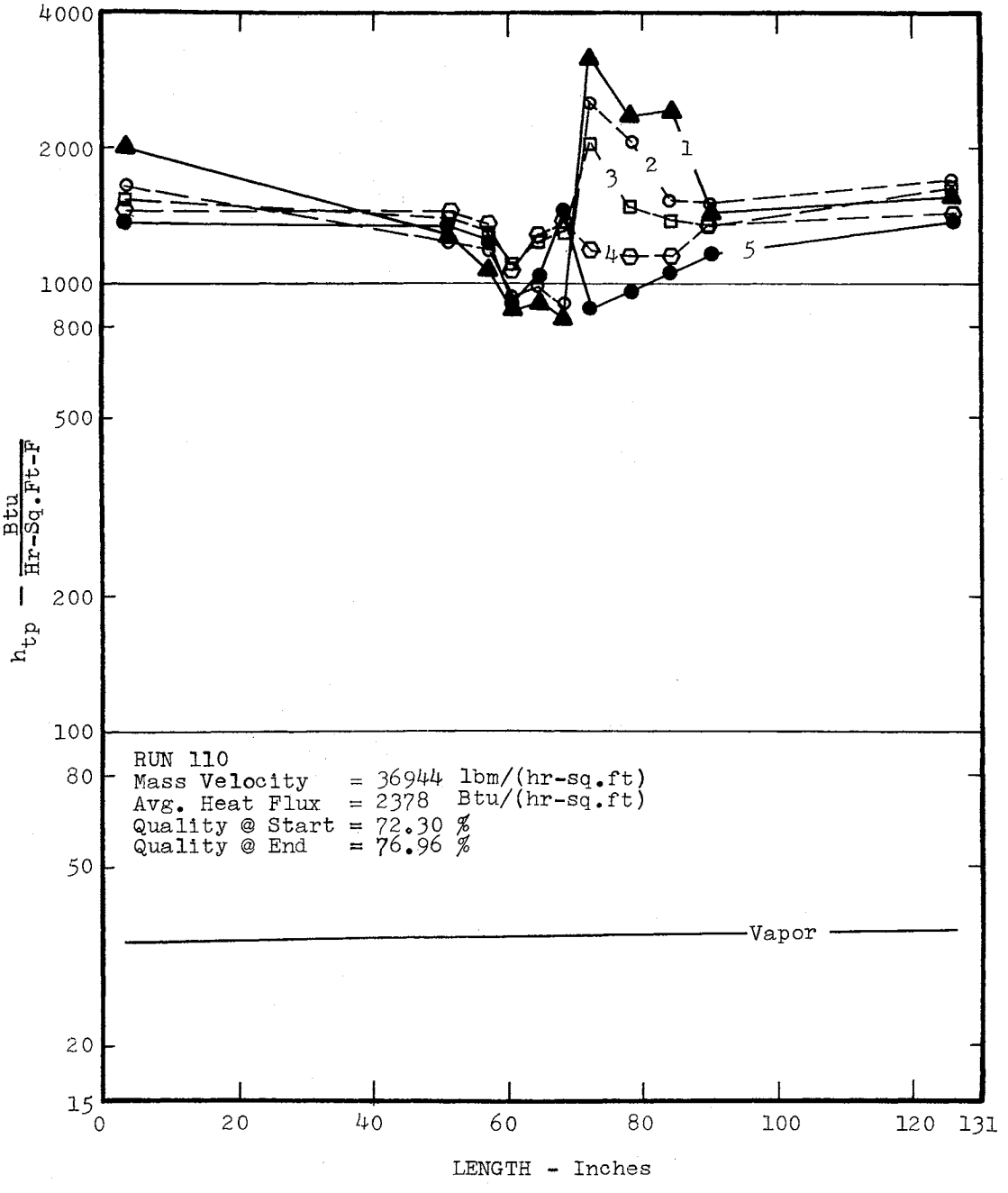

Figure 27. Heat Transfer Coefficients, Small Bend, Run 110

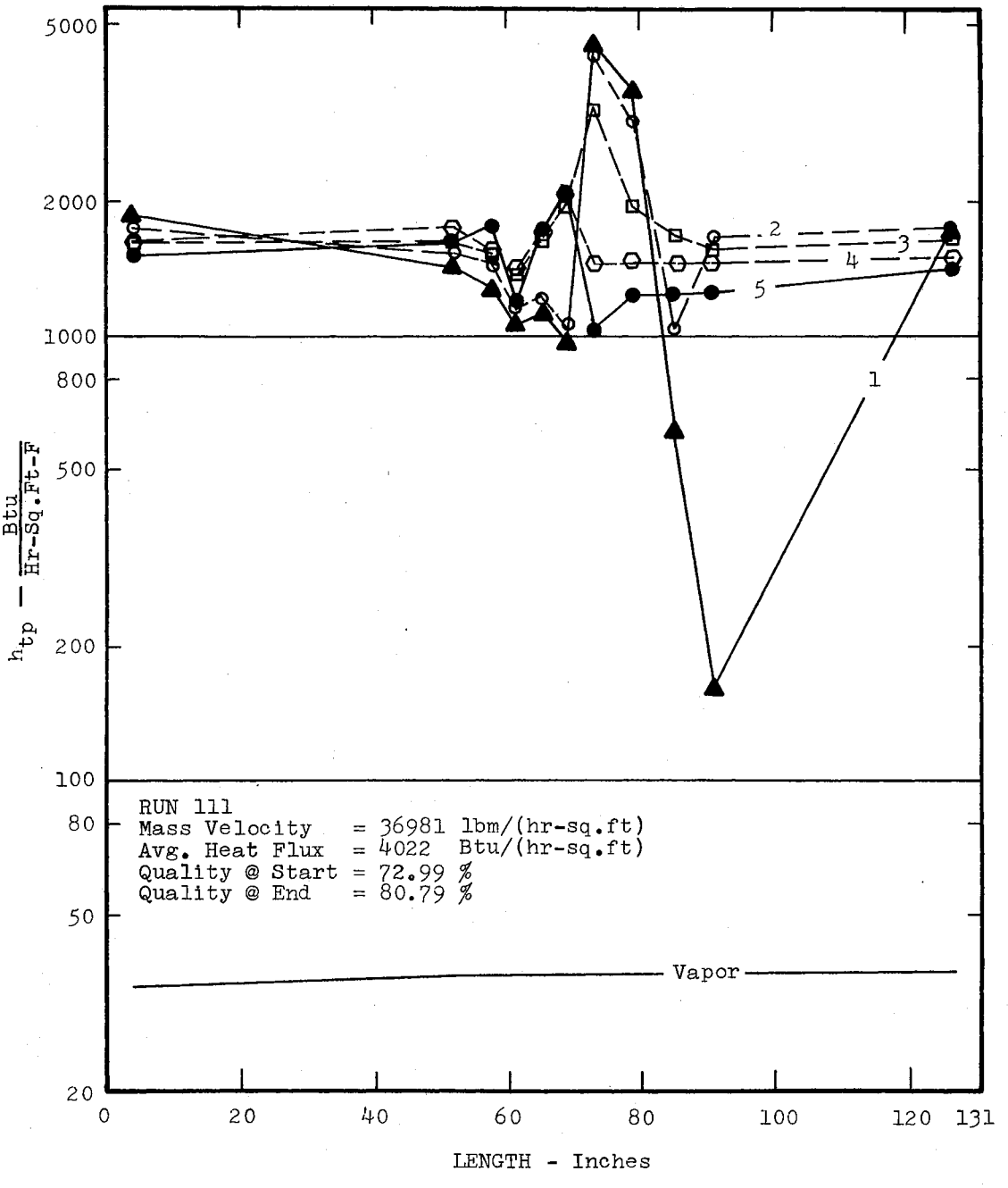

Figure 28. Heat Transfer Coefficients, Small Bend, Run 111

Data from Runs 112 and 113, shown in Figures 29 and 30, shows the onset of a dry patch and the establishment of a dry patch at axial location 9. The onset of a dry patch, shown in Figure 31, manifests itself in large amplitude wall temperature fluctuations due to intermittent wetting of the tube wall whereas an established dry patch, shown in Figure 32, is manifested in small amplitude wall temperature fluctuations due to occasional splatter of droplets on the wall and their subsequent evaporation.

The next series of runs was Runs 114, 115 and 116. The difficulty in maintaining a fixed mass velocity and inlet quality is noticeable in this series. Figures 33, 34 and 35 show the presence of a dry patch downstream of the bend.

Data from Runs 117 through 120, plotted on Figures 36 through 39, show the next series of runs where a dry patch was obtained for a "fixed" mass velocity and inlet quality and an increasing heat flux.

Figure 40 reveals that the liquid film becomes asymmetric with respect to the horizontal plane when a two phase mixture flows through a bend.

Data from Runs 122 and 123, plotted on Figures 41 and 42 indicates once again the onset and presence of a dry patch. The high heat transfer coefficients realized downstream of the bend are typical of thin liquid films evaporating rapidly prior to dryout. Collier (17) has noted that heat transfer coefficients up to 35,000 Btu/(hr.-sq. ft.-°F) have been reported for water evaporating from thin liquid films.

Figure 43 shows the data plotted for Run 124 and Figure 44 indicates the large amplitude wall temperature oscillations associated with the onset of dryout.

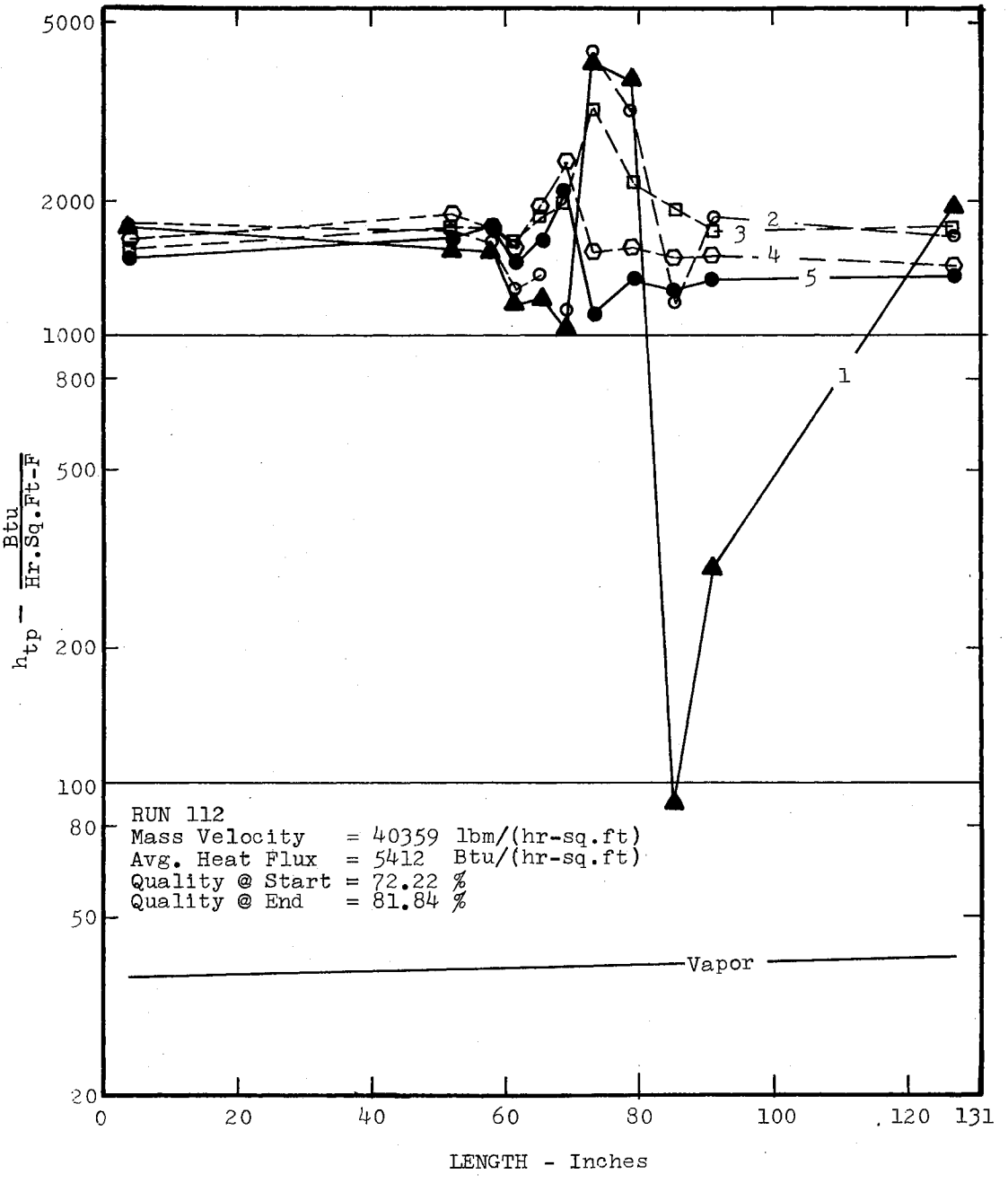

Figure 29. Heat Transfer Coefficients, Small Bend, Run 112

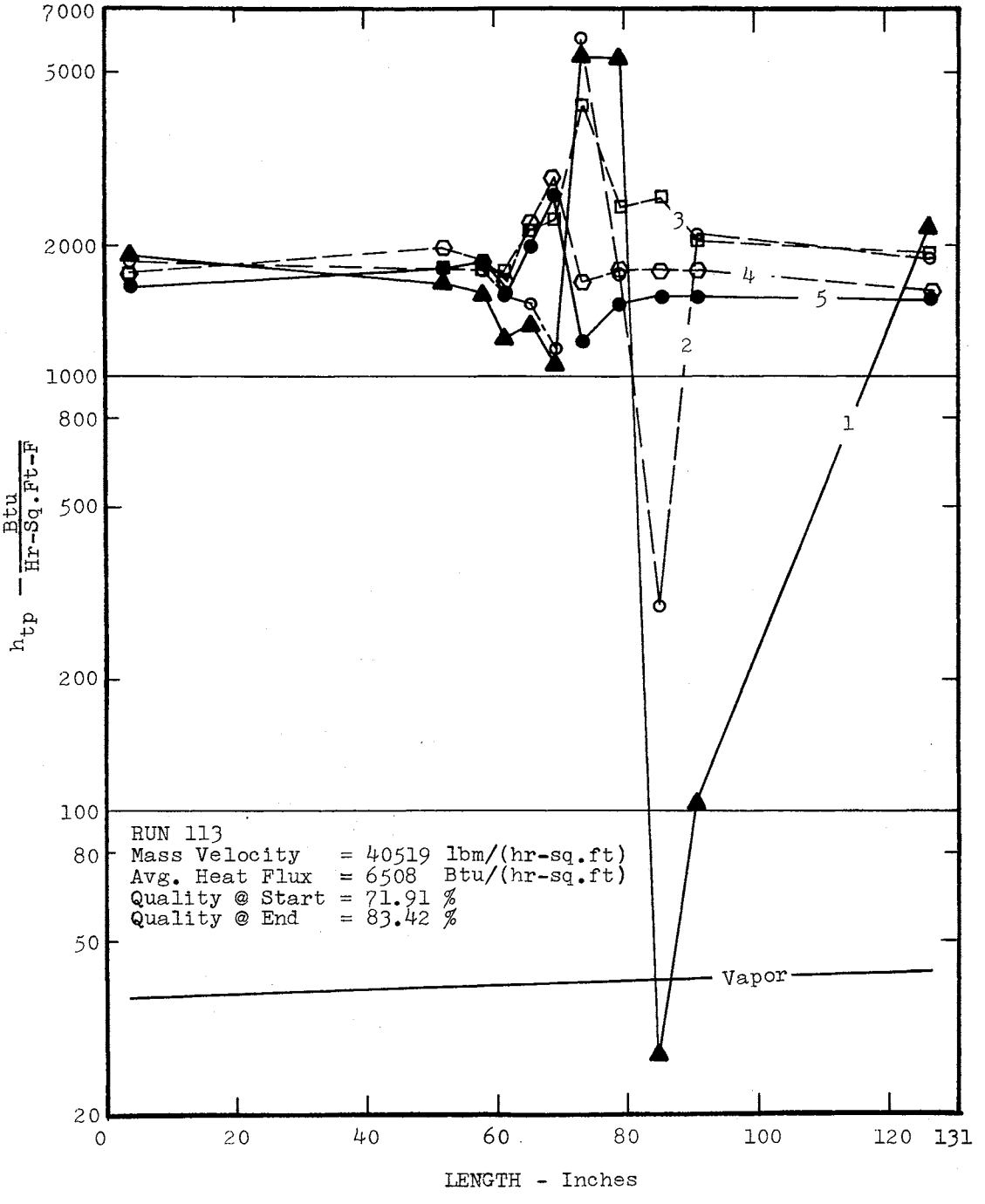

Figure 30. Heat Transfer Coefficients, Small Bend, Run 113

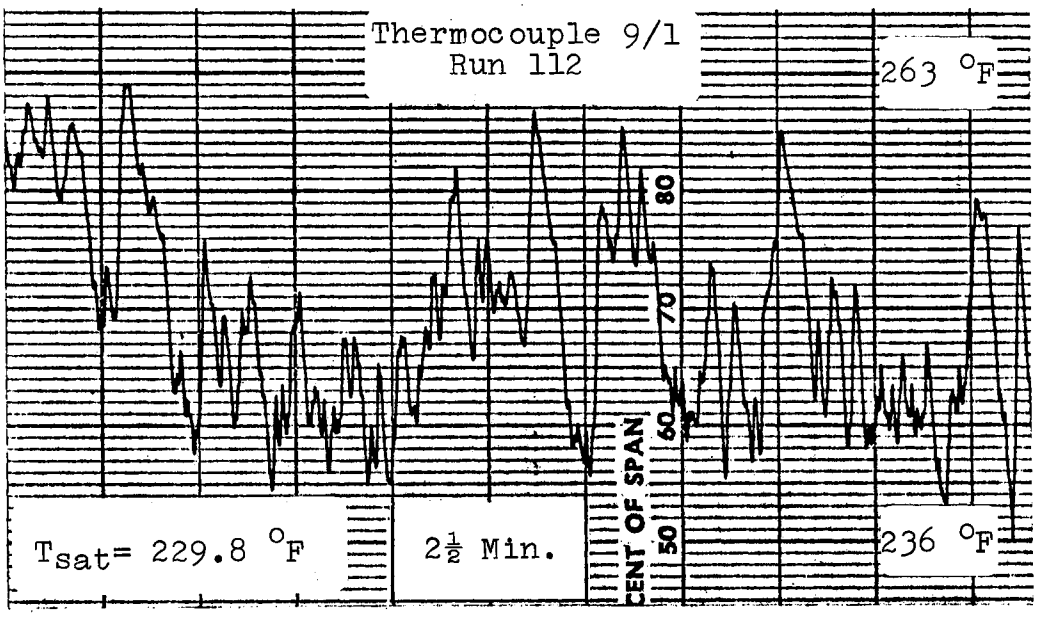

Figure 31. Temperature Trace Showing the Onset of a Dry Patch, Run 112

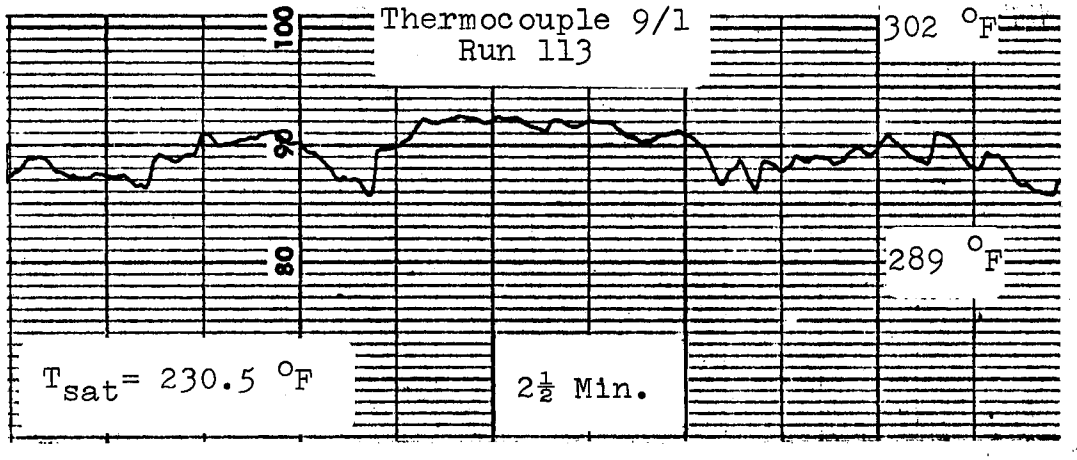

Figure 32. Temperature Trace of an Established Dry Patch, Run 113

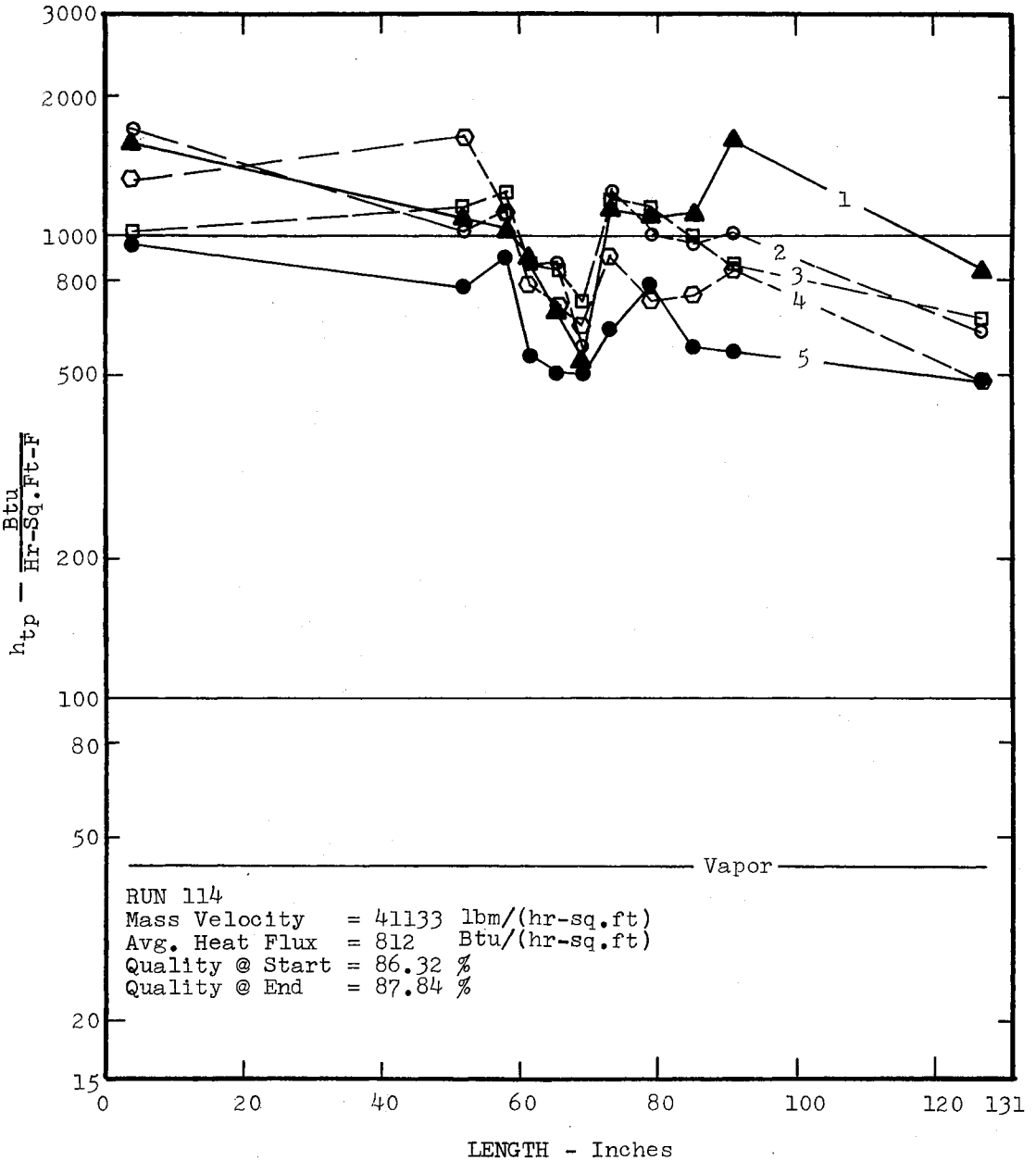

Figure 33. Heat Transfer Coefficients, Small Bend, Run 114

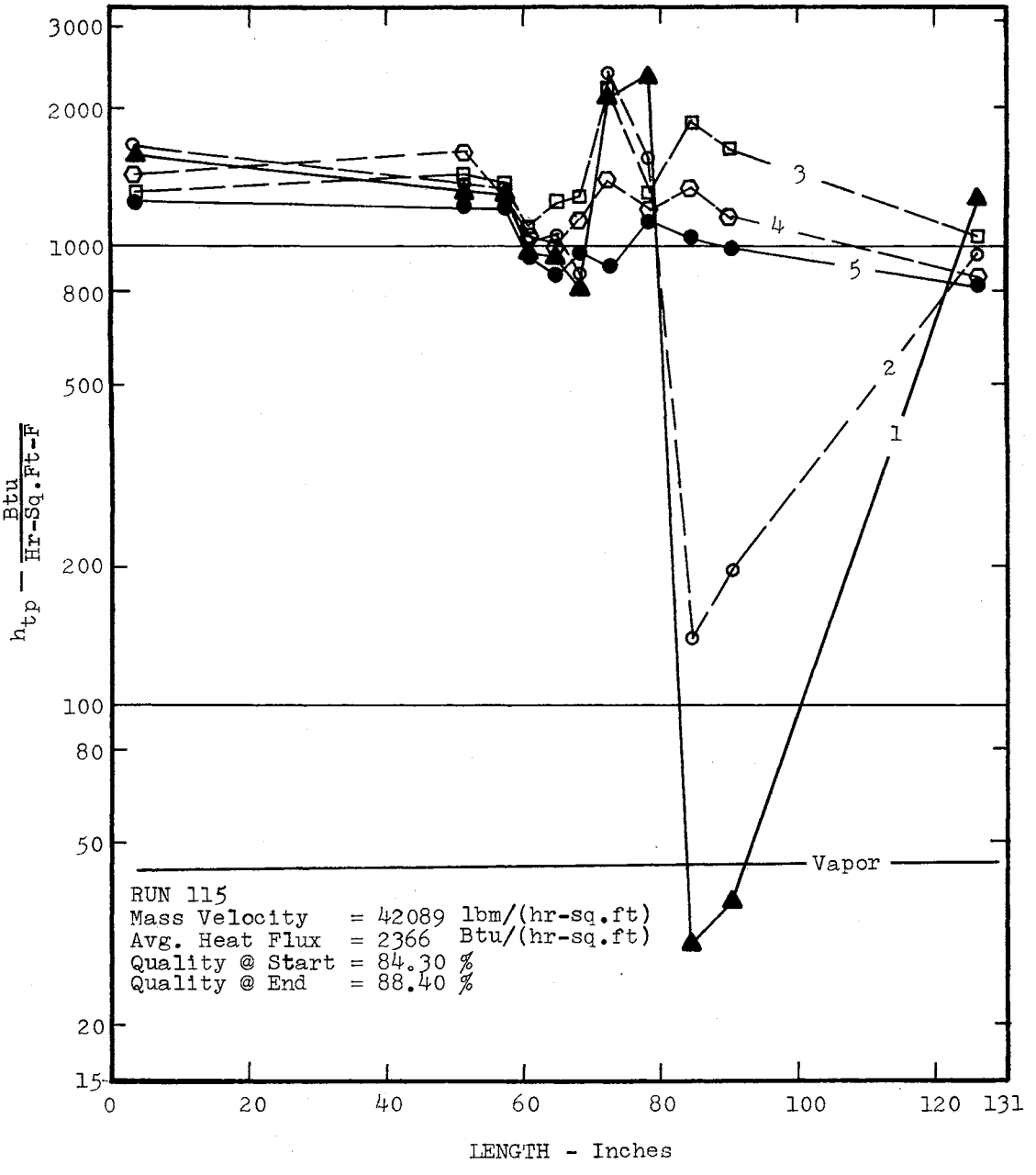

Figure 34. Heat Transfer Coefficients, Small Bend, Run 115

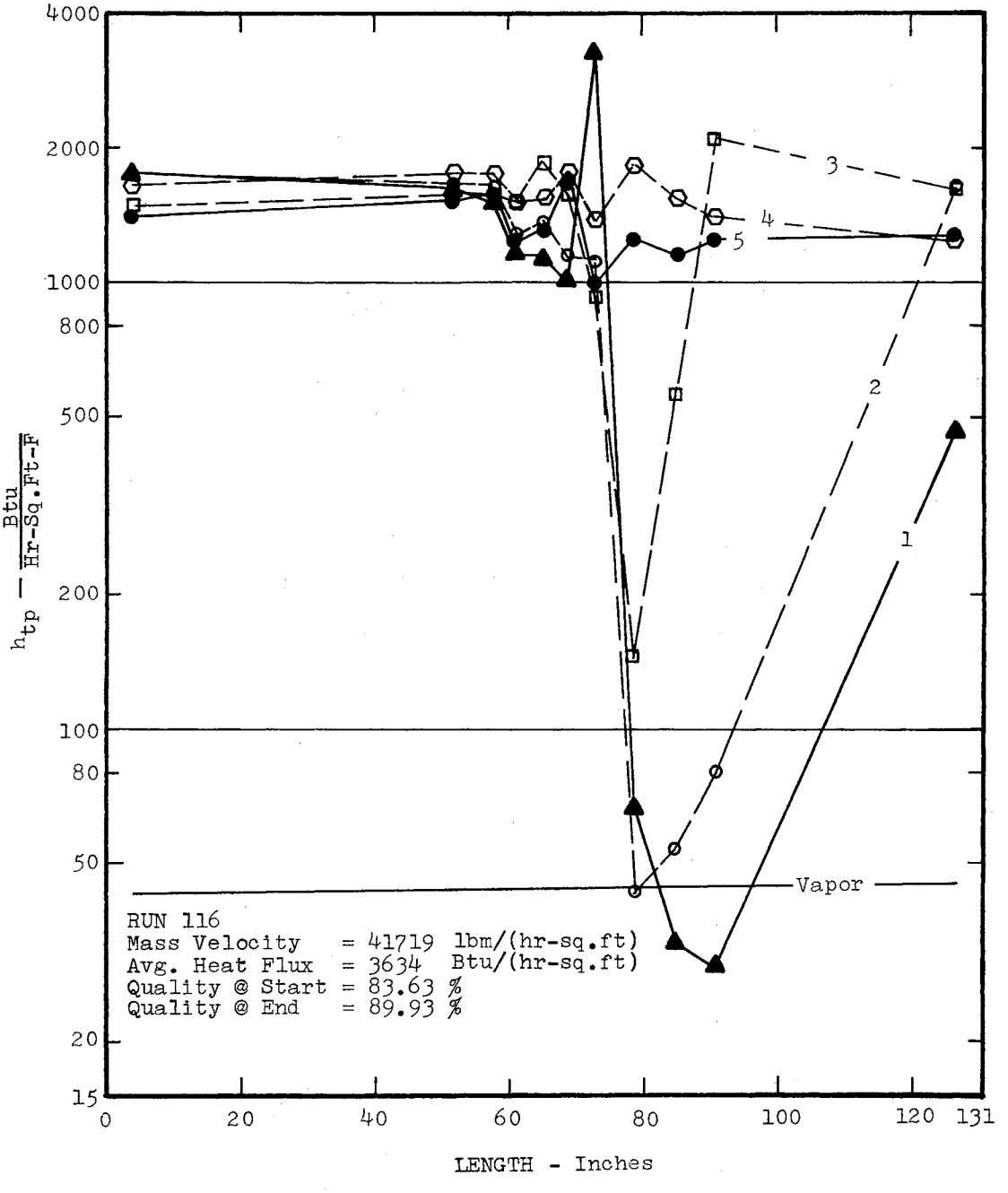

Figure 35. Heat Transfer Coefficients, Small Bend, Run 116

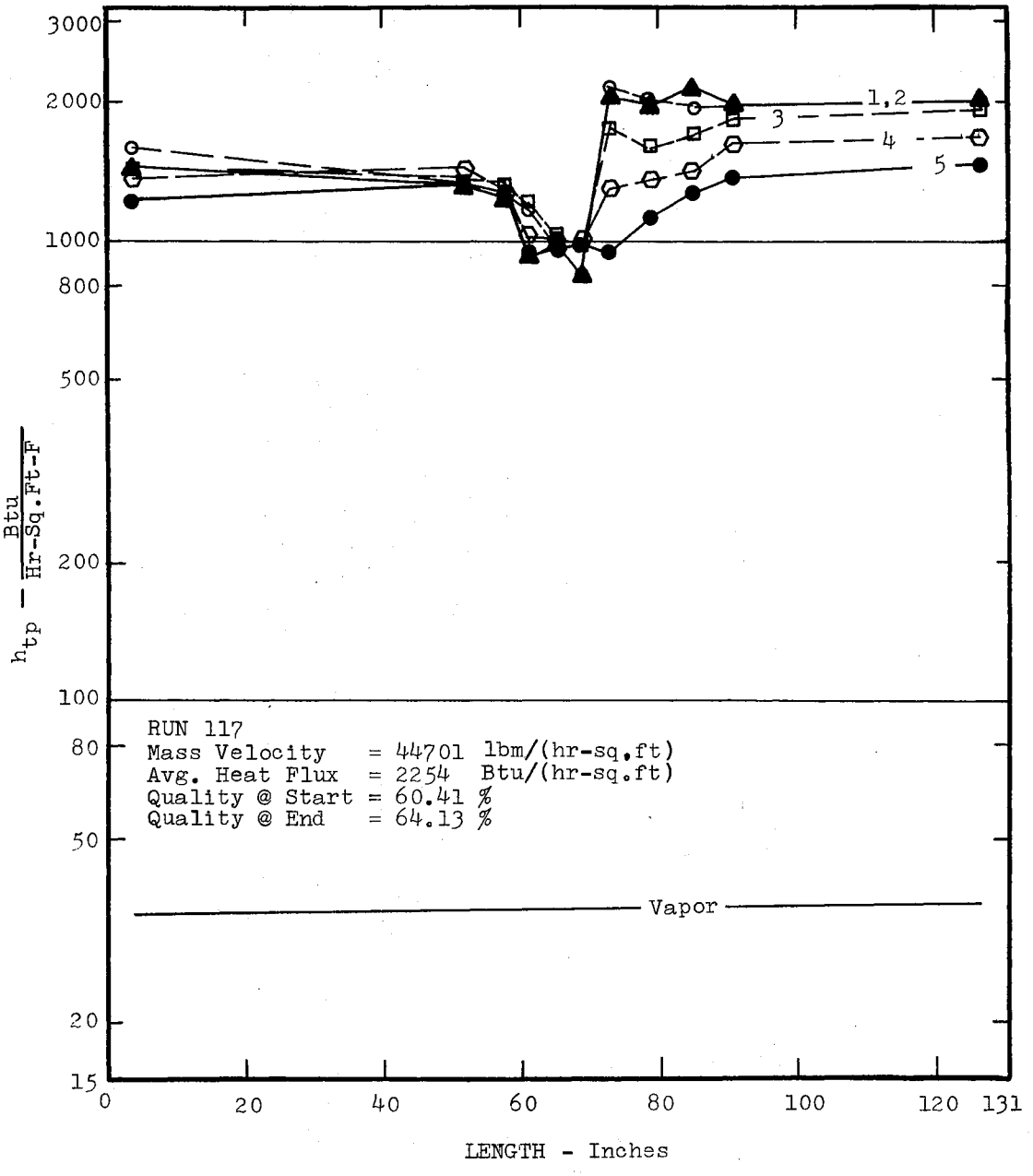

Figure 36. Heat Transfer Coefficients, Small Bend
Run 117

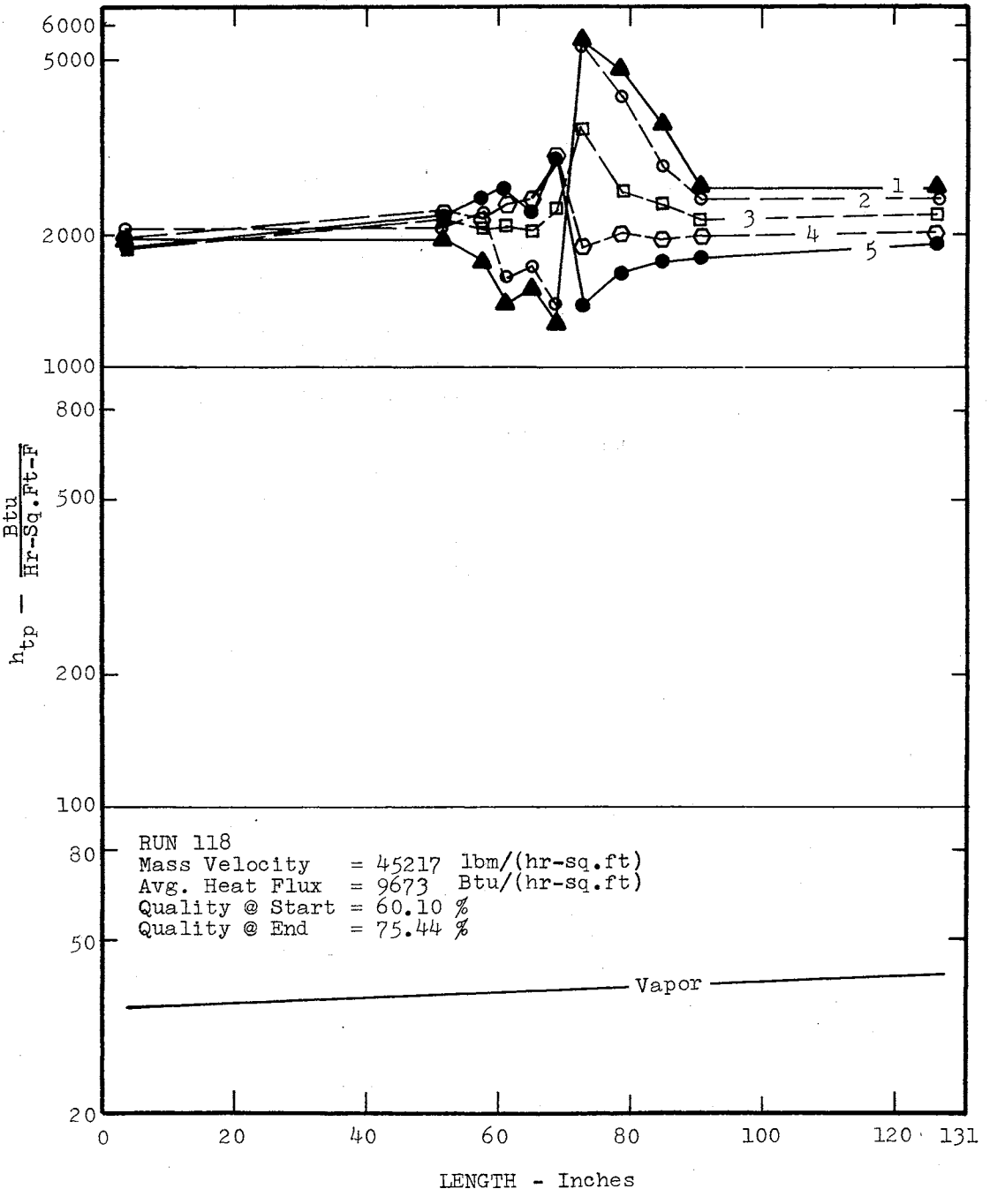

Figure 37. Heat Transfer Coefficients, Small Bend, Run 118

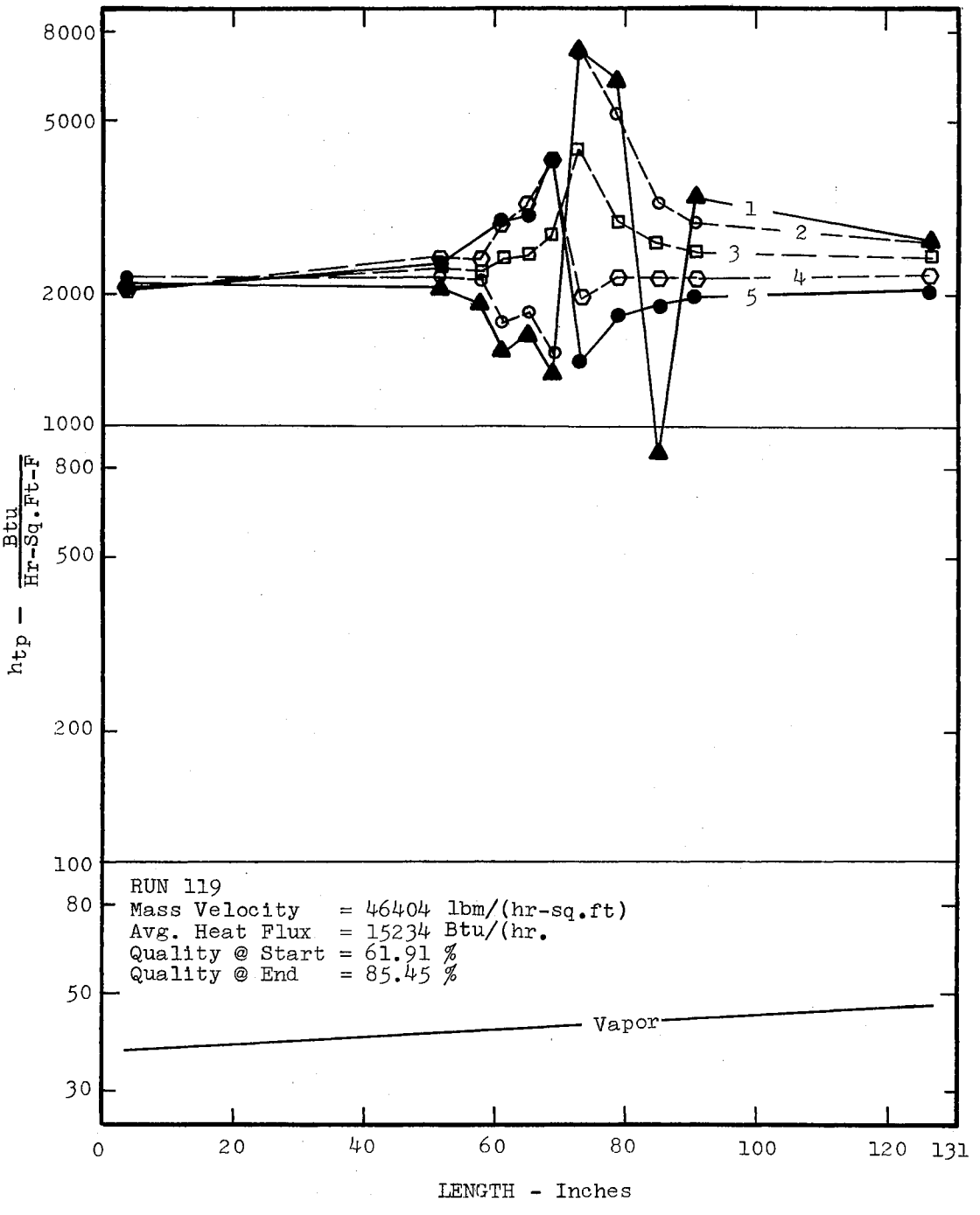

Figure 38. Heat Transfer Coefficients, Small Bend, Run 119

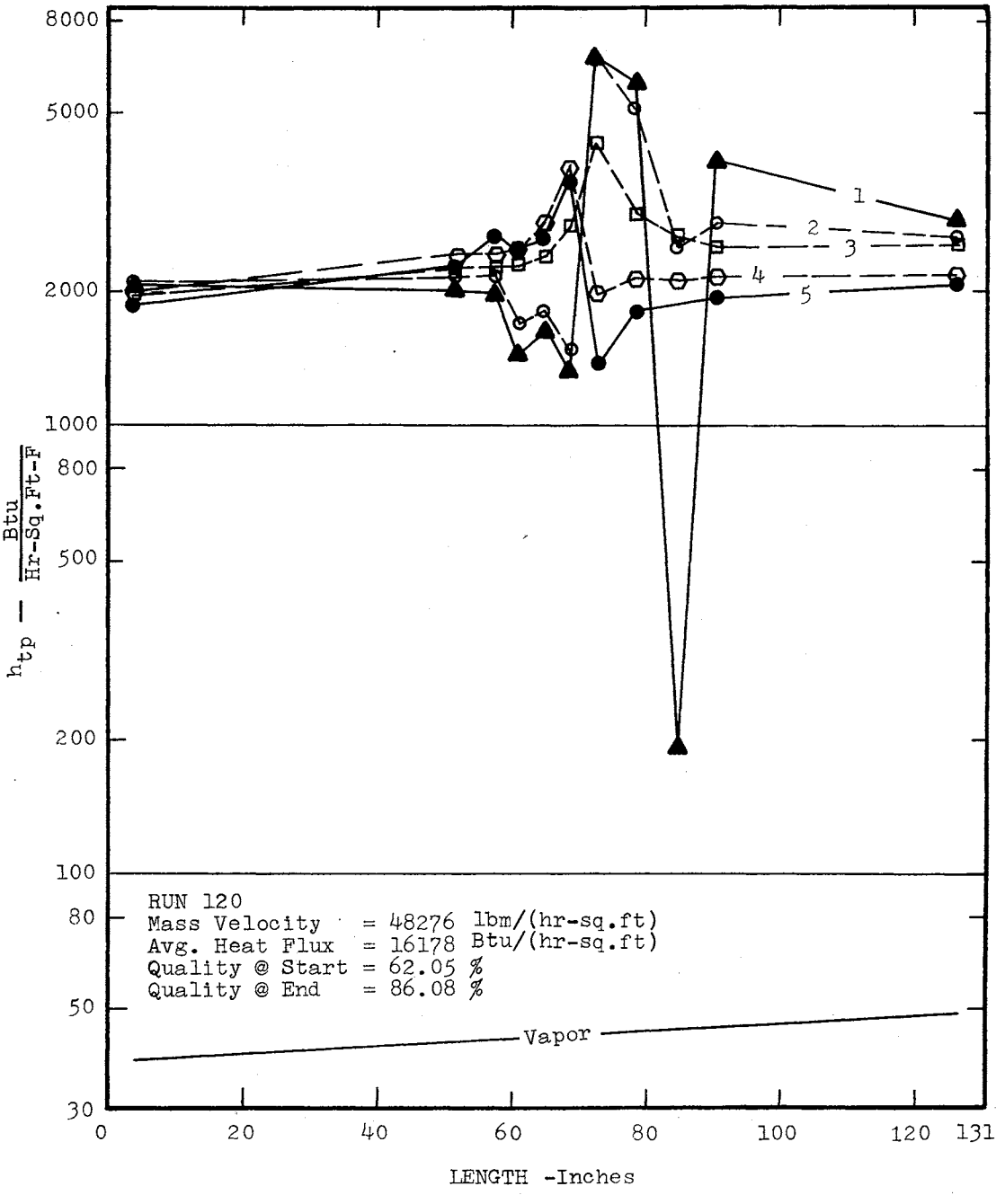

Figure 39. Heat Transfer Coefficients, Small Bend, Run 120

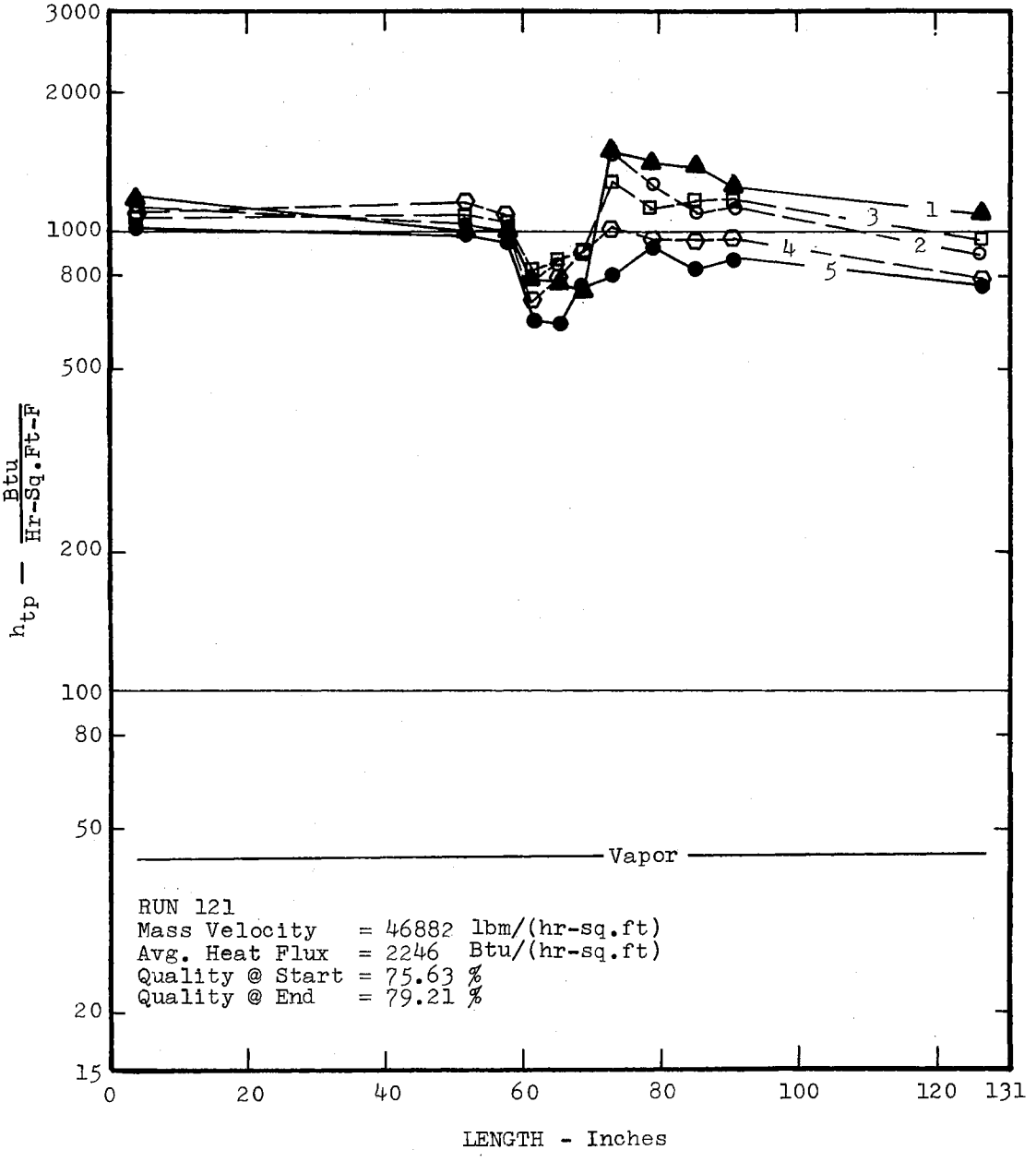

Figure 40. Heat Transfer Coefficients, Small Bend, Run 121

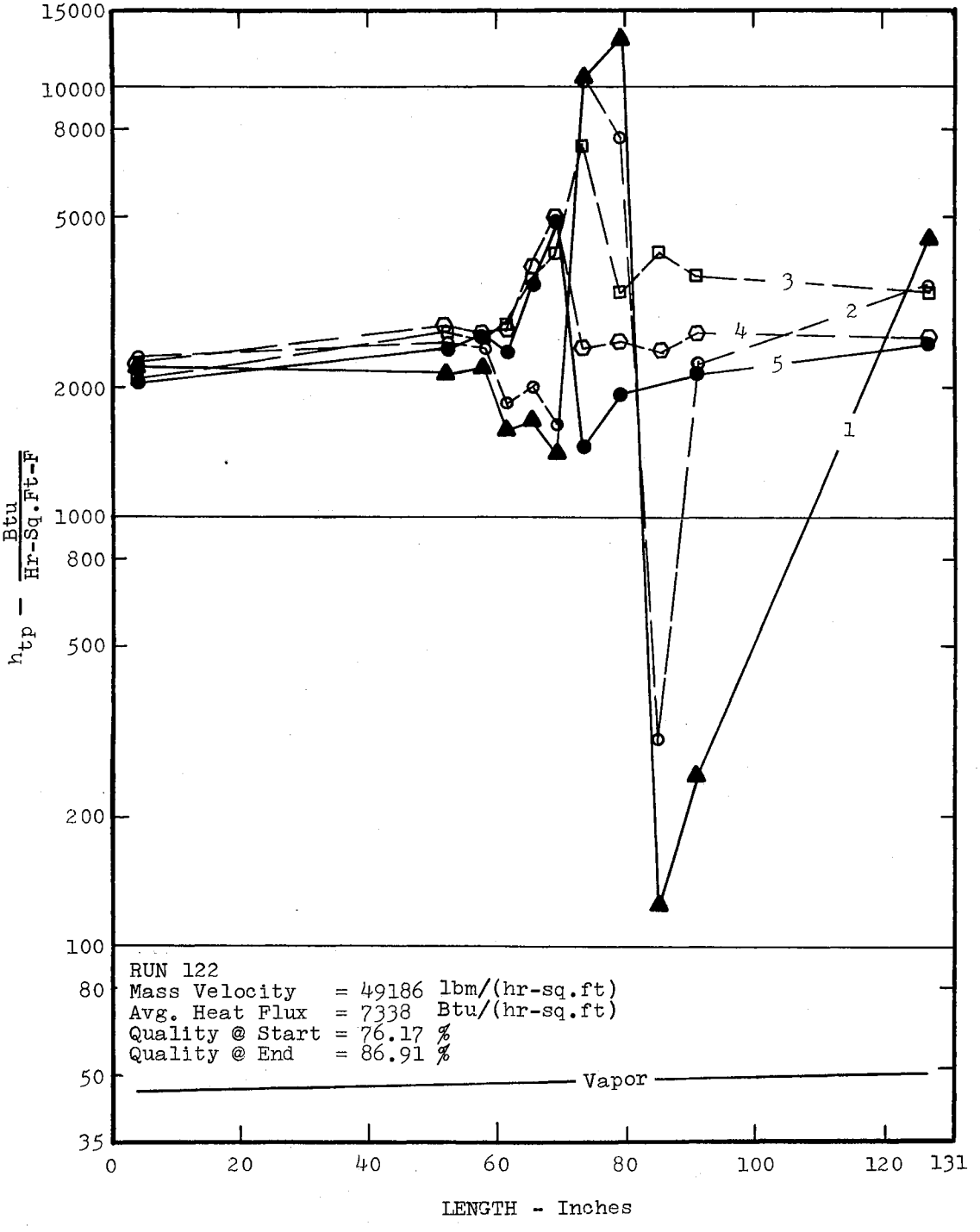

Figure 41. Heat Transfer Coefficients, Small Bend, Run 122

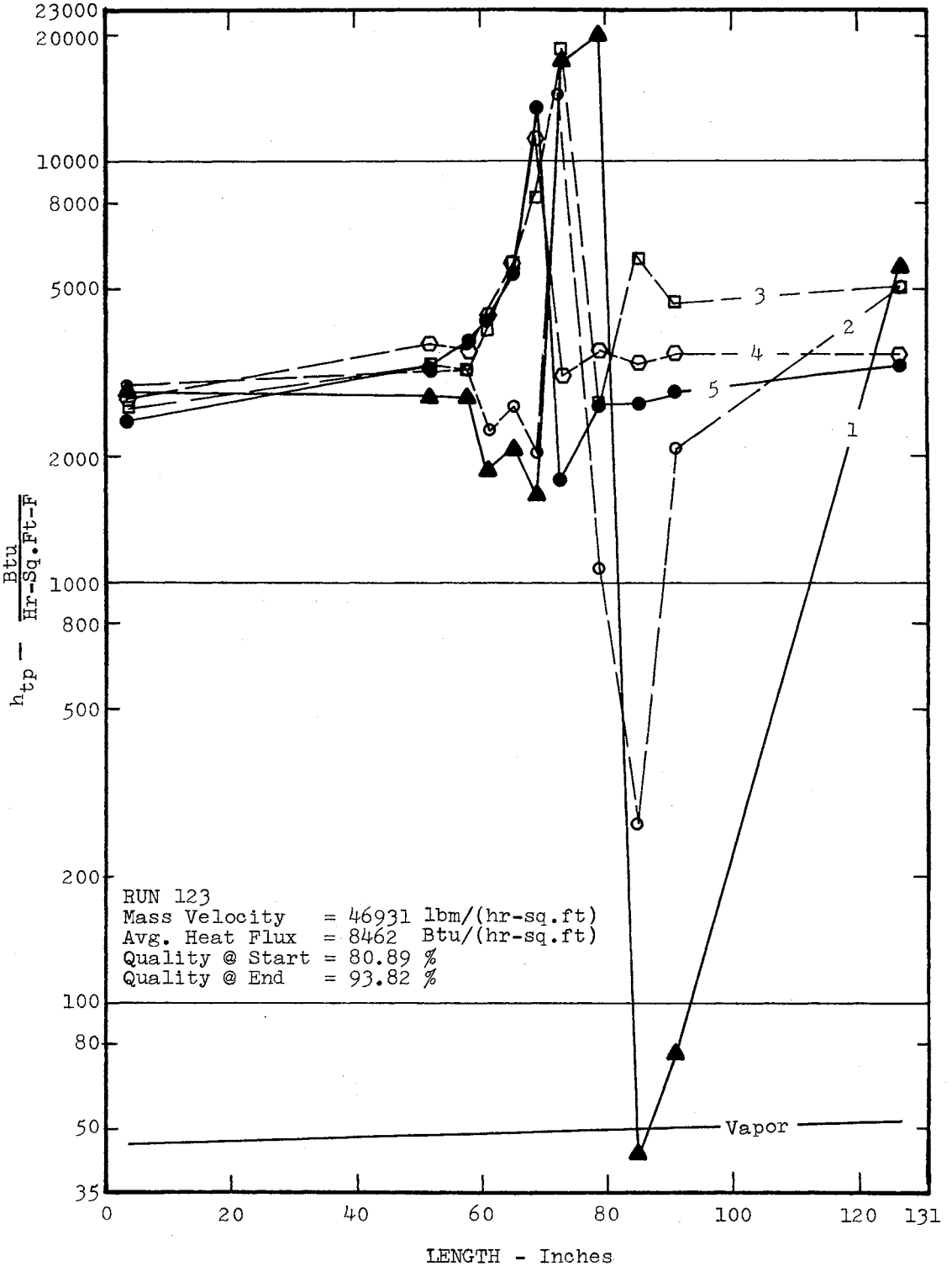

Figure 42. Heat Transfer Coefficients, Small Bend, Run 123

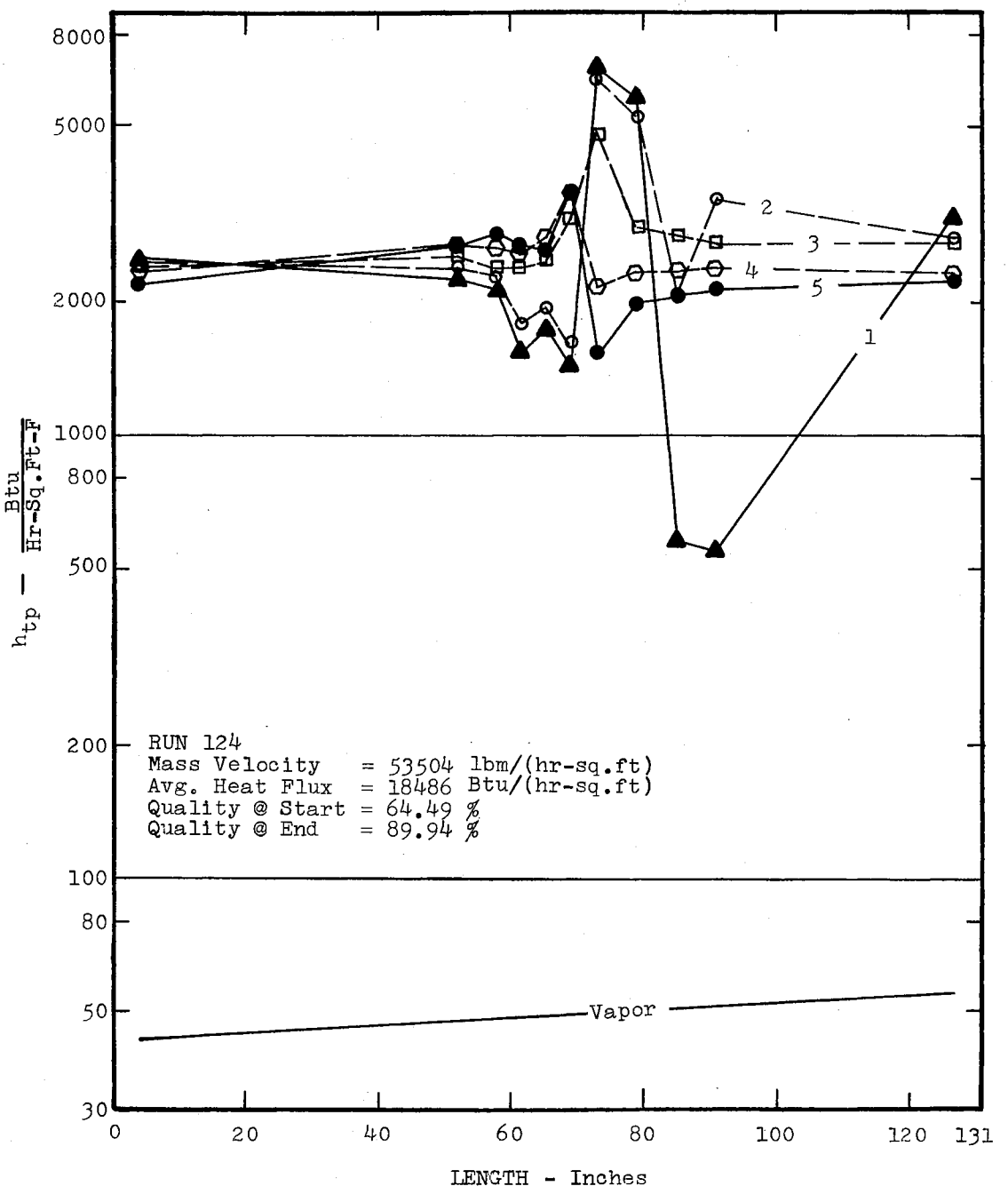

Figure 43. Heat Transfer Coefficients, Small Bend, Run 124

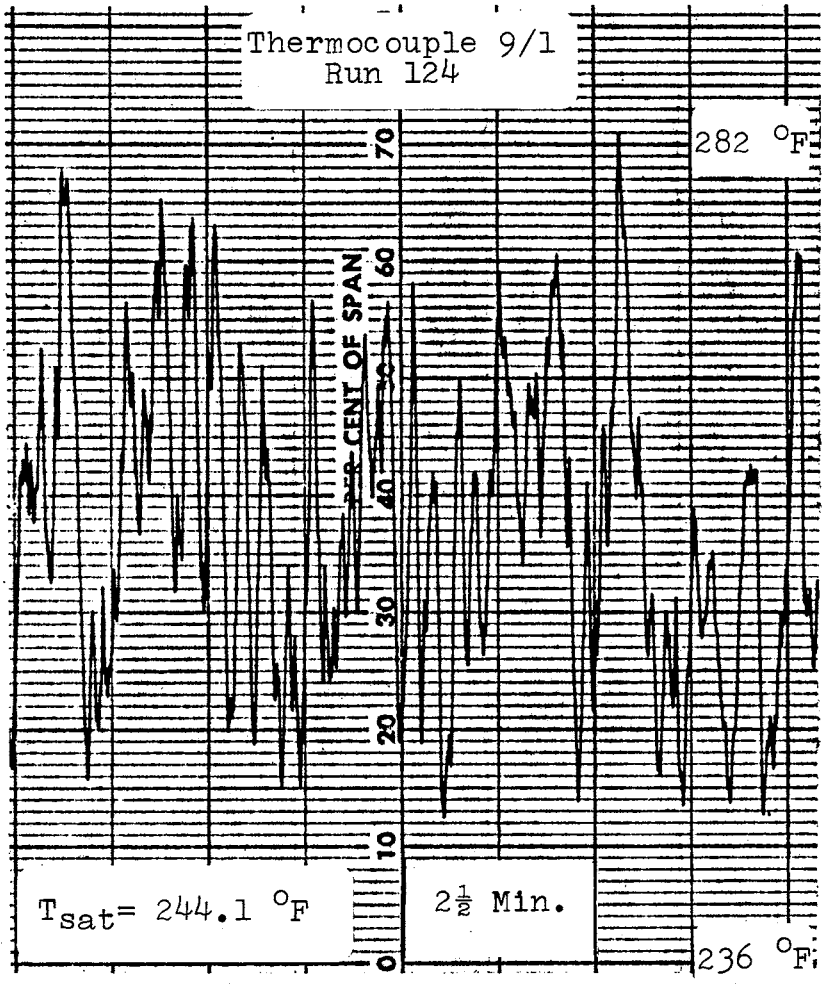

Figure 44. Temperature Trace Showing the Onset of a Dry Patch, Run 124

Figures 45 and 46 reveal that the mean heat transfer coefficient is enhanced when a two phase mixture flows through a 180° bend and no dry patches are created downstream of the bend.

Large Bend Tests

The heat transfer coefficients obtained from Runs 204 through 212 are plotted on Figures 47 through 55. The large bend runs were supposed to be replicates of some small bend runs. However, this was not possible in each case, due to the loop incapabilities mentioned earlier. The table below indicates the runs that were replicates.

TABLE III

REPLICATE RUNS WITH LARGE BENDS

Small Bend		Large Bend	
Figure	Run	Figure	Run
24	107	48	205
30	113	50	207
35	116	51	208
39	120	52	209
41	122	53	210
43	124	54	211
46	126	55	212

Tabulated results of all the steam-water runs are given in Table IV.

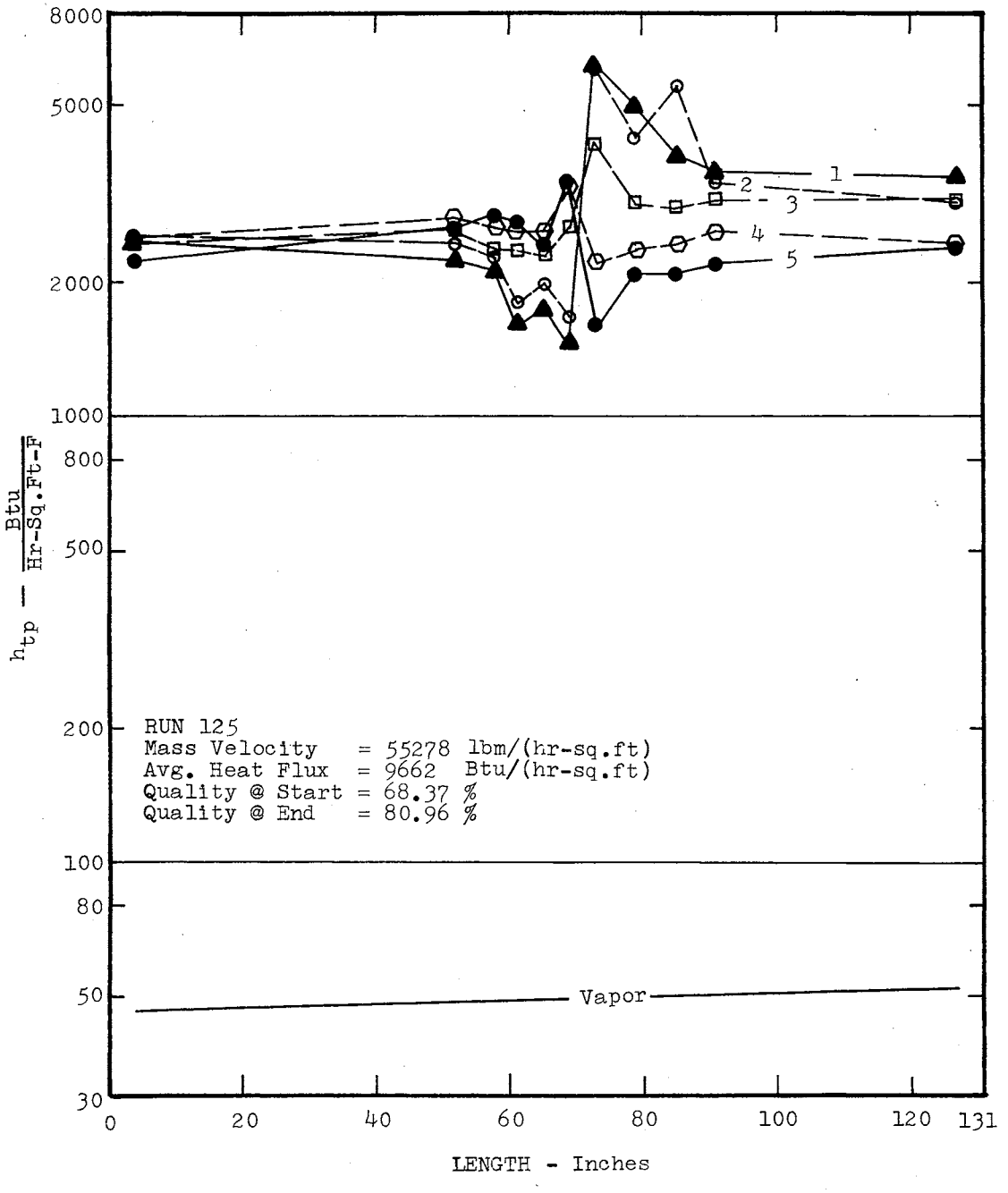

Figure 45. Heat Transfer Coefficients, Small Bend, Run 125

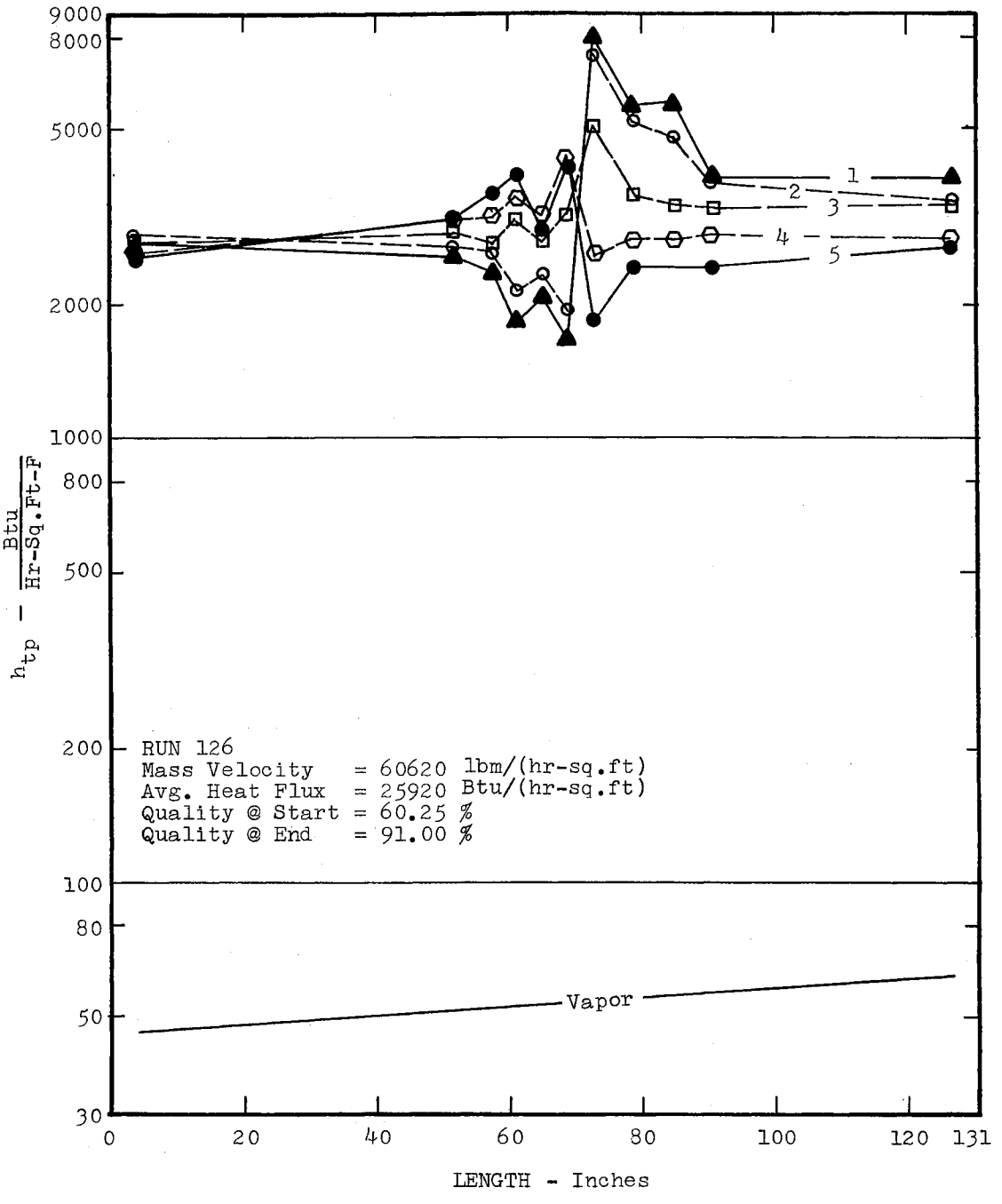

Figure 46. Heat Transfer Coefficients, Small Bend, Run 126

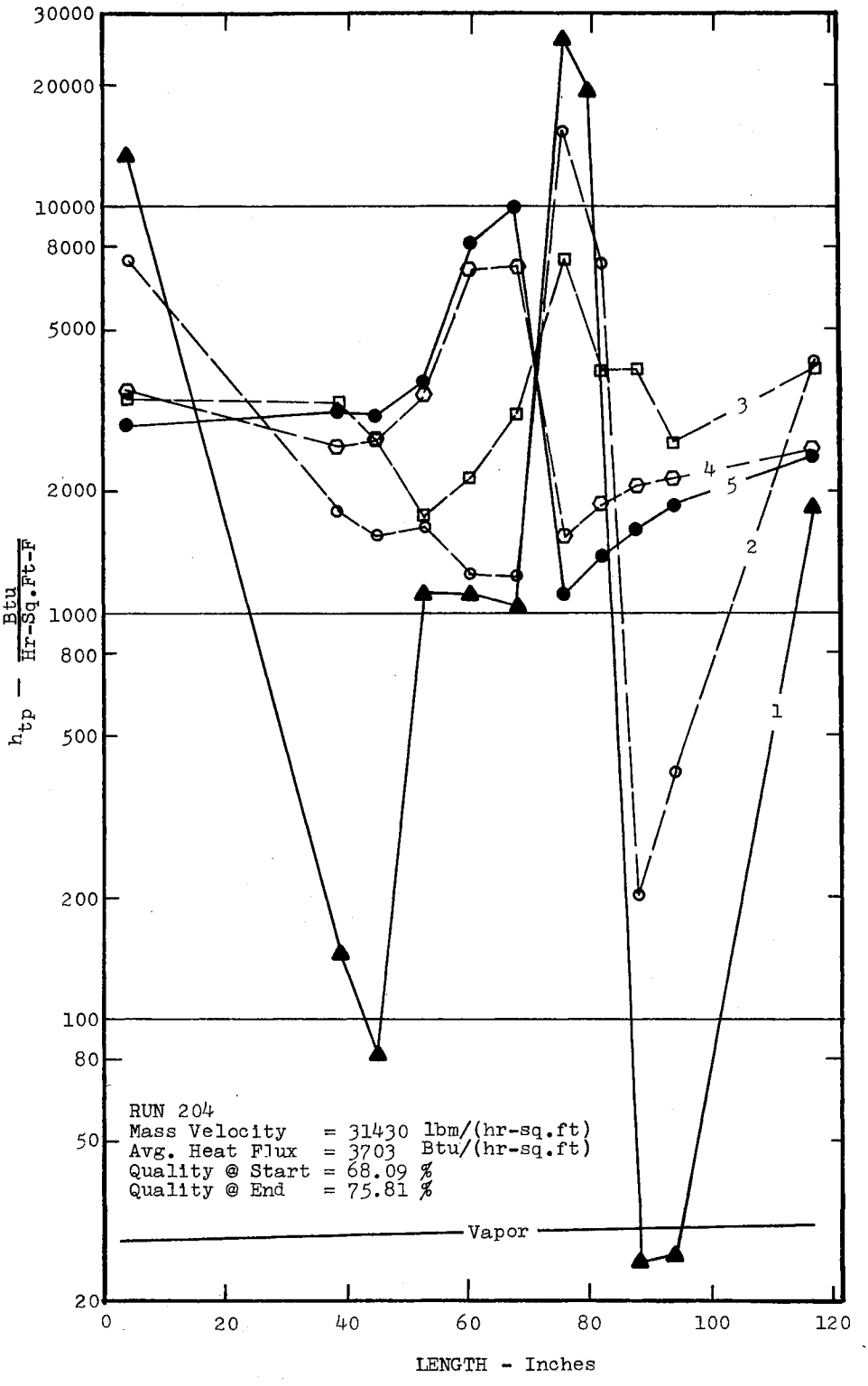

Figure 47. Heat Transfer Coefficients, Large Bend, Run 204

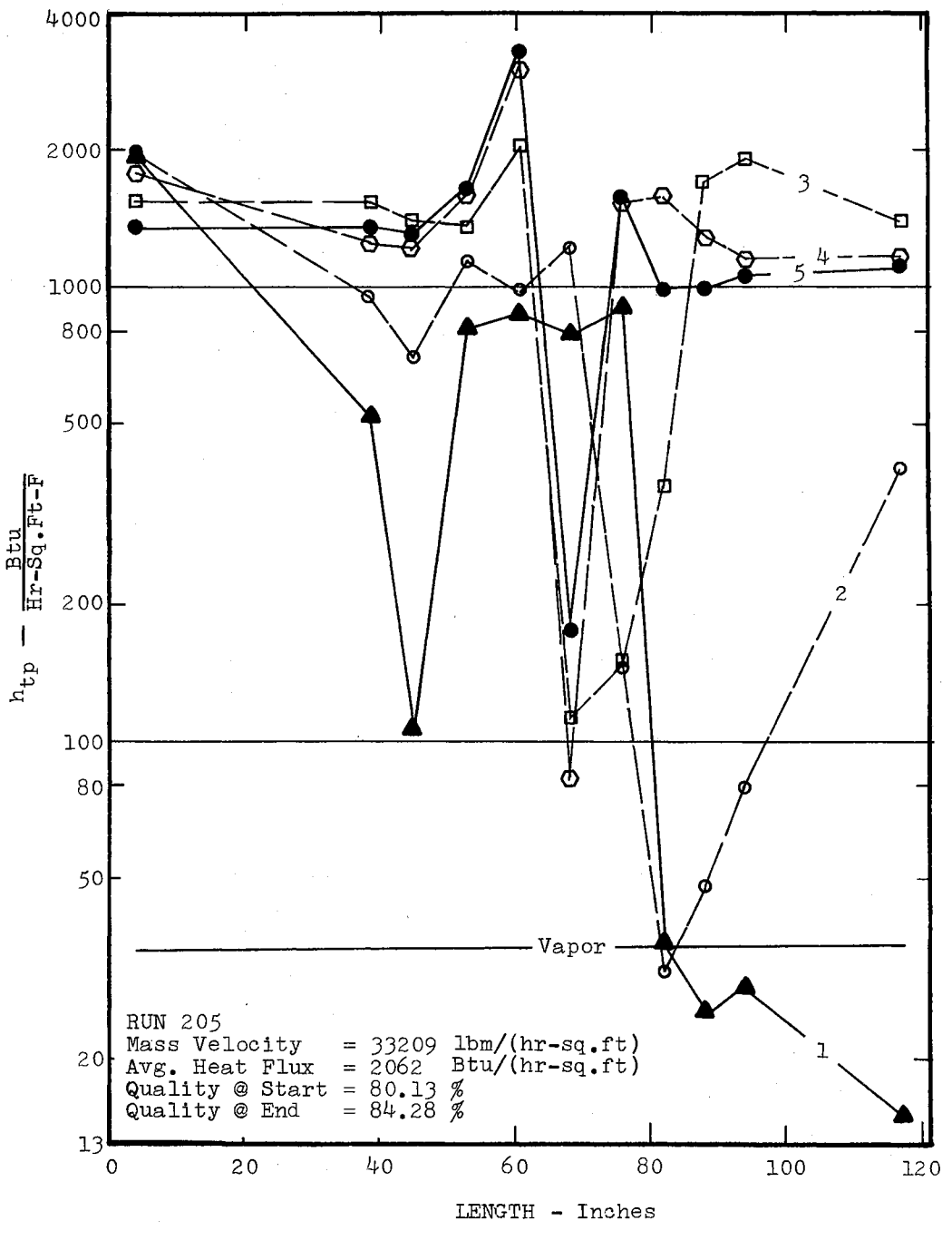

Figure 48. Heat Transfer Coefficients, Large Bend, Run 205

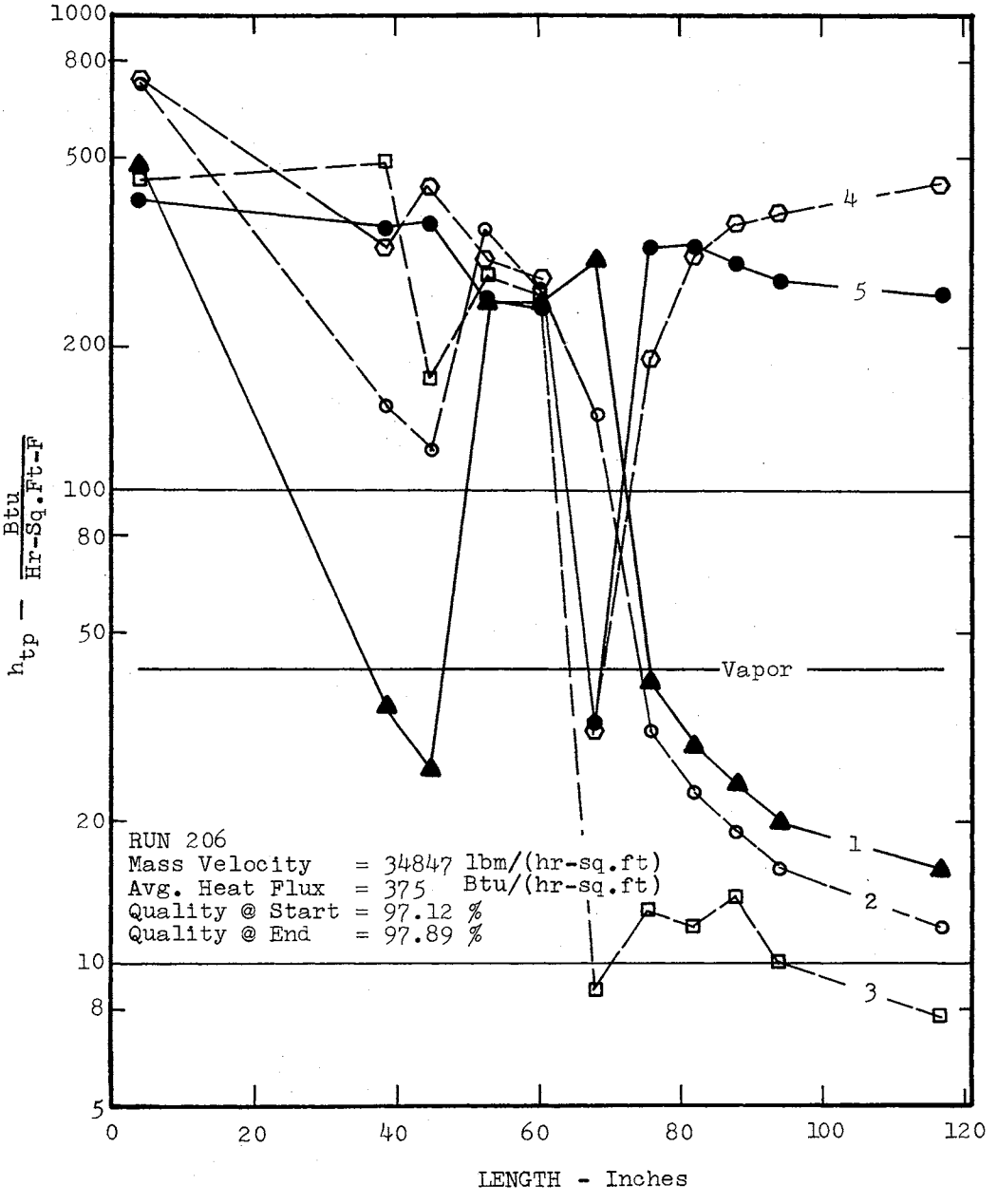

Figure 49. Heat Transfer Coefficients, Large Bend, Run 206

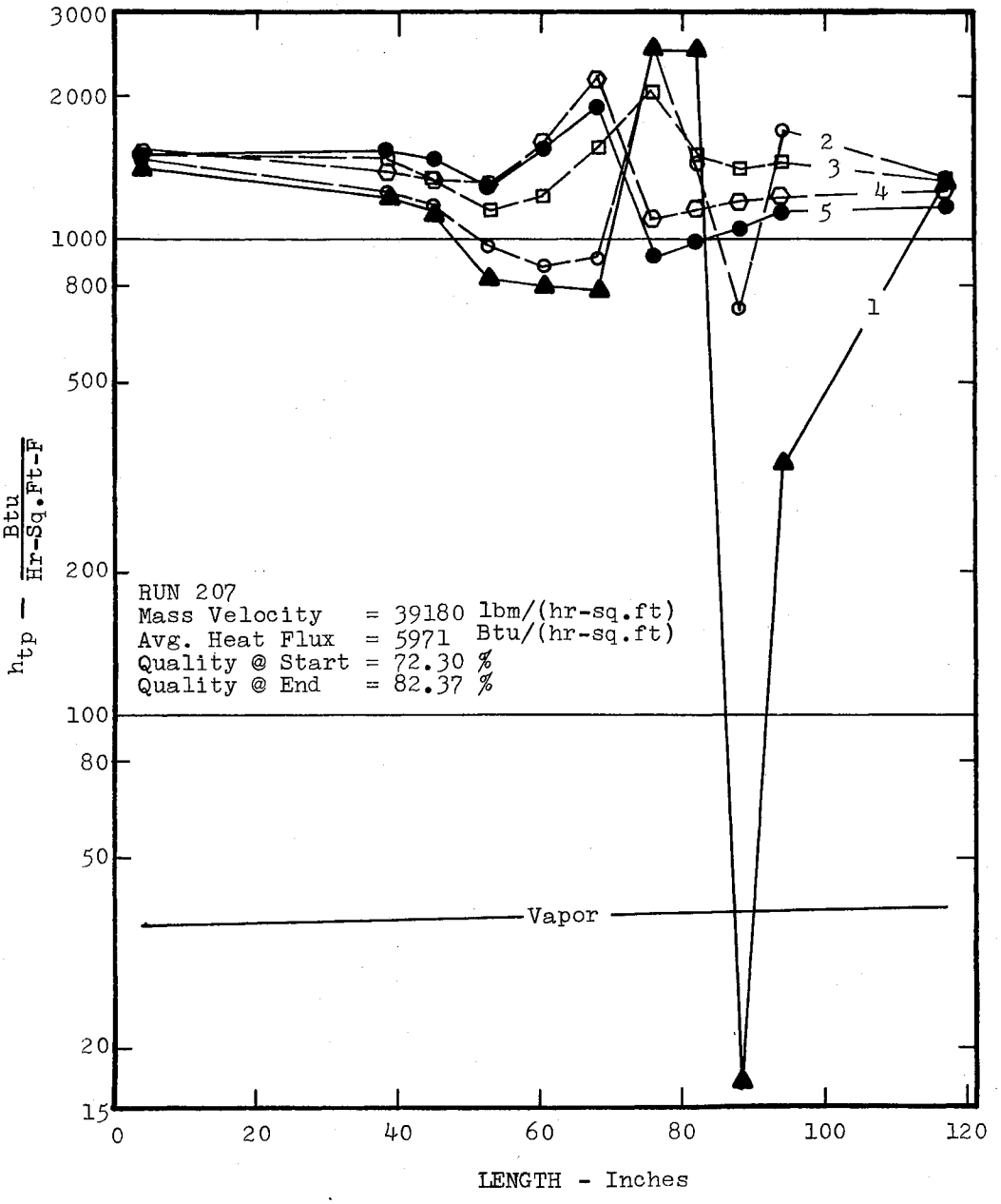

Figure 50. Heat Transfer Coefficients, Large Bend, Run 207

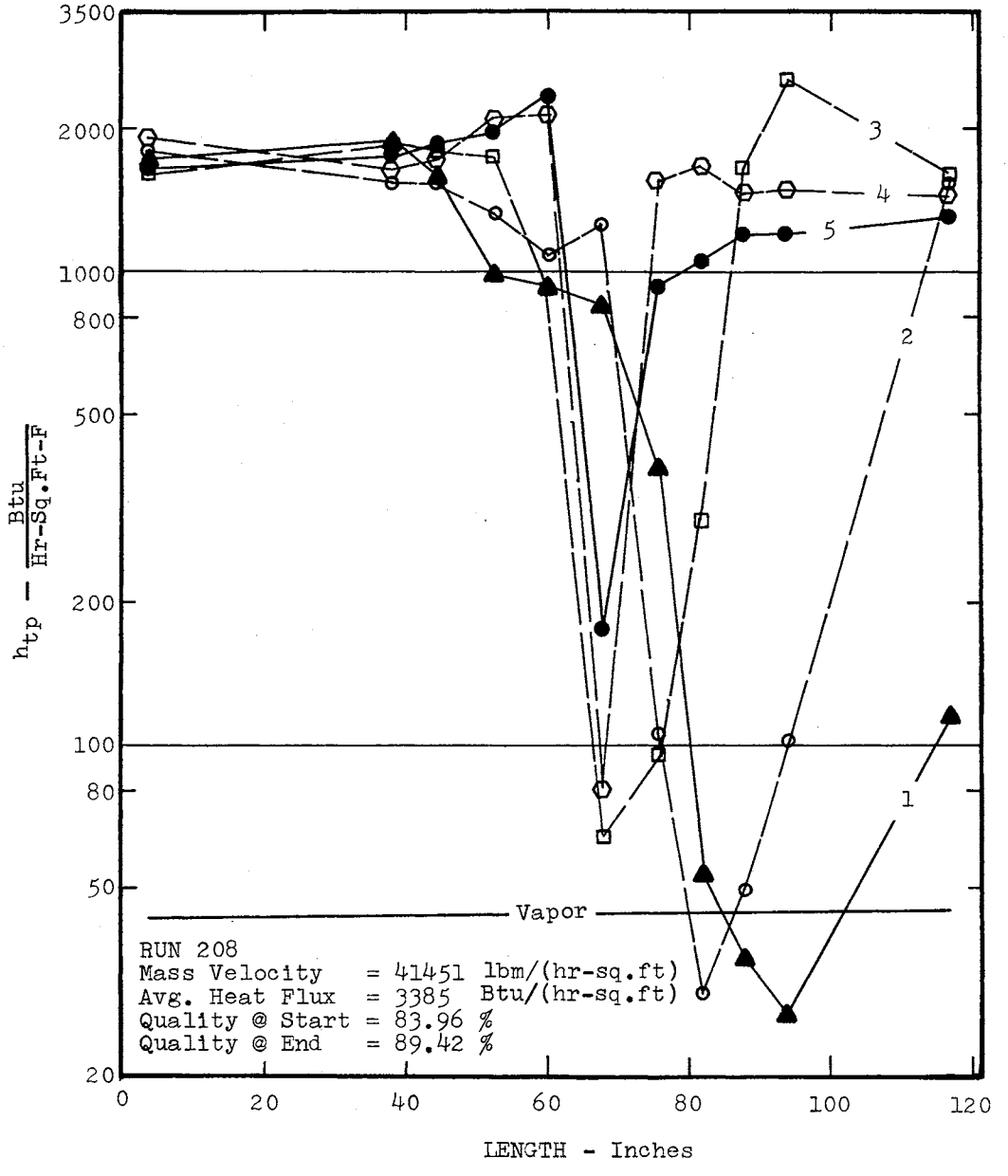

Figure 51. Heat Transfer Coefficients, Large Bend, Run 208

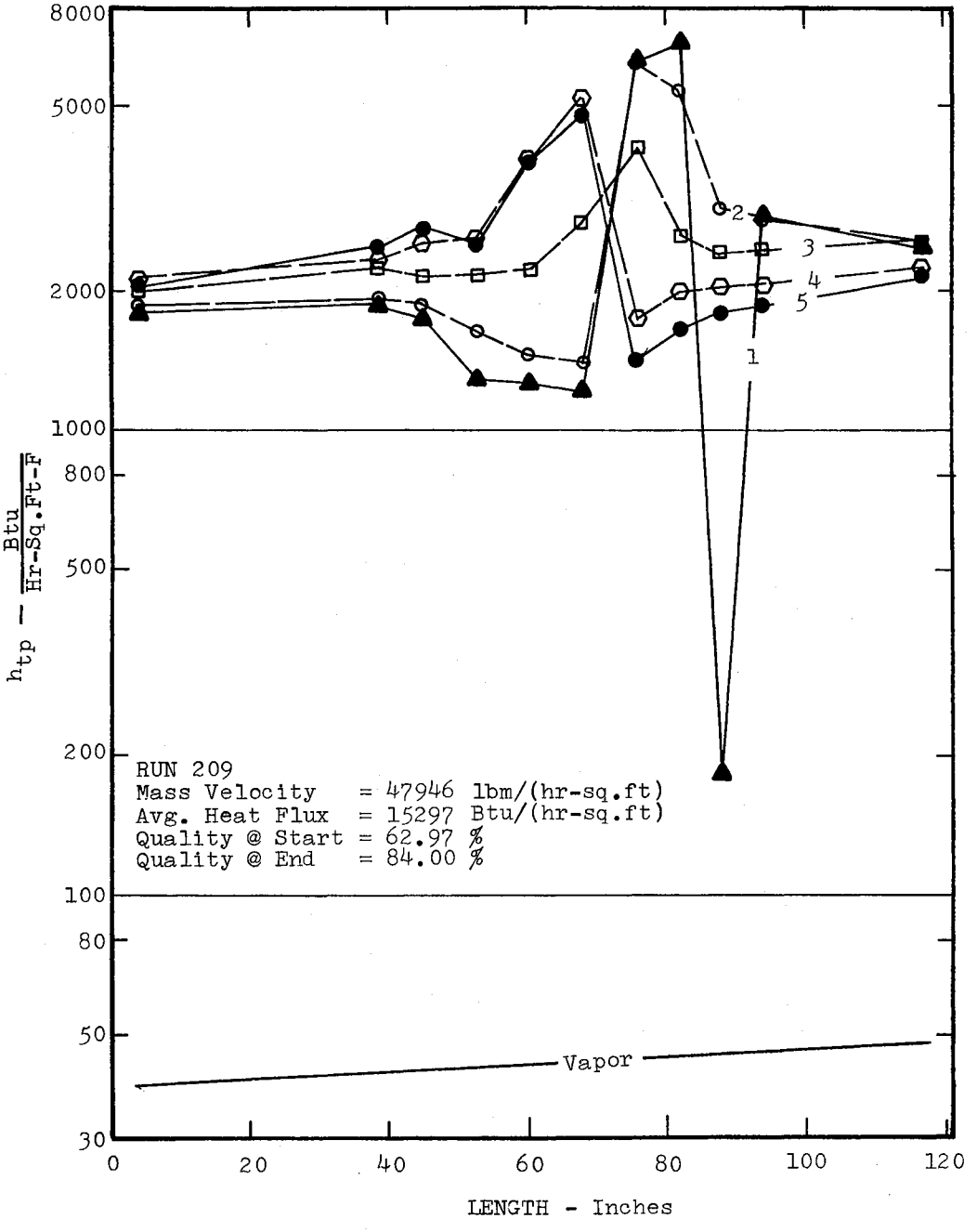

Figure 52. Heat Transfer Coefficients, Large Bend, Run 209

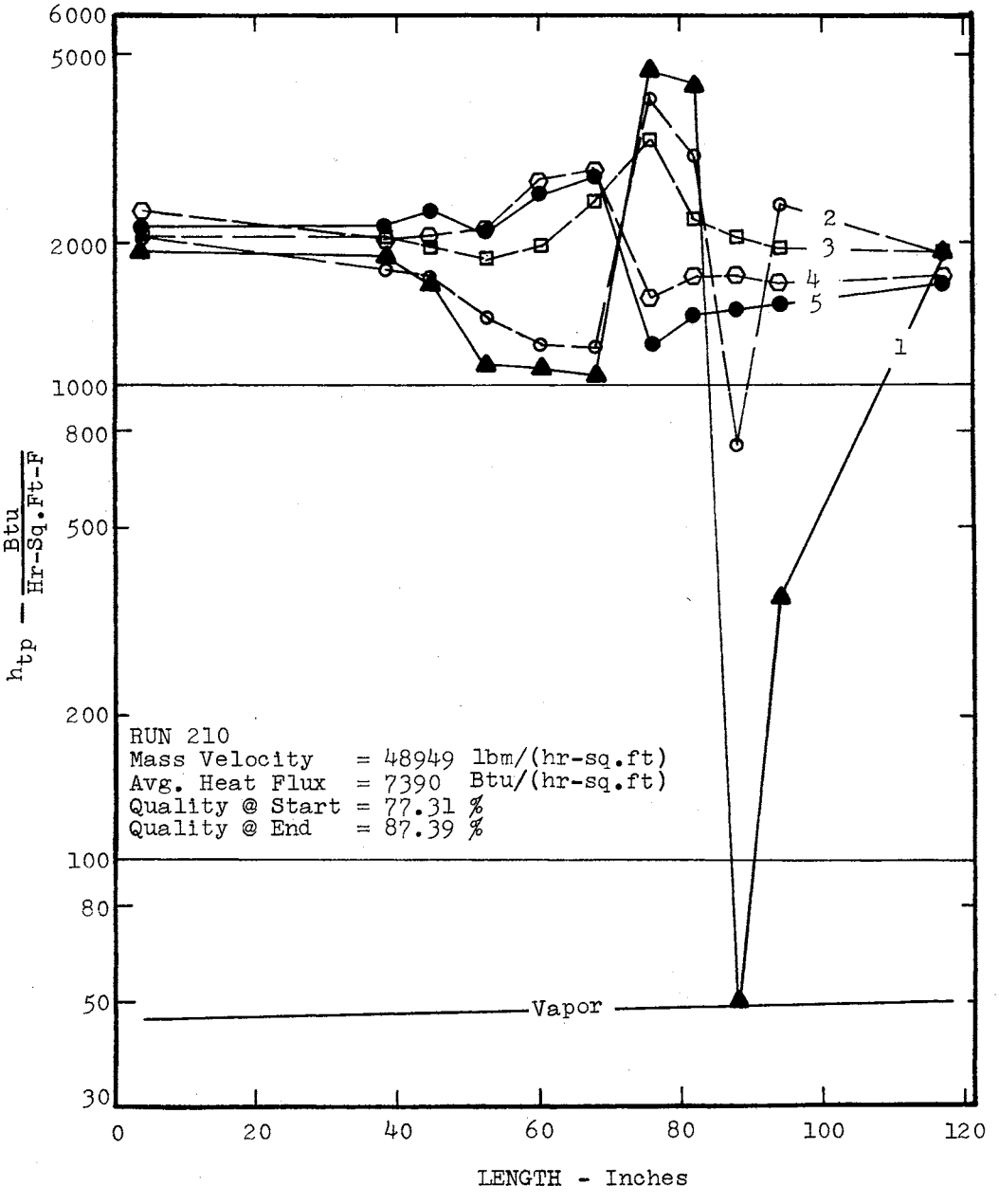

Figure 53. Heat Transfer Coefficients, Large Bend, Run 210

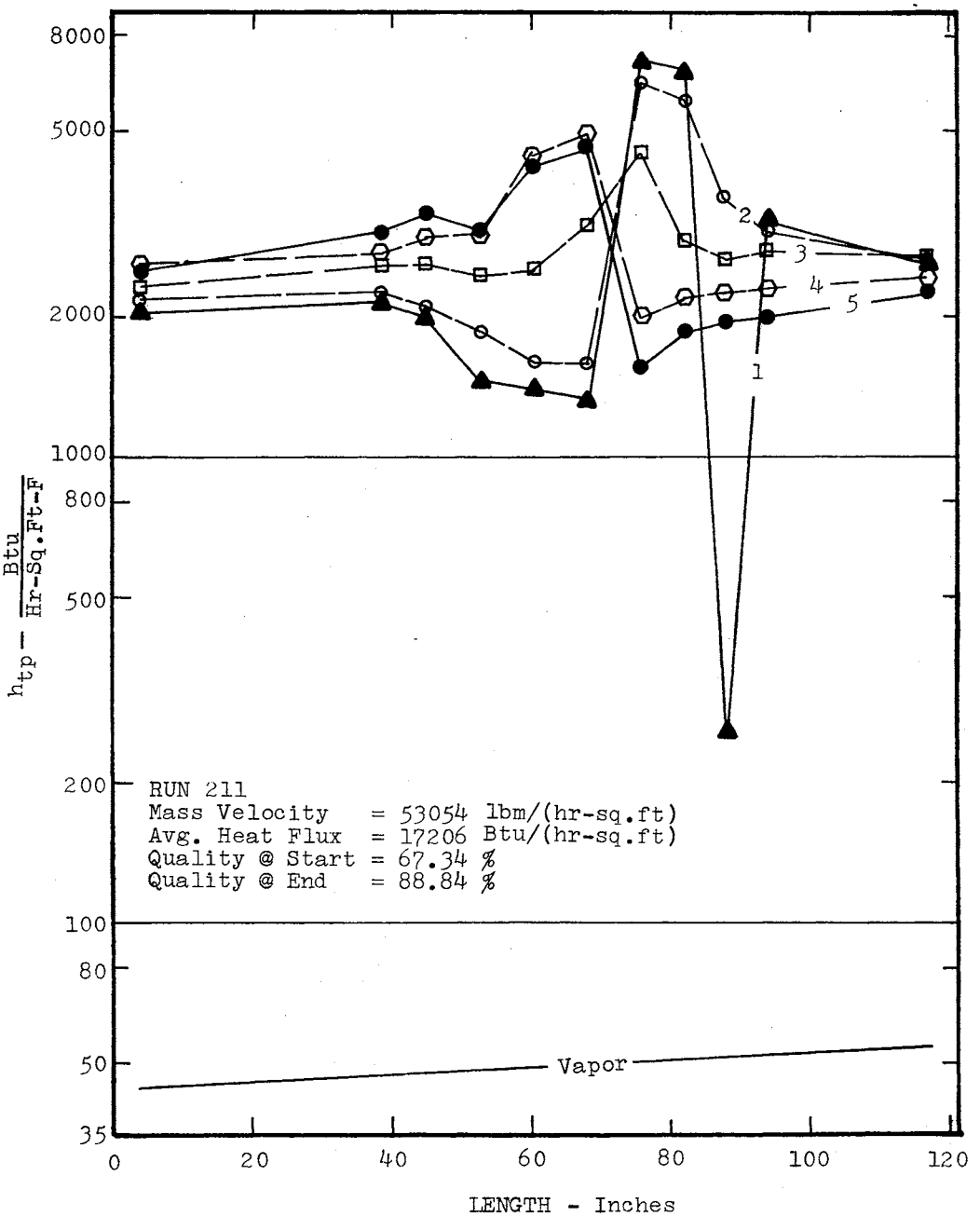

Figure 54. Heat Transfer Coefficients, Large Bend, Run 211

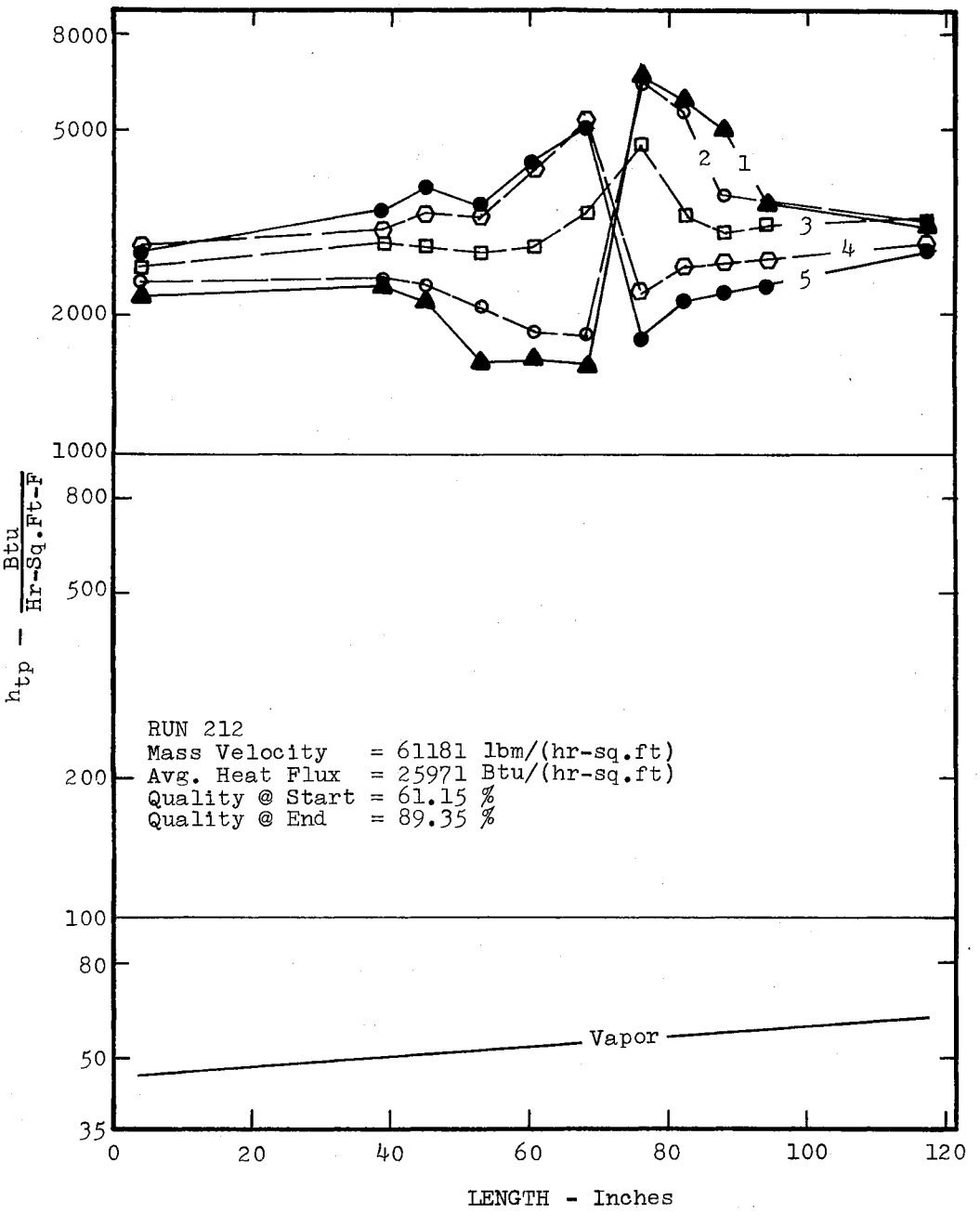

Figure 55. Heat Transfer Coefficients, Large Bend, Run 212

TABLE IV

EXPERIMENTAL CONDITIONS FOR STEAM-WATER RUNS

Run	Mass Velocity lbm/(hr.-sq. ft.)	Avg. Heat Flux Btu/(hr.-sq. ft.)	Quality, % Start	Quality, % End	Pressure, PSIA Start	Pressure, PSIA End	Temperature, °F Start	Temperature, °F End
104	28,105	699	89.57	91.39	19.39	18.88	226.3	224.9
105	32,413	385	83.53	84.45	19.82	19.22	227.5	225.8
106	32,472	816	82.94	84.80	19.75	19.08	227.3	225.5
107	34,690	2,244	82.60	87.26	20.08	19.41	228.2	226.4
108	33,388	3,650	65.47	73.27	16.79	16.17	218.8	216.9
109	37,034	378	95.50	96.30	22.86	22.11	235.2	233.3
110	36,944	2,378	72.30	76.96	18.37	17.59	223.5	221.2
111	36,981	4,022	72.99	80.79	18.50	17.62	223.8	221.3
112	40,359	5,412	72.22	81.84	21.30	20.41	231.3	229.0
113	40,519	6,508	71.91	83.42	21.57	20.67	232.0	229.7
114	41,133	812	86.32	87.84	22.85	21.89	235.1	232.8
115	42,089	2,366	84.30	88.40	22.31	22.36	236.2	234.0
116	41,719	3,634	83.63	89.93	23.75	22.81	237.3	235.0
117	44,701	2,254	60.41	64.13	18.94	18.01	225.1	222.4
118	45,217	9,673	60.10	75.44	20.11	18.76	228.2	224.6
119	46,404	15,234	61.91	85.45	24.53	23.27	239.0	236.1
120	48,276	16,178	62.05	86.08	24.77	23.55	239.6	236.8
121	46,882	2,246	75.63	79.21	20.31	19.00	228.8	225.2
122	49,186	7,338	76.17	86.90	25.55	24.76	241.3	239.5
123	46,931	8,462	80.89	93.82	26.14	25.60	242.5	241.4
124	53,504	18,486	64.49	89.40	28.03	26.41	246.5	243.1
125	55,278	9,662	68.37	80.96	23.00	21.71	235.5	232.4
126	60,620	25,920	60.25	91.00	25.68	23.46	241.6	236.6
204	31,430	3,703	68.09	75.81	17.50	17.17	220.9	219.9
205	33,209	2,062	80.13	84.28	20.10	19.47	228.2	226.5
206	34,847	375	97.12	97.89	22.43	21.73	234.1	232.4
207	39,180	5,971	72.30	82.37	18.65	17.77	224.3	221.7
208	41,451	3,385	83.96	89.42	23.59	22.73	236.9	234.9
209	47,946	15,298	62.97	84.00	20.65	19.58	229.7	226.8
210	48,949	7,390	77.31	87.39	25.22	24.06	240.6	238.0
211	53,054	17,206	67.34	88.84	22.87	21.26	235.2	231.2
212	61,181	25,971	61.15	89.35	25.39	23.39	240.9	236.4

Stability

The heat transfer loop was designed with various throttling devices so that any unstable condition could be controlled. Consequently, all runs were conducted under stable conditions. For some runs there was a tendency for long period flow and consequently temperature oscillations to be superimposed on an otherwise "stable" operation. Whenever these temperature oscillations were picked up on the Speedomax recorder, the test section inlet valve was throttled and the unstable situation was alleviated. An example of this type of an oscillation and its subsequent damping is shown in Figure 56. The oscillation period for this example was 12 minutes while the amplitude was 26°F. Crain (5) encountered this type of instability in his experiments also; however, he was unable to damp it due to the lack of an inlet orificing device.

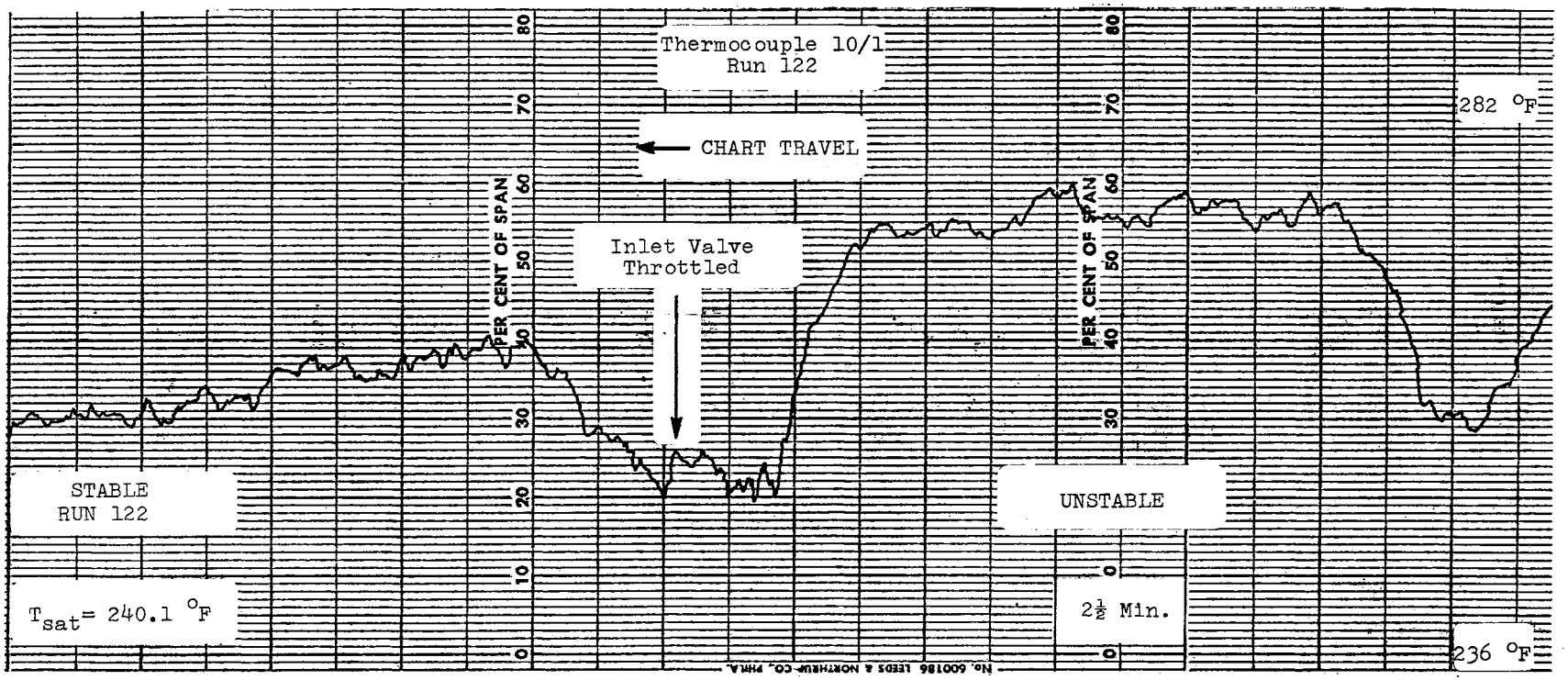

Figure 56. Long Period Oscillation and Subsequent Damping

CHAPTER VI

DISCUSSION

The amount of data taken for both the visual tests and the heat transfer tests was quite voluminous and the discussion for each test will be given separately except where similarity is to be compared.

Air-Water Tests

The hydrodynamic behavior in the bend was quite different than what was anticipated. The behavior in the bend was found to be a function of the flow direction as well as the liquid and gas mass flow rates. In general, however, the effect of the bend radius on the flow behavior could not be quantitatively described.

Low Liquid Flow Rates in Upflow

For low liquid flows the following behavior was observed as the gas flow rate was increased for constant liquid flow.

1. For low air flows, "flooding" in the bend was observed. Flooding is characterized by no net liquid flowing upwards in the tube for long periods of time. The liquid is eventually expelled from the bend when a slug of liquid is formed and carried out by the gas. Liquid pressure and flow oscillations mentioned in Chapter V coincide with the frequency of the slug ejection. The flooding velocity can be predicted

to within ± 20 percent (for $G_L/G_G < 30$) by the Diehl and Koppany (17) correlation:

The flooding velocity is given by

$$V_f = F_1 F_2 (\sigma/\rho)_g^{0.5} \quad (1)$$

where

$F_1 = (d_i/(\sigma/80))^{0.4}$; $d_i/(\sigma/80) < 1.0$;

$F_1 = 1.0$; $d_i/(\sigma/80) \geq 1.0$;

$F_2 = (G_G/G_L)0.25$;

σ = surface tension;

d_i = inside tube diameter.

2. As the air flow was increased, the liquid started to travel up the bend. However, some liquid would flow down on the inside of the bend until the gas flow was increased to the "flow reversal" point. At this point the liquid always flowed upwards and if the gas flow was decreased, some liquid would start to flow downwards on the inside of the bend again. From the air-water data it was determined that the flow reversal velocity can be predicted to within ± 20 percent by multiplying the flooding velocity by a factor of two.

$$V_{fr} = 2V_f \quad (2)$$

3. At low liquid flows ($G_L \Psi < 30$) and high air flows ($G_G/\Lambda > 1.0 \times 10^4$) the liquid film was inverted from the outside wall in the bend to the inside wall. The liquid then flowed on the bottom of the tube in the outlet leg. The factors controlling inversion were the ratio of centrifugal forces $[(\rho V_S^2)_G/(\rho V_s^2)_L]$ and secondary flow intensity in the vapor phase. The effect of the secondary flow was observed to exist up to a maximum of about 30 L/D's in the straight outlet leg. In

general, both factors seemed to control inversion in the bend whereas secondary flow intensity was the dominating factor in the straight outlet leg. Secondary flow influence was assumed when streaks of liquid, formed by de-entrainment of the liquid onto the outer wall, travelled in a spiralling fashion from the outside wall to the inside wall in the bend and from the top of the tube to the bottom of the tube downstream of the bend. The spiralling motion can be explained by the movement of the twin helices in the vapor core, as shown in Figure 1(c), dragging the liquid from the outside wall to the inside wall. Figure 18(a) shows this condition clearly. This phenomenon was recorded with better clarity on 16mm high speed color movies.

Figure 57 shows an example of liquid travelling mostly on the inside surface in the bend rather than on the outside due to the effect of a large air-water centrifugal force ratio (283 for the large bend, 337 for the small bend).

High Liquid Flow Rates in Upflow

For some high liquid flow rates the water was centrifuged and for gas velocities greater than the flow reversal velocity, vapor blanketing of the inside part of the bend as well as some length (maximum of 16 L/D's) of the outlet leg was observed. This phenomenon was generally observed in the slug flow type regimes. Zahn (10) observed the vapor blanketing of the straight leg in his study also (see Figure 14 in Zahn's paper).

An example of liquid being centrifuged is shown in Figure 58.

For some high liquid flow rates beyond the flow reversal point, the liquid would flow in the form of misty patches in the straight outlet

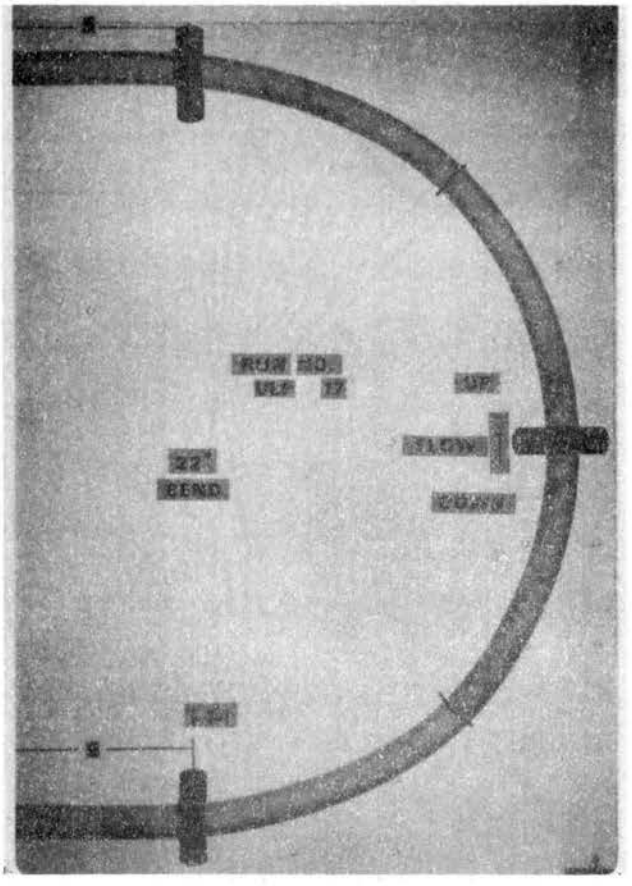

Figure 57. Example of Air Being Centrifuged

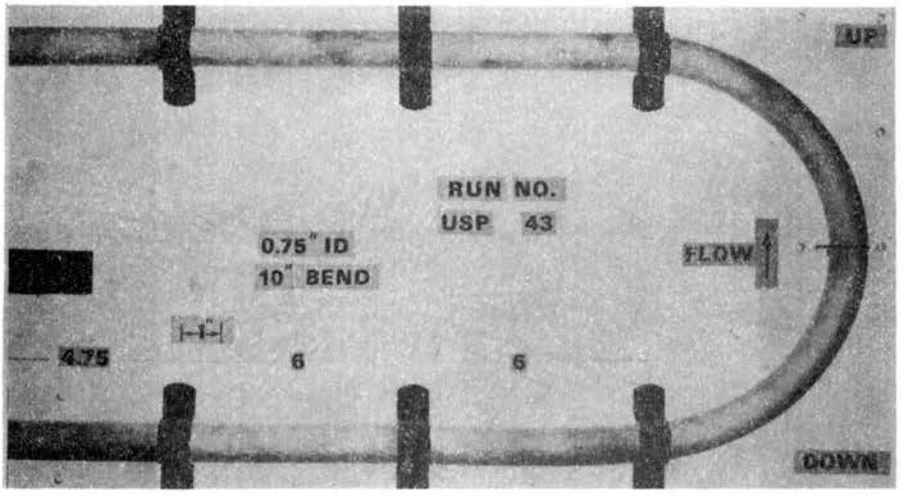

(a) Small Bend

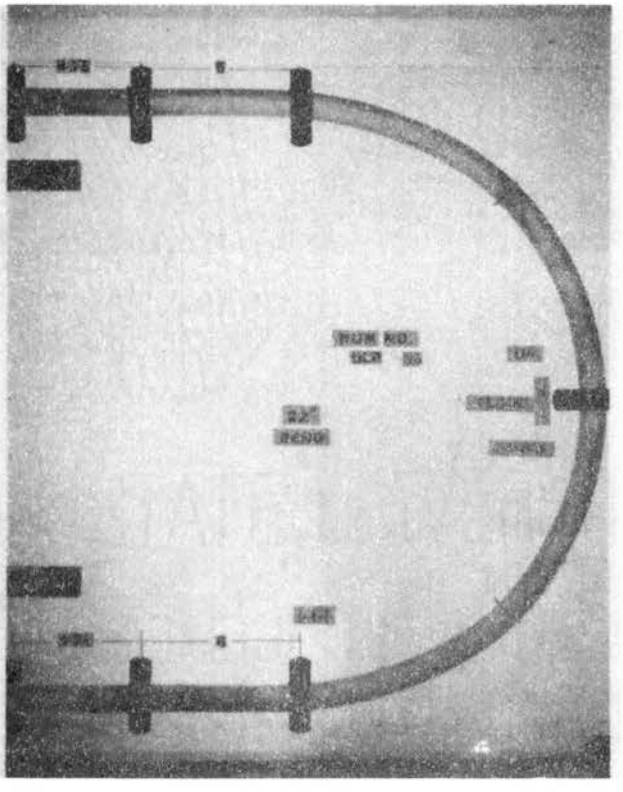

(b) Large Bend

Figure 58. Example of Liquid Being Centrifuged

leg downstream of the bend. The misty patches were generated by the liquid falling to the bottom of the tube due to gravity and in the process being entrained by the air travelling in the middle of the tube. The misty patches were observed for at least 20 L/D's downstream of the bend.

The "flow reversal" point could not be predicted for $G_L/G_G > 30$ since extrapolation of the Diehl-Koppany correlation for these conditions was unsatisfactory.

Low Liquid Flow Rates in Downflow

For low liquid flow rates and low air flow rates, the liquid trickled down on the bend and the controlling mechanisms were surface tension and gravity forces. For higher air flow rates the ratio of the centrifugal forces (air/liquid) was very large and the secondary flow intensity was strong enough that the liquid stayed on the inside of the bend. In the straight outlet leg the liquid slid along the wall to the bottom of the tube due to gravity forces acting on the liquid phase. This positional change of the liquid phase in the horizontal leg was a function of the secondary flow intensity. The stronger the intensity the farther the liquid travelled in the straight section before it reverted to the stable pattern. An example of this flow condition can be seen in Figure 59.

High Liquid Flow Rates in Downflow

For high liquid flow rates there was negligible difference in the flow pattern between the inlet and outlet legs. Liquid in the bend was usually observed to be concentrated on the outside tube wall.

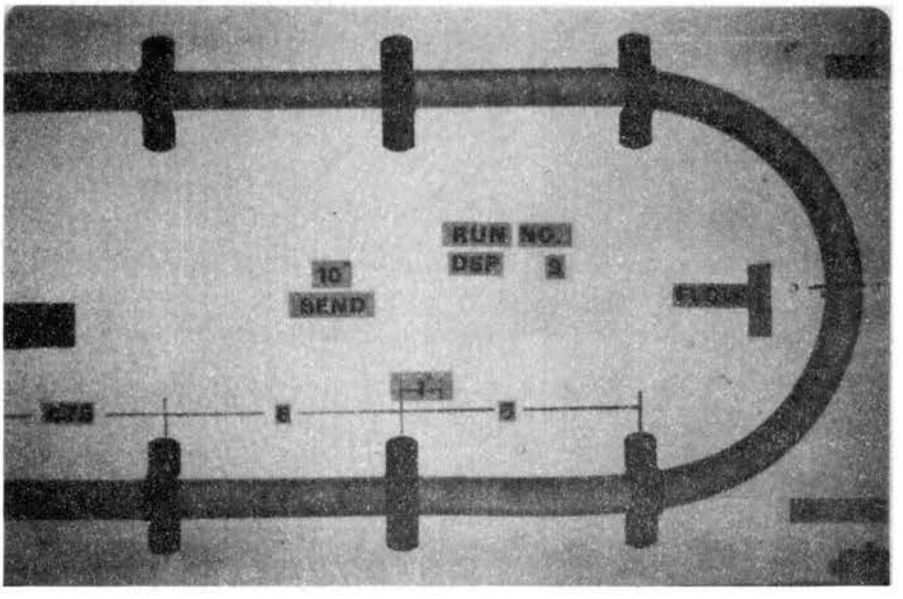

Figure 59. Vapor Blanket in the Annular Flow Regime (Downflow)

Effect of Bend Radius

It was somewhat difficult to quantitatively describe the influence of the bend size on the hydrodynamic behavior of the air-water flow. The only qualitative observation that can be made is that the resident time of a liquid particle in the bend is longer in the larger bend than in the smaller one for conditions below the flow reversal point.

Flow Regime Map for Horizontal Serpentine Tubes With Vertically Oriented Bends

The data from Figures 14, 15, 16 and 17 were superimposed onto one graph and a definite trend was observed in the flow pattern subdivisions. Using these points as a guide, a new flow regime map (Figure 60) which included these subdivisions was developed.

One area on the new map (below plug flow regime) is left undefined even though the data indicated that the regime should be classified as the Bubble flow regime. Although it seems logical that the Bubble flow regime should be located below the Plug flow regime, it is felt that the procedure used in mixing the gas phase could have a significant effect on the flow pattern for the prevailing flow conditions. This effect has also been pointed out by Hewitt and Hall-Taylor (19). Further experimentation with different mixing section designs would probably lead to a better boundary demarcation in this region

Zahn's (10) data were reduced and plotted on the new flow regime map in Figure 61. The data show that the subdivision delineation is quite good. The close similarity in Zahn's description of the flow patterns for diabatic flow and the author's description of flow patterns

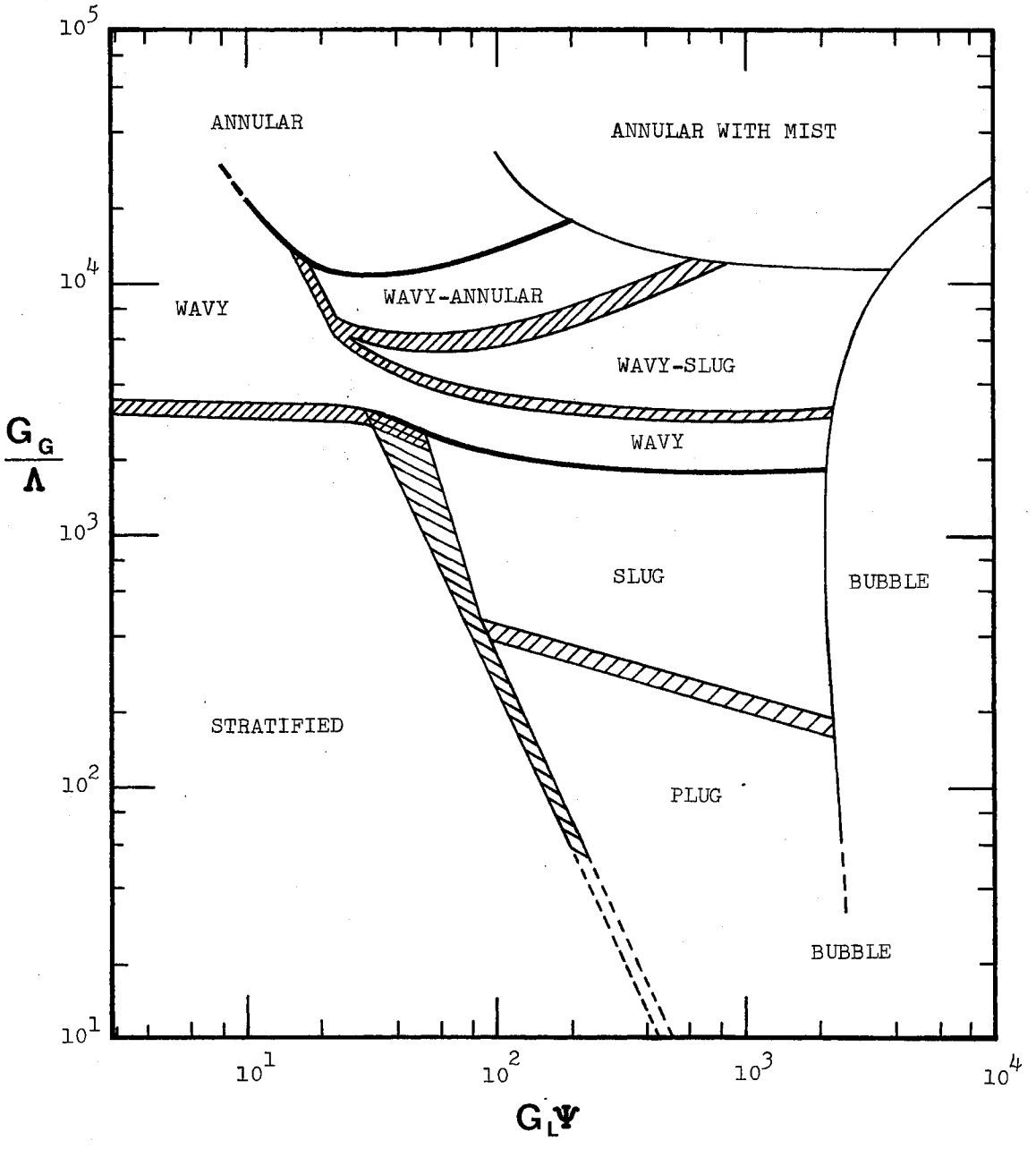

Figure 60. Flow Regime Map for Horizontal Serpentine Tubes With Vertically Oriented Bends

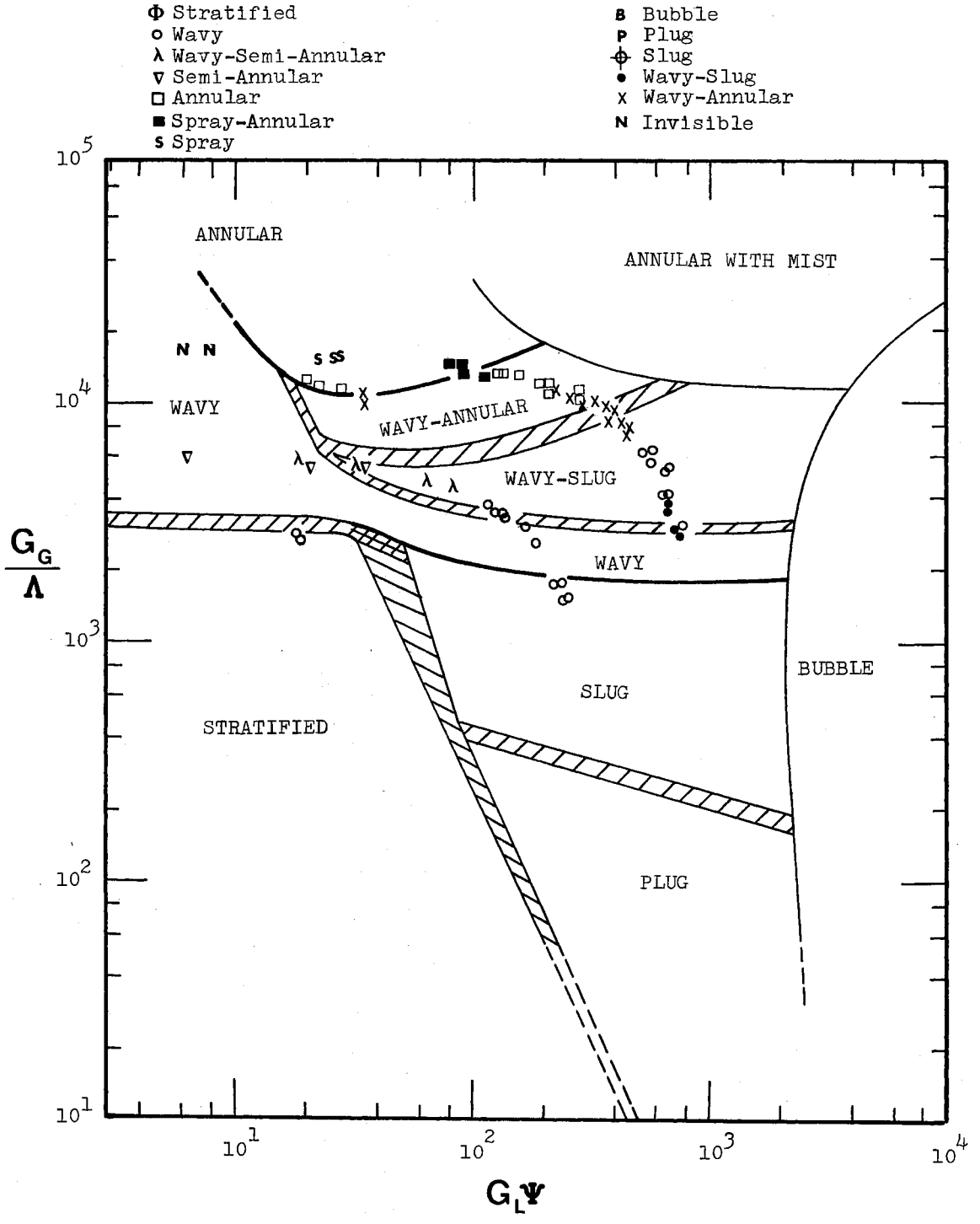

Figure 61. Zahn's Data on Author's Flow Regime Map

for adiabatic flow demonstrates that the new flow regime map may be used for flow pattern analysis of both evaporating flow with low heat fluxes and unheated flow with reasonable accuracy.

Steam-Water Tests

Steam-water heat transfer tests were conducted in the annular flow regime to see if the film inversion observed in the air-water tests could be duplicated.

The visual air-water tests revealed that for air-water centrifugal force ratios near 300, the liquid film would start to invert and for ratios in excess of 10,000 total destruction of annular flow in the bend would follow.

The centrifugal force ratios are defined in the following manner.

$$\text{Centrifugal Force Ratio} = \frac{(\rho V^2_S)_{\text{Gas}}}{(\rho V^2_S)_{\text{Liquid}}} \qquad (3)$$

The cross-hatched area shown in Figures 19 and 20 indicates that the flow regime where inversion was observed in the visual air-water was simulated in the steam-water tests. However, total disruption of the annular pattern was apparently never realized in the steam-water tests even when the ratios were in excess of 40,000. Moreover, since an increase in temperature decreases the liquid viscosity and consequently the wall shear stress at the liquid-wall interface, film inversion should be hastened for the steam-water tests.

The inability to obtain film inversion in the bend with the steam-water tests is explained in the next chapter.

In the semi-annular regime, however, film inversion similar to the one observed in the visual tests was apparently obtained. Figures 21 and 47 show this effect quite clearly since the heat transfer coefficient at station 6/5 indicates a vapor-type heat transfer coefficient.

Other conclusions that may be drawn from the heat transfer tests are itemized below.

1. The dry patch in the exit leg is caused by the secondary flow in the vapor core which inverts the liquid film from the outside wall to the inside wall in the bend and then with favorable gravity forces allows it to travel in the bottom half of the tube until the establishment of annular conditions further downstream. Butterworth (20) has shown that annular flow is maintained in a horizontal tube by "secondary flow" caused by asymmetry in the vapor flow velocity profile and by "wave-spreading" mechanisms and it is believed that these mechanisms are instrumental in re-establishing annular flow in the exit leg. Lis and Strickland (13) demonstrated the effect of gravity on "dryout" downstream of the bend by placing the bend in the horizontal plane and noting that the wall temperature oscillations were attenuated when compared to the oscillations encountered for tests with the bend in the vertical plane.

2. Although the quality changed by as much as 13 percent for some runs, annular flow was always re-established in the exit area of the test section. Therefore, a dry patch was caused as an after-effect of the bend rather than being generated by a quality change.

3. A dry patch always started at station 9 (L/D_i = 15) and grew toward the test section exit. Lis and Strickland (13) observed that a

dry patch in their tests started at an L/D_i of 14. Perhaps this information is more than coincidence since their bend-to-tube diameter ratio was 6.1 whereas the ratios in this study were 25.6 and 12.3.

Effect of Bend Radius

The effect of the bend radius was barely noticeable even though one bend was twice as large as the other bend. However, replicate runs with the large bend, in general, indicated that, under similar conditions, a dry patch could be established with a lower heat flux with the large bend than with the small bend.

Conduction Equation

The conduction equation used to calculate the wall temperature drop incorporated the peripheral conduction term. In all the runs that were made, this term was at the most 3 percent of the radial conduction term. However, the inclusion of this term was important since the film temperature drop for certain runs was fairly low. Generally the wall temperature drop was at least four orders of magnitude less than the film temperature drop. The only time that the ratio was reversed was when dryout was imminent.

Heat Transfer Coefficients

Heat transfer correlations for two phase flow in the forced convective region have been correlated with reasonable success, by various investigators,[1] in the following manner.

---

[1] Rohsenow and Hartnett (21) summarize the various correlations.

$$h_{tp} = h_L c\left(\frac{1}{x_{tt}}\right)^n \tag{4}$$

where

$$h_L = .023 \frac{K_L}{d_i} (R_e)_L^{0.8} (P_r)_L^{0.4};$$

c = constant;

n = constant;

$$x_{tt} = \left(\frac{x}{1-x}\right)^{0.9} \left(\frac{\rho_L}{\rho_G}\right)^{0.5} \left(\frac{\mu_G}{\mu_L}\right)^{0.1}.$$

It was not possible to correlate the data acquired in this study in this fashion due to the wide scatter caused by the dry patch and the small range of $1/x_{tt}$ covered.

In general, it can be seen from Figures 36 through 46 that the local heat transfer coefficients before the bend are almost equal to the mean heat transfer coefficients whereas after the bend they are spread out. This type of variation in the local heat transfer coefficient also adds to the difficulty in correlating the data.

CHAPTER VII

CONCLUSIONS AND RECOMMENDATIONS

Flow visualization tests with air-water mixtures and forced convective boiling tests with steam-water mixtures were conducted inside horizontal serpentine tubes with bends in the vertical plane.

The air-water tests revealed that, in the annular flow regime at the entrance to the bend, it was possible to invert the liquid film from the outside wall to the inside wall in the bend. The liquid film was then observed to travel in the bottom half of the straight tube to as much as 30 diameters downstream of the bend before it occupied the whole tube surface and annular flow conditions were re-established. This phenomenon may be attributed to the influence of the strong secondary flow circulation induced in the vapor core, by the bend, that aids in dragging the liquid film from the outer tube wall to the inner tube wall. Downstream of the bend, gravity forces favor the liquid film being maintained in the bottom half of the tube. However, as the secondary flow intensity decays in the straight leg "secondary flow" caused by the asymmetric nature of vapor core velocity profile and "wave-spreading" mechanisms help in re-establishing the annular type flow conditions.

This phenomena could not be completely duplicated with the steam-water tests since a dry patch only materialized about 15 diameters downstream of the bend and apparently never in the bend. Since the flow regime was apparently duplicated in the tests and the ratio of

centrifugal forces for steam-water were four times larger than the ratios calculated for the air-water tests when film inversion was observed, the following conclusions may be drawn.

1. The ratio of gas-liquid centrifugal forces which help in inverting the liquid film from the outer wall to the inner wall in the bend is only one of the many factors controlling the film inversion phenomenon.

2. Secondary flow in the vapor core is another controlling factor.

3. Surface wetting characteristics may be a controlling factor. The TYGON test section used in the air-water tests has poor wetting characteristics.

4. Surface finish may be a controlling factor. The TYGON test section was very smooth compared to the INCONEL test section.

5. Butterworth (20) has shown that surface tension cannot be an important factor in maintaining the film at the top of the tube in horizontal annular flow. Therefore, it may be assumed that it is not an important factor in inducing film inversion. However, surface tension coupled with the factors mentioned above may have been at least a second-order parameter for inducing film inversion in the bend.

6. Perhaps the most important factor that is not readily obvious in explaining the discrepancy in the film inversion phenomenon for the two tests is that of liquid entrainment in the vapor core. For the steam-water tests the mixture was routed through a needle valve which thoroughly mixed the two phases and consequently the annular flow that existed in the bend most likely had a thin film with a large amount of entrainment in the vapor core. In the air-water tests, air was injected through a tee with water flowing in the straight run. Since the liquid

flow rates were very low, for runs where complete film inversion in the bend was observed, the liquid would be forced to assume an annular profile in a fairly short distance and very little entrainment would be possible. In fact, the color movies of this phenomenon and visual observations indicated that streaks of liquids spiralling from the outside wall to the inside wall in the bend were very thin and discrete. However, with the steam-water runs the larger amount of entrainment would have resulted in the droplets being deposited onto the outside wall in the bend due to centrifuging, and this de-entrainment (similar to mist flow regime suppression in helical coils, see Crain (5)) was probably sufficient to keep the outside wall wet for the annular runs.

Hewitt and Hall-Taylor (19) have presented a detailed discussion on different mixing techniques and have shown that film flow rate variations due to different injection systems could persist for distances greater than 160 diameters.

A two phase flow regime map with more subdivisions than Baker's map was developed for mixtures flowing in horizontal serpentine tubes with bends in the vertical plane. The extra subdivisions include flow patterns typically observed in serpentine tubes. It was also shown that the map may be used with reasonable success in identifying flow patterns for evaporating flows with low heat fluxes.

The "flow reversal" velocity necessary in allowing the total flow to travel upward in the vertical bend can be calculated to within ± 20 percent (for $G_L/G_G < 30$) by multiplying the flooding velocity calculated from the Kiehl-Koppany (17) correlation, by a factor of two.

Even though it was somewhat difficult to observe differences caused by the bend radius, it may be concluded that the larger bend hastens the

onset of a dry patch downstream of the bend. This is probably due to the fact that the large centrifugal forces ($\rho V^2/R$) on the entrained droplets are more efficient in de-entraining the droplets onto the outside wall in the small bend than in the large bend. The de-entrainment of these droplets increases the liquid film thickness in the outer tube wall region in the bend and consequently in the upper half of the straight tube downstream of the bend. The thicker liquid film in the small bend test section makes it less susceptible to dryout than the large bend test section. Another mechanism that may also aid in thickening the liquid film in the outer wall region of the small bend is the centrifuging of the wave crests from the inner wall to the outer wall.

The following observation derived from this study may be of practical use to designers working with serpentine coils.

Avoid operating equipment, for qualities less than 95 percent, near the wavy-annular border for G_G/Λ less than 4×10^4. The region where film inversion was observed was for values of G_G/Λ between 1.5×10^4 and 3.0×10^4.

This study reveals that the film inversion phenomenon, which can be very detrimental to steam generator designs incorporating horizontal serpentine tubes with vertically oriented bends, is quite complex and that there is scope for further research in trying to understand this anomalous behavior. The following recommendations are being made for future research in this area.

1. Study the effect of the bend radius by using a very tight bend and a very easy bend, e.g., 7/8 inch tube with a 2½ inch radius bend and a 10 inch radius bend.

2. Study the effect of tube diameter on film inversion behavior, e.g., 1/2 inch diameter tube through a 2 inch diameter tube.

3. Since the film inversion phenomenon is mostly a hydrodynamic problem, it is felt that the initial investigations should be carried out in detail with air-water mixtures. It is also felt that measurements of film thickness are quite important in analyzing film inversion in the bend. Therefore it is suggested that a film thickness measurement should be made, at least half-way in the bend, three-quarters in the bend, and up to 20 diameters in the downstream leg. The detailed presentation on liquid film measurement techniques given by Hewitt and Hall-Taylor (19) can be used as a guide in designing a film thickness measurement probe.

The film thickness measurements may lead to better understanding of the effects of bend radius, droplet entrainment and tube diameter on film inversion in the bend.

4. All the experiments should be conducted with the same loop so that any discrepancies associated with injection techniques and other operating parameters can be avoided. If this is possible then, conducting only a few runs with each test section would probably give better insight to the problem than conducting numerous experiments with only two or perhaps three test sections.

5. For heat transfer experiments, it is suggested that the two phase mixture be generated from one source rather than mixing it ahead of the test section. This type of an experiment will make the mass velocity and the inlet quality independent variables rather than dependent variables.

BIBLIOGRAPHY

(1) Carver, J. R., C. R. Kakarala, and J. S. Slotnik, "Heat Transfer in Coiled Tubes With Two Phase Flow," U.S.A.E.C. Report, TID-20988, 1964.

(2) Miropolskiy, Z. L., V. J. Picus, and M. E. Shitsman, "Regimes of Deteriorated Heat Transfer at Forced Flow of Fluids in Curvilinear Channels," 3rd Intl. Heat Transfer Conf., Chicago, Ill., V. 2, 1966, P. 95.

(3) Owhadi, A., K. J. Bell, and B. Crain, Jr., "Forced Convection Boiling Inside Helically Coiled Tubes," Intl. J. of Heat and Mass Transfer, V. 11, 1968, P. 1779.

(4) Banerjee, S., E. Rhodes, and D. S. Scott, "Film Inversion of Co-Current Two-Phase Flow in Helical Coils," AIChE Journal, V. 13(1), 1967, P. 189.

(5) Crain, Berry, Jr., "Forced Convection Heat Transfer to a Two-Phase Mixture of Water and Steam in a Helical Coil," Ph. D. thesis, Oklahoma State University, Stillwater, Okla. (1973).

(6) Lis, J. and M. J. Thelwell, "Experimental Investigation of Turbulent Heat Transfer in a Pipe Preceded by a 180° Bend," Proc. Inst. of Mech. Engrs., V. 178, Pt. 3I, 1963-64, P. 17.

(7) Ede, A. J., "The Effect of a 180° Bend on Heat Transfer to Water in a Tube," 3rd Intl. Heat Transfer Conf., Chicago, Ill., V. 1, 1966, P. 99.

(8) Alves, G. E., "Co-Current Liquid-Gas Flow in a Pipe-Line Contactor," Chem. Eng. Prog., V. 50, 1954, P. 449.

(9) Baker, O., "Simultaneous Flow of Oil and Gas," Oil and Gas J., V. 53(12), 1954, P. 185.

(10) Zahn, W. R., "A Visual Study of Two Phase Flow While Evaporating in Horizontal Tubes," J. of Heat Transfer, ASME Trans., V. 86, 1964, P. 417.

(11) Rounthwaite, C., "Two-Phase Heat Transfer in Horizontal Tubes," J. of Inst. of Fuel, Feb. 1968, P. 66.

(12) Lunn, D. C. F. and J. Harvey, "Corrosion at Trawsfyndd," Engineering, Feb. 1970, P. 189.

(13) Lis, J. and J. A. Strickland, "Local Variations of Heat Transfer in a Horizontal Steam Evaporator Tube," 4th Intl. Heat Transfer Conf., Paris, Paper B4.6, 1970.

(14) Robertson, J. M., "Dryout in Horizontal Hairpin Waste-Heat Boiler Tubes," 13th Natl. Heat Transfer Conf., Denver, Colo., A. I. Ch. E. Preprint No. 17, Aug. 1972.

(15) Scott, D. S., "Properties of Cocurrent Gas-Liquid Flow," Advances in Chemical Engineering, New York, Academic Press, 1963.

(16) Bell, K. J. J. Taborek and J. T. Fenoglio, "Interpretation of Horizontal In-Tube Condensation Heat Transfer Correlations With a Two Phase Flow Regime Map," Chem. Eng. Prog. Symp. Ser., No. 102, V. 66, 1970, P. 150.

(17) Collier, J. G., Convective Boiling and Condensation, New York, McGraw-Hill Book Co., 1972.

(18) Diehl, J. E. and C. R. Koppany, "Flooding Velocity Correlation for Gas-Liquid Counterflow in Vertical Tubes," Chem. Eng. Prog. Symp., No. 92, V. 65, 1968, P. 77.

(19) Hewitt, G. F. and N. S. Hall-Taylor, Annular Two-Phase Flow, Oxford, Pergamon Press, 1970.

(20) Butterworth, D., "Air-Water Annular Flow in a Horizontal Tube," AERE R-6687, Feb. 1967.

(21) Rohsenow, W. M. and J. P. Hartnett, Handbook of Heat Transfer, New York, McGraw-Hill Book Co., 1973.

(22) Dittus, F. W., and L. M. K. Boelter, Univ. of Calif. (Berkeley) Eng. Pub., V. 2, 1930, P. 443.

(23) Sieder, E. N., and C. E. Tate, "Heat Transfer and Pressure Drop of Liquids in Tubes," Ind. Eng. Chem., V. 28, 1936, P. 1429.

(24) Steltz, W. G., and G. J. Silvestri, "The Formulation of Steam Properties for Digital Computer Application," ASME Trans., V. 80, 1958, P. 967.

(25) Farukhi, M. N., "FORTRAN Subroutines for Calculating the Keenan and Keyes Steam Tables on the IBM 360 O.S. in Double Precision," Westinghouse Elec. Corp. Report, Tampa Div., WTD-LM-70-20, Aug. 1970.

(26) Anon., "Engineering Properties of INCONEL 600," International Nickel Co., Huntington, West Virginia, Technical Bulletin T-7, 1969.

APPENDIX A

AIR-WATER VISUAL TESTS

Loop Description

The Schematic diagram of the air-water loop is shown in Figure 62 and a photographic view is shown in Figure 63.

Laboratory air was delivered through an air filter to a pressure regulator. Air flowed from the regulator to an air-water mixing tee after passing through a rotameter (with interchangeable tubes and floats) and a control valve. The valve was used to control the air flow rate while the regulator was used to maintain a constant pressure in the air line.

A mixture of hot and cold city water was used for the liquid phase. Hot water was mixed with the cold water only when the cold water temperature was below 60°F. The inlet valves always throttled to damp out possible flow oscillations in the liquid supply lines. The water mixture flowed from the mixing tee to a flow control valve. Water from the valve flowed to an air-water mixing tee after passing through a small rotameter, a large rotameter and a venturi. A 200 cubic inch surge tank was incorporated in the water line between the control valve and the small rotameter to damp out possible flow oscillations in the supply line.

Liquid dye (green or red), an 8% solution of food coloring, was injected into the liquid stream at the throat of the venturi. The dye

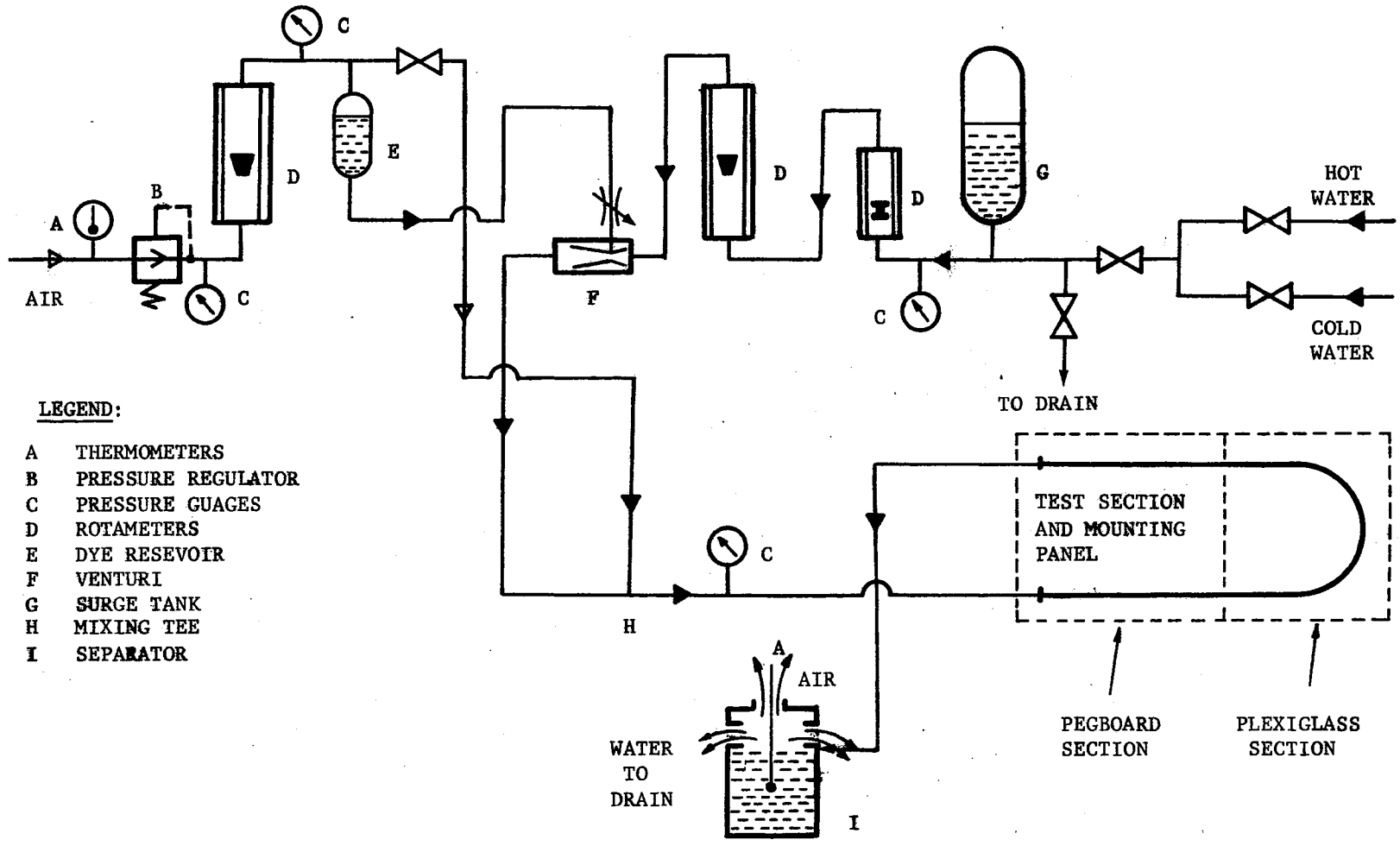

Figure 62. Air-Water Loop

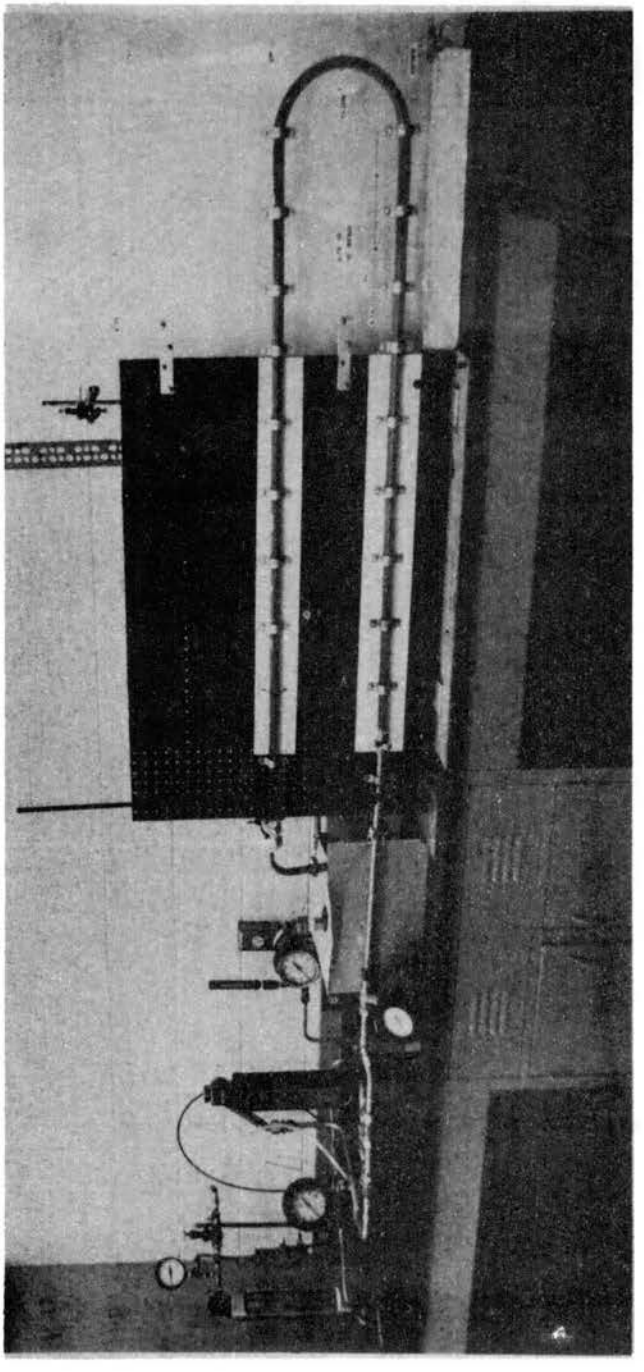

Figure 63. Photograph of the Air-Water Loop

reservoir was pressurized by air tapped from the air line upstream of the air valve. The injection rate was controlled by a needle valve.

Test Section Description

The clear test section was made from an 11-foot, 3/4-inch ID, TYGON tube. TYGON was chosen as the test section material because it is flexible and it could be bent to the 10-inch and 22-inch bend configurations that needed to be tested.

A schematic diagram of the test sections is given in Figure 64 with the appropriate dimensions. The test sections were mounted on a 1/4-inch thick pegboard-plexiglass stand. The pegboard dimensions were 28 inches high by 42 inches wide while those for the plexiglass were 26 inches high by 24 inches wide.

Instrumentation

The following parameters were recorded for all runs.

1. Air temperature upstream to the air filter using a mercury thermometer.

2. Air pressure upstream to the rotameter using a pressure gauge (0-160 PSIG).

3. Air pressure downstream to the rotameter using a pressure gauge (0-30 PSIG).

4. Air flow rate in SCFM using a Fischer and Porter interchangeable rotameter (0.25 to 27.5 SCFM).

5. Water flow rates in GPM using Fischer and Porter rotameters (0.06 to 0.6 GPM and 0.6 to 6.0 GPM, respectively).

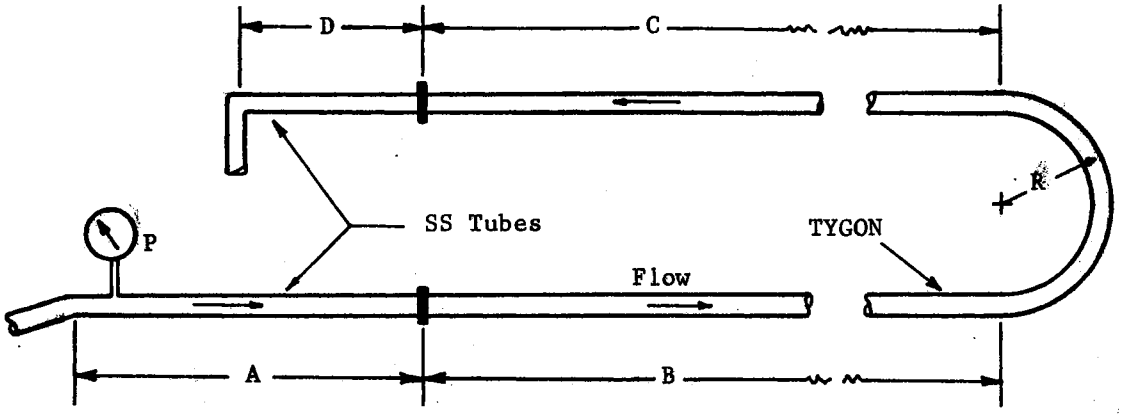

UPWARD FLOW TEST SECTION

R	A	B	C	D		E	F	G	H
10 inches	35	52¼	58½	5		8½	58½	52¼	7½
22 inches	35	47	47	13		18½	47½	47	9

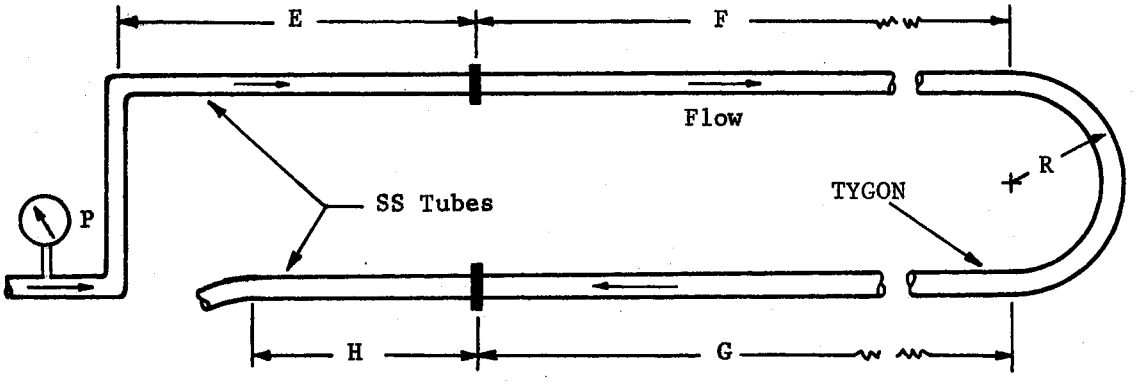

DOWNWARD FLOW TEST SECTION

Figure 64. TYGON Test Sections

6. Air-water mixture pressure after the mixing tee by using a pressure guage (0 to 30 PSIG).

7. Mixture temperature in the exit chamber using a mercury thermometer.

Photographic Techniques

Most of the runs were recorded on 35mm color slides while some duplicate runs were recorded on 16mm movie film.

Diffused back lighting was used for illumination. This was accomplished by passing the light from two 300 watt photoflood lamps, inside parabolic reflectors, and three 100 watt photofloods, inside conical reflectors, through a sheet of tracing paper which was placed behind the plexiglass section.

A MINOLTA SR-7 single lens reflex camera with 55mm lens was used for the slide pictures. High speed EKTACHROME film (ASA 125), a shutter speed of 1/1000 and a lens opening between f4 and f5.6 were used for the still photography.

A 16mm BOLEX camera, with a 25mm and a 50mm lens, was used for taking movies. High speed EKTACHROME (ASA 125) film, a lens opening of f5.6 and a frame speed of 64fps were used for taking the motion pictures.

Loop Operating Procedure

The loop was started by opening the water flow control valve. The valve was then intermittently opened and closed to deaerate the system. Some air was intentionally trapped in the surge tank so that the tank could serve as a capacitor.

Once the system had been deaerated, several runs were made by holding the liquid flow rate constant while varying the air flow rate from about a minimum to a maximum. All of the still pictures were taken after the initial transient introduced by varying the air flow had decayed and a flow pattern had been established. Movie films were taken after a series of still pictures were taken by duplicating the runs.

The amount of dye injected, in most runs, was low enough that corrections to the liquid flow rate were unnecessary. However, in some runs that were labelled "special," only the dye solution was used for the liquid phase and the liquid flow rate was measured by timing a known volume of dye flowing through the test section.

APPENDIX B

NUMERICAL SOLUTION OF WALL TEMPERATURE GRADIENT WITH INTERNAL HEAT GENERATION

A numerical solution of the conduction equation with internal heat generation and variable thermal conductivity and electrical resistivity is outlined in this appendix. A discussion on how the variation in wall thickness in the bend was accommodated in the solution is also given.

Heat Balance on an Incremental Element

Assumptions and Conditions

The following assumptions and conditions are used in deriving the numerical solution.

1. Electrical resistivity is a function of temperature.
2. Thermal conductivity is a function of temperature.
3. Peripheral wall conduction exists.
4. Axial conduction is negligible.
5. Steady state conditions exist.
6. Heat losses to the atmosphere are present.

The tube wall was divided into ten equal slices and the inside surface temperature was obtained directly (since the outside wall temperature was known) by performing heat balances on each node in the radial direction. The tube cross-section was divided into octants.

Interior Nodes

Consider the cross-section of a typical interior element as shown in Figure 65.

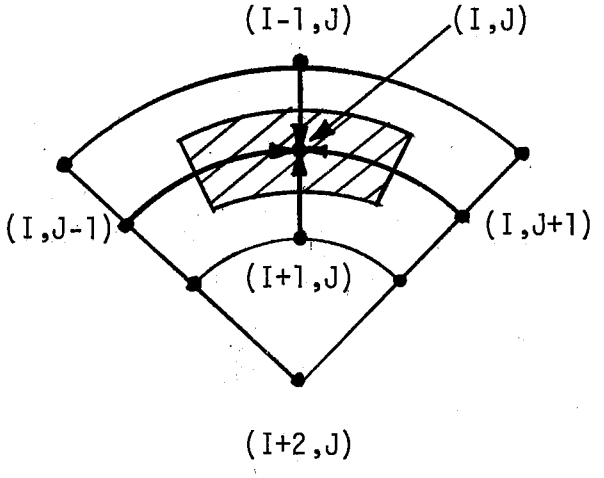

Figure 65. Interior Element

An energy balance on the element gives,

$$q_1 + q_2 + q_3 + q_4 + q_g = 0. \tag{1}$$

From Fourier's law we know that

$$q = -KA \frac{dt}{dx} \tag{2}$$

Now using subscripts I and J for the radial and peripheral direction, respectively (as shown in Figure 65), and writing Fourier's equation for side 1, we obtain

$$q_1 = q_{(I-1,J)} = -K_{avg}(rd\phi)_{I-\frac{1}{2}}(dz)[t_{(I-1,J)} - t_{(I,J)}]/ (r_{(I-1)} - r_I) \tag{3}$$

where

$$d\phi = \pi/4 \text{ (eight thermocouple locations)}$$

$$(r_{(I-1)} - r_I) = \Delta r \text{ (taking equal increments)}$$

$$K_{avg} = (K_{I-1} + K_I)/2.0$$

$$r_{I-\frac{1}{2}} = (r_{I-1} - \frac{\Delta r}{2}) \text{ and } r_{I+\frac{1}{2}} = (r_{I+1} + \frac{\Delta r}{2}).$$

Assuming that heat transfer into the element is positive and since Δr is a negative term, the minus sign can be deleted from Equation (3).

Substituting the definitions into Equation (3) gives

$$q_{I-1,J} = \frac{(K_{I-1,J} + K_{I,J})}{2} (\frac{\pi}{4}) (r_{I-1} - \frac{\Delta r}{2}) \frac{(t_{I-1,J} - t_{I,J})}{\Delta r} . \quad (4)$$

Similarly for side 3,

$$q_{I+1,J} = \frac{(K_{I+1,J} + K_{I,J})}{2} (\frac{\pi}{4}) (r_{I+1} + \frac{\Delta r}{2}) \frac{(t_{I+1,J} - t_{I,J})}{\Delta r} dz. \quad (5)$$

Writing Fourier's equation for side 2 gives

$$q_2 = q_{I,J+1} = K_{avg}(dr\ dz)\ (t_{I,J+1} - t_{I,J})/(r_I d\phi). \quad (6)$$

Substituting the definitions for some of the variables gives

$$q_{I,J+1} = \frac{(K_{I,J+1} + K_{I,J})}{2} (\Delta r)(\frac{4}{\pi r_I})(t_{I,J+1} - t_{I,J})\ dz. \quad (7)$$

Similarly for side 4,

$$q_{I,J-1} = \frac{(K_{I,J-1} + K_{I,J})}{2} (\Delta r)(\frac{4}{\pi r_I})(t_{I,J-1} - t_{I,J})\ dz. \quad (8)$$

The heat generation term is calculated from the equation for Joulean heating.

$$q_g = I^2R \quad (9)$$

where

$$R = \frac{\rho dz}{A_{cs}} (3.412)$$

ρ = electrical resistivity and a function of temperature at node (I,J)

and

$$A_{cs} = \frac{\pi}{4}(r_I\ \Delta r). \tag{10}$$

Substituting the above definitions into Equation (9) gives

$$q_g = (3.412)\left(\frac{4}{\pi r\ \Delta r}\right)(\rho)(I^2)\ dz. \tag{11}$$

Combining Equations (4), (5), (7), (8), and (10) and rearranging the terms give

$$t_{I+1,J} = t_{I,J} - \{\left(\frac{3.412}{X\ AREA}\right)(eI^2) + \left(\frac{DPHI}{2\ DELR}\right)(K_{I-1,J} + K_{I,J})$$
$$(r_{I-1,J} - \frac{DELR}{2})(t_{I-1,J} - t_{I,J}) + \left(\frac{DELR}{2\ DPHI}\right)$$
$$(K_{I,J-1} + K_{I,J})\left(\frac{1}{r_I}\right)(t_{I,J-1} - t_{I,J})$$
$$+ \left(\frac{DELR}{2\ DPHI}\right)(K_{I,J+1} + K_{I,J})\left(\frac{1}{r_I}\right)(t_{I,J+1} - t_{I,J})\}/$$
$$\{\left(\frac{DPHI}{2\ DELR}\right)(K_{I+1,J} + \frac{DELR}{2})(K_{I+1,J} + K_{I,J})\}, \tag{12}$$

where

DPHI = $\pi/4$

X AREA = $(r_{I,J})(\pi/4)(\Delta r)$

DELR = Δr.

Equation (12) is used for all the interior elements. For the outside wall element, which is really a "half-size" element, Equations (5), (7), (8), and (9) are solved simultaneously in conjunction with the following equation, which accounts for the heat loss.

$$q_L = \left(\frac{q_\ell}{8L_t}\right)\left(\frac{t_{room} - t_{I,J}}{t_o - t_{or}}\right)\ dz \tag{13}$$

where

q_e = heat loss for element (from calibration run)

L_t = heated tube length

t_o = surface temperature during calibration run

t_{or} = room temperature during calibration run.

For the outside wall node the temperatures for nodes (I-1,J), (I, J+1) and (I,J-1), are known since the first node condition is given by Equation (13) and the other three nodal temperatures are thermocouple readings. Consequently, the temperature at node (I+1,J) can be calculated. After all the (I+1,J) temperature values are calculated, successive use of Equation (12) gives the temperature at the inside surface.

Heat Flux at Inside Wall

The procedure for performing heat balances outlined above gives the radial heat flux at the inside wall when the heat balance is made on the inside surface ("half-size") node. This heat flux value was used in calculating the heat transfer coefficients.

Wall Thickness Calculations in the Bend

The variations in wall thickness in the bend were incorporated in the computer program by using a procedure similar to the one outlined by Carver et al. (1).

Assumptions

The following assumptions were made for the tube geometry.

1. Negligible ovality.

2. Conservation of tube material volume during bending.

For a straight tube the cross-section would be similar to the one shown in Figure 66 and for a bent tube it would be similar to the one shown in Figure 67.

The mean length for the three different elements can be written as

$$L_o = (R + r + \frac{T_o}{2})\, d\theta \tag{14}$$

$$L_i = (R - r - \frac{T_i}{2})\, d\theta \tag{15}$$

$$L_c = Rd\theta. \tag{16}$$

Using the conservation of material volume assumption gives

$$\{(rd\alpha + (r + T_o)d\alpha)\frac{T_o}{2} \quad (R + r + \frac{T_o}{2})d = (rd\alpha + (r + T_c)$$

$$d\alpha)\frac{F_c}{2}\} Rd\theta \tag{17}$$

The terms $d\alpha$ and $d\theta$ drop out of the equation and the following equation is then obtained.

$$(2r + T_o)(T_o)(R + r + \frac{T_o}{2}) = (2r + T_c)(F_c)(R). \tag{18}$$

Similarly

$$(2r + T_i)(T_i)(R - r - \frac{T_i}{2}) = (2r + T_c)(T_c)(R). \tag{19}$$

In Equations (18) and (19) all the variables except T_o and T_i are known. Solving these equations by trial and error gives the values for the maximum and minimum thickness. For the thickness at the other peripheral and axial locations, an average value of the adjacent thicknesses were used.

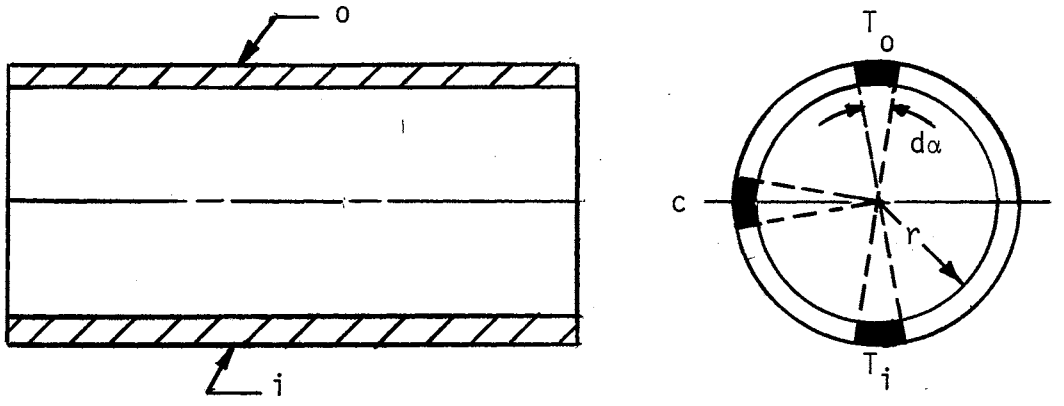

Figure 66. Cross-Section for Straight Tube

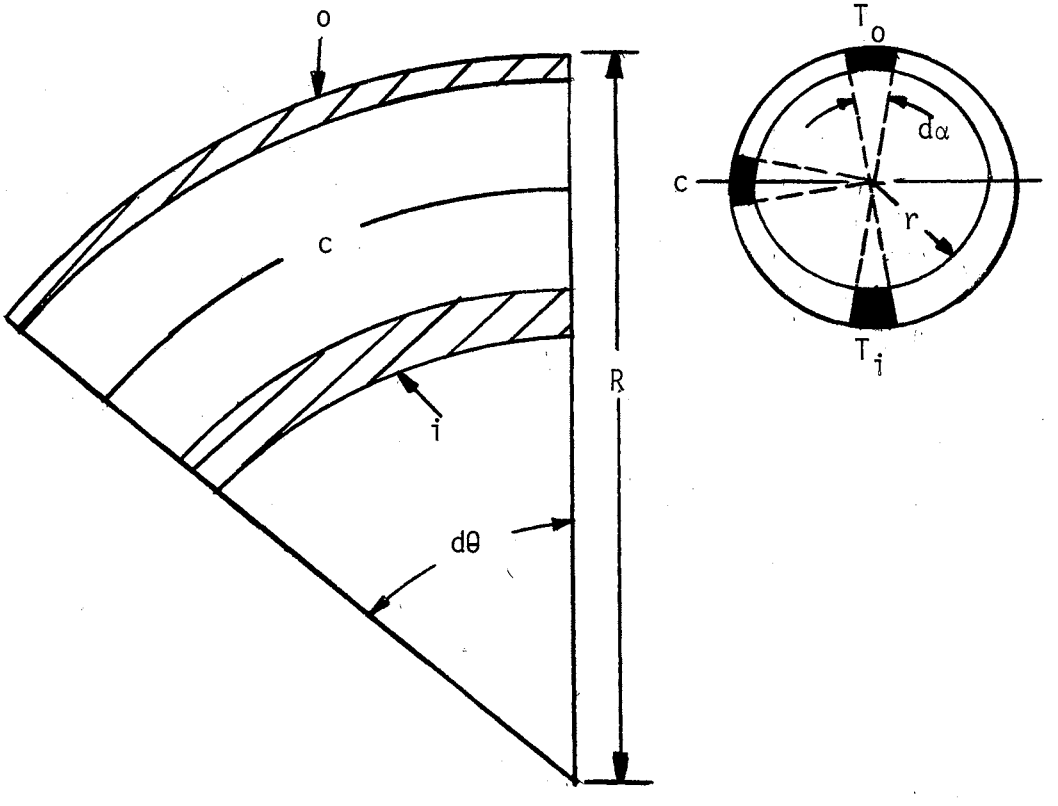

Figure 67. Cross-Section for Curved Tube

APPENDIX C

SINGLE PHASE HEAT TRANSFER TESTS

Two single phase heat transfer runs were made to check the accuracy of the calculated average heat transfer coefficients with the well-known Dittus-Boelter (22) and Sieder-Tate (23) correlations. The results indicate that the data fit the correlations quite accurately. The single phase run, Run 103, for the small bend was made in the turbulent region whereas the run for the large bend, Run 203, was made in the upper range of the transition region. It was intended that both runs be made with Reynolds number greater than 10,000, but this was only possible when the inlet temperatures were greater than 170°F due to pump limitations. Run 103 was made for this condition but Run 203 was made with the inlet temperature of 85°F since there was a tendency to initiate subcooled boiling with low heat fluxes for the higher inlet temperatures. Consequently, Run 203 was made with the Reynolds number equal to 7,295. A summary of the results is given in Tables V and VI below.

The tabulated results show that the average heat transfer coefficients immediately after the bend are enhanced. Similar findings were reported by Ede (7) with his investigations of single phase heat transfer inside 180 degree bends in the turbulent region. The laminarization effect of the bend on single phase fluid flow is also indicated in the

tabulated results in that the heat transfer coefficients for axial locations 5, 6, and 7 are generally lower than values obtained from either the Dittus-Boelter correlation or the Sieder-Tate correlation.

TABLE V

SINGLE PHASE EXPERIMENTAL CONDITIONS

Conditions	Run 103	Run 203
Average Heat Flux--Btu/(hr.-sq. ft.)	2,615	11,342
Mass Velocity--lbm/(hr.-sq. ft.)	143,515	173,865
Reynolds Number	11,000	7,295
Inlet Temperature--°F	172.2	85.7
Outlet Temperature--°F	184.4	127.9

TABLE VI

CIRCUMFERENTIAL AVERAGE HEAT TRANSFER COEFFICIENTS--BTU/(HR.-SQ. FT.-°F)

	Axial Locations										
Investigators	1	2	3	4	5	6	7	8	9	10	11
Run 103											
Author	327	344	348	265	266	273	342	400	406	381	314
Dittus-Boelter	318	322	323	323	323	324	324	325	325	326	328
Sieder-Tate	356	361	362	363	363	364	364	365	365	366	372
Run 203											
Author	281	348	355	239	242	312	416	350	299	321	327
Dittus-Boelter	258	275	278	282	286	289	293	296	299	302	312
Sieder-Tate	288	305	309	317	322	324	327	331	336	339	352

APPENDIX D

SAMPLE CALCULATIONS

This appendix shows how the heat transfer coefficients for the steam-water tests were calculated. The sample calculation shown below is for thermocouple location 1 at axial station 1 and for Run 112. Raw data for the run is shown in Table VII below. Since most of the calculations are quite tedious, only the highlights will be given here.

TABLE VII

RAW DATA FOR RUN 112

Data		Units
Exit Water Flow Rate	=	23.12 lbm/hour
Exit Steam Flow Rate	=	107.73 lbm/hour
Current to Tube	=	302.00 amps
Voltage Drop in Tube	=	12.35 volts
Atmospheric Pressure	=	29.17 inches hg
Avg. Loop Temperature	=	215.80 degrees F
Room Temperature	=	86.00 degrees F
Uncorrected Inlet Temperature	=	232.30 degrees F
Uncorrected Outlet Temperature	=	229.20 degrees F
Uncorrected Inlet Pressure	=	7.10 psig
Uncorrected Outlet Pressure	=	6.28 psig
Uncorrected Pressure at 1	=	7.02 psig
Uncorrected Pressure at 2	=	6.72 psig
Uncorrected Pressure at 3	=	6.88 psig
Uncorrected Pressure at 4	=	6.55 psig
Thermocouple 1/1 Reading	=	235.50 degrees F

All thermal and transport properties for the steam-water mixtures were calculated from the Keenan and Keyes steam tables (24) that were reformulated by Farukhi (25) and stored on disk. The values for the thermal conductivity of INCONEL 600 were obtained from the INCO technical bulletin (26).

The inlet mixture thermocouple reading was corrected by the following equation:

$$t_{in} = t_{in} - 0.7/(210.7 - 72.0) \times (t_{in} - t_{room})$$

and the corrected temperature is

$$t_{in} = 231.6°F.$$

Similarly the outlet temperature reading was corrected by

$$t_{out} = t_{out} - 0.9/(210.7 - 72.0) \times (t_{out} - t_{room})$$

and

$$t_{out} = 228.3°F.$$

The heat lost from the test section was calculated by using the heat loss value obtained from the calibration runs and the following equation:

$$Q_{loss} = 596/(211.5 - 78.2) \times [(t_{in} + t_{out})/2 - t_{room}].$$

The heat losses and the temperature readings were assumed to be proportional to the difference between the room temperature and the recorded temperature.

Pressure readings for stations 3, 4, and outlet were corrected for pressure changes due to fluid in the connecting lines. The values were then used to calculate corresponding saturation temperatures using the steam tables. There were minor differences between the inlet and outlet saturation temperature values obtained from the pressure readings and

the values obtained from the thermocouple readings. It was felt that the thermocouple readings were more reliable since they were calibrated in situ and consequently they were used for further calculations. However, the ratios of the temperatures obtained from the pressure readings (based on tube length) were used to establish the saturation temperatures at the 11 thermocouple station locations.

The saturation temperature for axial location 1 is:

$$t_{sat} = 231.27°F.$$

The total mass flow rate is:

$$W_t = W_w + W_s$$

$$= 23.12 + 107.73$$

$$= 130.85 \text{ lbm/hr.}$$

The mass velocity is:

$$G_t = W_t/A_i$$

$$= 130.85/0.00324$$

$$= 40358.7 \text{ lbm/(hr.-sq. ft.)}.$$

The exit quality at the cyclone, obtained from the raw data is:

$$X_e = W_s/W_t$$

$$= 107.73/130.85$$

$$= 82.33\%.$$

The outlet quality at the test section was calculated by allowing for loop losses. Once again the loop losses for this run were calculated by using the loop losses obtained during the calibration runs. The quality at the exit electrode was then calculated by using the loop losses for the section between the exit electrode and the exit thermocouple. The qualities for the axial stations were calculated by

allowing for the heat losses as well as the heat addition to the test section. Using this method the quality at the inlet electrode was eventually calculated. The values for steam qualities given in Appendix E are the values at the inlet and exit electrode, i.e., start of heating and end of heating.

The quality at station 1 is:

$$X_1 = 72.52\%.$$

Values of the enthalpies were calculated by starting from the exit electrode and proceeding to the inlet electrode. The calculations were performed simultaneously with the steam quality calculations.

The inside wall temperatures were obtained via the conduction equation outlined in Appendix B after the thermocouple reading was corrected.

The inside wall temperature at location 1/1 is:

$$t_i = 234.32°F.$$

The heat flux at each thermocouple location was obtained by performing a heat balance on the inside node as explained in Appendix B.

At location 1/1 the heat flux value is:

$$Q/A_i = 5388.25 \text{ Btu/(hr.-sq. ft.)}.$$

Finally, the heat transfer coefficient at location 1/1 is:

$$h_{tp} = \frac{Q/A_i}{t_i - t_{sat}}$$

$$= 5388.25/(234.32 - 321.27)$$

$$= 1766.5 \text{ Btu/(hr.-sq. ft.-°F)}.$$

APPENDIX E

EXPERIMENTAL DATA FROM STEAM-WATER TESTS

RUN NUMBER 104

VOLTAGE DROP IN TUBE	= 5.0	VOLTS	
CURRENT TO TEST SECTION	= 122.0	AMPS	
CALCULATED HEAT GENERATION	= 2026.9	BTU/HOUR	(Q=I*I*R)
HEAT LOSS IN TEST SECTION	= 487.9	BTU/HOUR	(HEATED PART)
HEAT TRANSFERRED TO THE MIXTURE	= 1539.0	BTU/HOUR	(QIN=QGEN-QLOSS)
TOTAL MASS VELOCITY	= 28104.6	LBM/(HR-SQ.FT)	
AVERAGE HEAT FLUX	= 698.9	BTU/(HR-SQ.FT)	

AXIAL STATION	QUALITY %	ENTHALPY BTU/HOUR	SAT TEMP DEGREE F	SAT PRESS PSIA
START	89.57	1055.39	226.31	19.39
1	89.62	1055.86	226.27	19.37
2	90.29	1062.12	225.84	19.22
3	90.37	1062.86	225.76	19.19
4	90.43	1063.40	225.68	19.16
5	90.48	1063.85	225.60	19.13
6	90.53	1064.29	225.52	19.10
7	90.58	1064.74	225.45	19.07
8	90.67	1065.57	225.36	19.04
9	90.75	1066.32	225.31	19.02
10	90.83	1067.07	225.26	19.01
11	91.33	1071.75	224.95	18.89
END	91.39	1072.28	224.91	18.88

CORRECTED OUTSIDE WALL TEMPERATURES - DEGREES F

AXIAL STATION LOCATIONS

	1	2	3	4	5	6	7	8	9	10	11
1	227.2	246.6	248.0	227.6	227.3	227.4	243.6	247.7	248.9	250.1	254.6
2	227.2	244.2	245.9	227.1	226.8	230.0	243.3	246.3	245.4	248.4	251.8
3	227.3	237.7	238.6	226.9	226.8	235.7	241.0	242.1	241.9	241.7	243.2
4	227.1	227.6	227.7	226.7	226.7	235.3	232.9	232.0	230.3	229.3	228.6
5	227.7	227.5	227.3	227.1	226.9	237.5	227.1	226.8	226.9	226.9	227.0
6	227.4	228.0	227.7	227.0	227.1	239.1	233.3	231.2	228.9	228.7	230.1
7	227.3	237.7	237.6	227.1	226.8	239.2	241.7	243.3	241.8	241.8	245.1
8	227.2	244.8	245.5	227.1	226.8	230.5	243.7	247.2	247.5	248.5	253.8

RUN NUMBER 105

VOLTAGE DROP IN TUBE	= 4.1	VOLTS	
CURRENT TO TEST SECTION	= 100.0	AMPS	
CALCULATED HEAT GENERATION	= 1361.2	BTU/HOUR	(Q=I*I*R)
HEAT LOSS IN TEST SECTION	= 512.1	BTU/HOUR	(HEATED PART)
HEAT TRANSFERRED TO THE MIXTURE	= 849.1	BTU/HOUR	(QIN=QGEN-QLOSS)
TOTAL MASS VELOCITY	= 32413.4	LBM/(HR-SQ.FT)	
AVERAGE HEAT FLUX	= 385.6	BTU/(HR-SQ.FT)	

AXIAL STATION	QUALITY %	ENTHALPY BTU/HOUR	SAT TEMP DEGREE F	SAT PRESS PSIA
START	83.53	997.91	227.47	19.82
1	83.56	998.17	227.45	19.81
2	83.88	1001.09	227.13	19.69
3	83.93	1001.52	227.02	19.65
4	83.96	1001.75	226.89	19.60
5	83.99	1001.98	226.76	19.55
6	84.02	1002.20	226.63	19.51
7	84.05	1002.44	226.51	19.46
8	84.09	1002.76	226.38	19.41
9	84.13	1003.12	226.32	19.39
10	84.17	1003.47	226.26	19.37
11	84.42	1005.70	225.88	19.23
END	84.45	1005.99	225.84	19.22

CORRECTED OUTSIDE WALL TEMPERATURES - DEGREES F

AXIAL STATION LOCATIONS

	1	2	3	4	5	6	7	8	9	10	11
1	227.7	227.4	227.3	227.3	227.5	227.6	226.9	226.5	227.0	230.4	228.7
2	227.7	227.4	227.3	227.2	227.4	227.3	226.8	226.6	227.0	229.4	226.7
3	227.7	227.4	227.3	227.1	227.3	227.1	226.9	226.8	226.8	226.9	226.7
4	227.7	227.4	227.3	227.1	227.3	227.0	227.1	226.8	226.8	226.9	226.5
5	227.8	227.5	227.4	227.1	227.2	227.0	227.3	227.0	226.9	227.0	226.8
6	227.9	227.6	227.5	227.1	227.4	227.1	227.0	226.9	226.8	226.9	226.6
7	227.9	227.6	227.5	227.1	227.1	227.1	226.9	226.8	226.7	226.9	226.5
8	227.8	227.5	227.4	227.1	227.3	227.4	227.0	226.7	226.8	229.0	227.2

RUN NUMBER 106

VOLTAGE DROP IN TUBE	= 5.4	VOLTS	
CURRENT TO TEST SECTION	= 130.0	AMPS	
CALCULATED HEAT GENERATION	= 2300.2	BTU/HOUR	(Q=I*I*R)
HEAT LOSS IN TEST SECTION	= 504.2	BTU/HOUR	(HEATED PART)
HEAT TRANSFERRED TO THE MIXTURE	= 1796.1	BTU/HOUR	(QIN=QGEN-QLOSS)
TOTAL MASS VELOCITY	= 32472.0	LBM/(HR-SQ.FT)	
AVERAGE HEAT FLUX	= 815.6	BTU/(HR-SQ.FT)	

AXIAL STATION	QUALITY %	ENTHALPY BTU/HOUR	SAT TEMP DEGREE F	SAT PRESS PSIA
START	82.94	992.14	227.29	19.75
1	83.00	992.68	227.21	19.72
2	83.70	998.97	226.29	19.38
3	83.78	999.70	226.20	19.35
4	83.83	1000.16	226.17	19.34
5	83.88	1000.64	226.15	19.33
6	83.94	1001.20	226.12	19.32
7	83.99	1001.67	226.09	19.31
8	84.07	1002.41	226.03	19.29
9	84.16	1003.24	225.97	19.26
10	84.24	1003.98	225.90	19.24
11	84.75	1008.70	225.51	19.10
END	84.80	1009.20	225.47	19.08

CORRECTED OUTSIDE WALL TEMPERATURES - DEGREES F

AXIAL STATION LOCATIONS

	1	2	3	4	5	6	7	8	9	10	11
1	227.9	230.2	231.5	228.1	228.0	228.2	227.1	226.9	236.7	237.7	232.8
2	228.0	227.8	228.4	228.0	227.9	227.9	227.1	227.5	232.4	232.6	227.5
3	228.0	227.7	227.7	227.6	227.5	227.4	227.1	227.1	227.1	227.2	226.9
4	228.0	227.6	227.9	227.5	227.4	227.3	227.5	227.2	227.2	227.0	227.0
5	228.3	227.9	227.8	227.5	227.4	227.2	227.9	227.5	227.3	227.3	227.1
6	228.4	227.6	227.9	227.6	227.5	227.4	227.6	227.3	227.2	227.0	227.0
7	228.2	227.7	228.0	227.6	227.5	227.4	227.1	227.1	227.0	227.0	226.8
8	227.9	228.0	227.7	227.9	227.9	228.0	227.1	227.5	229.7	231.9	228.9

RUN NUMBER 107

VOLTAGE DROP IN TUBE	= 8.2	VOLTS	
CURRENT TO TEST SECTION	= 200.0	AMPS	
CALCULATED HEAT GENERATION	= 5445.5	BTU/HOUR	(Q=I*I*R)
HEAT LOSS IN TEST SECTION	= 504.7	BTU/HOUR	(HEATED PART)
HEAT TRANSFERRED TO THE MIXTURE	= 4940.8	BTU/HOUR	(QIN=QGEN-QLOSS)
TOTAL MASS VELOCITY	= 34689.6	LBM/(HR-SQ.FT)	
AVERAGE HEAT FLUX	= 2243.6	BTU/(HR-SQ.FT)	

AXIAL STATION	QUALITY %	ENTHALPY BTU/HOUR	SAT TEMP DEGREE F	SAT PRESS PSIA
START	82.60	989.33	228.18	20.08
1	82.75	990.71	228.14	20.07
2	84.45	1006.83	227.70	19.90
3	84.66	1008.80	227.59	19.86
4	84.80	1010.09	227.47	19.82
5	84.93	1011.28	227.35	19.77
6	85.07	1012.57	227.23	19.73
7	85.20	1013.76	227.11	19.68
8	85.42	1015.82	226.99	19.64
9	85.63	1017.81	226.92	19.61
10	85.84	1019.79	226.85	19.59
11	87.12	1031.91	226.43	19.43
END	87.26	1033.26	226.38	19.41

CORRECTED OUTSIDE WALL TEMPERATURES - DEGREES F

AXIAL STATION LOCATIONS

	1	2	3	4	5	6	7	8	9	10	11
1	229.5	236.5	240.3	229.8	229.6	230.0	228.2	267.1	265.3	260.7	244.5
2	229.8	229.4	230.6	229.4	229.0	229.2	228.3	259.7	252.1	247.8	230.1
3	229.9	229.4	229.1	228.7	228.2	228.2	230.4	238.0	230.3	228.8	228.0
4	229.9	229.3	229.2	228.5	228.1	228.0	228.9	228.9	228.6	228.6	228.1
5	230.2	229.5	229.2	228.6	228.0	227.8	229.7	229.1	228.9	229.0	228.4
6	230.2	229.3	229.2	228.7	228.1	227.9	229.0	229.0	228.7	228.7	228.2
7	230.1	229.4	230.9	228.9	228.3	228.1	233.1	241.3	229.7	228.9	228.0
8	229.6	231.6	229.4	229.5	229.2	229.4	229.5	261.8	254.8	247.8	234.1

RUN NUMBER 108

VOLTAGE DROP IN TUBE	= 10.3	VOLTS	
CURRENT TO TEST SECTION	= 250.0	AMPS	
CALCULATED HEAT GENERATION	= 8502.7	BTU/HOUR	(Q=I*I*R)
HEAT LOSS IN TEST SECTION	= 465.1	BTU/HOUR	(HEATED PART)
HEAT TRANSFERRED TO THE MIXTURE	= 8037.6	BTU/HOUR	(QIN=QGEN-QLOSS)
TOTAL MASS VELOCITY	= 33388.0	LBM/(HR-SQ.FT)	
AVERAGE HEAT FLUX	= 3649.9	BTU/(HR-SQ.FT)	

AXIAL STATION	QUALITY %	ENTHALPY BTU/HOUR	SAT TEMP DEGREE F	SAT PRESS PSIA
START	65.47	819.38	218.80	16.79
1	65.71	821.64	218.75	16.78
2	68.56	848.86	218.19	16.59
3	68.92	852.27	218.08	16.56
4	69.15	854.44	217.98	16.53
5	69.37	856.51	217.88	16.49
6	69.59	858.58	217.78	16.46
7	69.82	860.74	217.67	16.43
8	70.17	864.06	217.56	16.39
9	70.53	867.50	217.48	16.37
10	70.89	870.94	217.40	16.34
11	73.03	891.36	216.91	16.19
END	73.27	893.63	216.85	16.17

CORRECTED OUTSIDE WALL TEMPERATURES - DEGREES F

AXIAL STATION LOCATIONS

	1	2	3	4	5	6	7	8	9	10	11
1	221.6	233.5	233.5	223.0	222.9	223.3	219.6	226.5	271.9	258.0	220.0
2	221.7	222.1	222.6	222.2	222.0	222.2	219.6	225.6	249.7	235.4	220.2
3	222.2	221.6	221.6	221.0	220.9	220.7	219.9	220.9	221.7	220.8	220.7
4	222.2	221.5	221.6	220.8	220.5	220.0	221.5	221.2	221.2	221.1	221.0
5	222.8	222.0	221.8	221.0	220.5	219.9	222.6	221.7	221.8	221.6	221.3
6	222.7	221.9	221.6	221.2	220.9	220.0	221.6	221.4	221.4	221.1	221.4
7	222.6	221.8	222.1	221.4	221.1	220.5	220.0	221.9	221.2	220.9	220.4
8	221.8	222.5	221.9	222.3	222.1	222.7	219.7	231.7	253.0	234.0	221.1

RUN NUMBER 109

VOLTAGE DROP IN TUBE	= 4.1	VOLTS	
CURRENT TO TEST SECTION	= 100.0	AMPS	
CALCULATED HEAT GENERATION	= 1362.0	BTU/HOUR	(Q=I*I*R)
HEAT LOSS IN TEST SECTION	= 529.9	BTU/HOUR	(HEATED PART)
HEAT TRANSFERRED TO THE MIXTURE	= 832.1	BTU/HOUR	(QIN=QGEN-QLOSS)
TOTAL MASS VELOCITY	= 37033.7	LBM/(HR-SQ.FT)	
AVERAGE HEAT FLUX	= 377.9	BTU/(HR-SQ.FT)	

AXIAL STATION	QUALITY %	ENTHALPY BTU/HOUR	SAT TEMP DEGREE F	SAT PRESS PSIA
START	95.50	1115.82	235.15	22.86
1	95.52	1115.99	235.11	22.84
2	95.81	1118.57	234.61	22.63
3	95.85	1118.92	234.51	22.59
4	95.87	1119.07	234.41	22.55
5	95.90	1119.32	234.31	22.51
6	95.92	1119.47	234.21	22.47
7	95.95	1119.72	234.11	22.43
8	95.98	1119.97	234.00	22.38
9	96.02	1120.32	233.92	22.35
10	96.06	1120.67	233.84	22.31
11	96.27	1122.50	233.38	22.13
END	96.30	1122.75	233.33	22.10

CORRECTED OUTSIDE WALL TEMPERATURES - DEGREES F

AXIAL STATION LOCATIONS

	1	2	3	4	5	6	7	8	9	10	11
1	236.2	235.8	235.5	236.0	236.0	235.9	240.8	243.8	244.9	245.7	247.5
2	236.2	235.7	235.6	235.9	235.6	235.9	240.9	243.4	242.3	244.7	246.0
3	236.4	235.8	235.7	235.7	235.7	235.7	240.5	241.5	241.5	241.5	241.0
4	236.2	235.6	235.6	235.8	235.7	235.4	237.1	236.6	235.8	235.8	235.3
5	236.5	236.0	235.9	235.9	235.8	235.5	235.5	235.1	235.3	235.3	235.3
6	236.4	235.7	235.6	235.8	236.0	235.5	237.4	236.5	235.9	235.6	235.9
7	236.2	235.5	235.5	235.8	235.5	235.7	241.0	242.3	241.6	241.8	242.3
8	236.0	235.6	235.7	235.7	235.7	235.8	241.2	244.1	244.4	245.0	247.5

RUN NUMBER 110

VOLTAGE DROP IN TUBE	= 8.3	VOLTS	
CURRENT TO TEST SECTION	= 205.0	AMPS	
CALCULATED HEAT GENERATION	= 5718.1	BTU/HOUR	(Q=I*I*R)
HEAT LOSS IN TEST SECTION	= 481.4	BTU/HOUR	(HEATED PART)
HEAT TRANSFERRED TO THE MIXTURE	= 5236.8	BTU/HOUR	(QIN=QGEN-QLOSS)
TOTAL MASS VELOCITY	= 36944.3	LBM/(HR-SQ.FT)	
AVERAGE HEAT FLUX	= 2378.0	BTU/(HR-SQ.FT)	

AXIAL STATION	QUALITY %	ENTHALPY BTU/HOUR	SAT TEMP DEGREE F	SAT PRESS PSIA
START	72.30	887.85	223.46	18.37
1	72.44	889.19	223.41	18.35
2	74.14	905.20	222.74	18.12
3	74.36	907.25	222.61	18.07
4	74.49	908.44	222.49	18.03
5	74.63	909.72	222.36	17.98
6	74.76	910.91	222.24	17.94
7	74.90	912.19	222.11	17.90
8	75.11	914.15	221.98	17.85
9	75.33	916.22	221.89	17.82
10	75.54	918.20	221.80	17.79
11	76.82	930.27	221.28	17.62
END	76.96	931.57	221.22	17.60

CORRECTED OUTSIDE WALL TEMPERATURES - DEGREES F

AXIAL STATION LOCATIONS

	1	2	3	4	5	6	7	8	9	10	11
1	225.1	225.1	225.3	225.8	225.7	225.6	223.4	223.5	223.4	223.9	223.3
2	225.2	225.1	225.1	225.3	225.1	224.9	223.5	223.6	223.9	223.8	223.3
3	225.3	224.9	224.8	224.6	224.4	224.1	223.8	224.1	224.0	224.1	223.2
4	225.4	224.9	224.9	224.4	224.0	223.8	224.7	224.5	224.4	224.1	223.5
5	225.6	225.0	225.0	224.5	224.0	223.7	225.2	224.9	224.6	224.3	223.5
6	225.7	224.9	224.9	224.5	224.1	224.0	224.5	224.6	224.5	224.1	223.4
7	225.6	225.0	225.1	224.7	224.3	224.3	223.8	224.1	224.2	224.0	223.2
8	225.5	225.1	225.1	225.3	225.1	225.3	223.6	223.7	223.8	223.8	223.1

RUN NUMBER 111

VOLTAGE DROP IN TUBE	= 10.7	VOLTS	
CURRENT TO TEST SECTION	= 262.0	AMPS	
CALCULATED HEAT GENERATION	= 9340.8	BTU/HOUR	(Q=I*I*R)
HEAT LOSS IN TEST SECTION	= 482.6	BTU/HOUR	(HEATED PART)
HEAT TRANSFERRED TO THE MIXTURE	= 8858.2	BTU/HOUR	(QIN=QGEN-QLOSS)
TOTAL MASS VELOCITY	= 36981.3	LBM/(HR-SQ.FT)	
AVERAGE HEAT FLUX	= 4022.5	BTU/(HR-SQ.FT)	

AXIAL STATION	QUALITY %	ENTHALPY BTU/HOUR	SAT TEMP DEGREE F	SAT PRESS PSIA
START	72.99	894.70	223.84	18.50
1	73.23	897.00	223.79	18.48
2	76.07	924.02	223.18	18.27
3	76.43	927.43	223.05	18.22
4	76.66	929.57	222.92	18.18
5	76.88	931.63	222.79	18.13
6	77.10	933.68	222.67	18.09
7	77.33	935.83	222.54	18.05
8	77.69	939.22	222.38	17.99
9	78.05	942.63	222.26	17.95
10	78.41	946.03	222.13	17.91
11	80.55	966.30	221.39	17.65
END	80.79	968.58	221.31	17.63

CORRECTED OUTSIDE WALL TEMPERATURES - DEGREES F

AXIAL STATION LOCATIONS

	1	2	3	4	5	6	7	8	9	10	11
1	226.8	226.8	227.0	227.7	227.6	227.7	224.3	224.4	229.3	238.3	224.6
2	226.8	226.6	226.8	226.9	226.6	226.7	224.3	224.7	227.4	226.0	224.6
3	226.9	226.4	226.4	226.0	225.5	225.2	224.7	225.2	225.5	225.5	224.7
4	226.9	226.3	226.5	225.6	225.1	224.7	226.2	225.9	225.8	225.7	225.0
5	227.3	226.5	226.4	225.7	224.8	224.6	227.2	226.4	226.3	226.1	225.1
6	227.4	226.4	226.5	225.8	225.1	224.9	226.1	226.1	226.1	225.8	224.9
7	227.4	226.7	226.8	226.2	225.6	225.2	224.7	225.4	225.7	225.6	224.7
8	227.1	226.7	226.6	227.0	226.9	227.2	224.5	224.5	226.9	226.0	224.6

RUN NUMBER 112

VOLTAGE DROP IN TUBE	= 12.3	VOLTS	
CURRENT TO TEST SECTION	= 302.0	AMPS	
CALCULATED HEAT GENERATION	= 12418.0	BTU/HOUR	(Q=I*I*R)
HEAT LOSS IN TEST SECTION	= 500.2	BTU/HOUR	(HEATED PART)
HEAT TRANSFERRED TO THE MIXTURE	= 11917.8	BTU/HOUR	(QIN=QGEN-QLOSS)
TOTAL MASS VELOCITY	= 40358.7	LBM/(HR-SQ.FT)	
AVERAGE HEAT FLUX	= 5411.9	BTU/(HR-SQ.FT)	

AXIAL STATION	QUALITY %	ENTHALPY BTU/HOUR	SAT TEMP DEGREE F	SAT PRESS PSIA
START	72.22	891.37	231.32	21.30
1	72.52	894.19	231.27	21.28
2	76.04	927.57	230.60	21.01
3	76.48	931.72	230.47	20.96
4	76.76	934.34	230.35	20.92
5	77.03	936.87	230.23	20.87
6	77.31	939.49	230.11	20.82
7	77.59	942.11	229.99	20.78
8	78.03	946.26	229.85	20.72
9	78.47	950.44	229.76	20.69
10	78.91	954.61	229.67	20.65
11	81.55	979.66	229.11	20.44
END	81.84	982.45	229.04	20.41

CORRECTED OUTSIDE WALL TEMPERATURES - DEGREES F

AXIAL STATION LOCATIONS

	1	2	3	4	5	6	7	8	9	10	11
1	235.5	235.2	235.1	236.3	236.3	236.6	232.5	232.5	259.5	244.3	233.1
2	235.3	234.9	234.8	235.3	234.9	235.4	232.5	232.7	236.5	234.2	233.1
3	235.6	234.8	234.6	233.9	233.6	233.5	233.0	233.5	233.8	233.9	233.6
4	235.4	234.5	234.7	233.6	233.0	232.7	234.7	234.4	234.4	234.4	233.9
5	236.0	235.0	234.7	233.6	233.0	232.7	235.9	235.0	235.1	234.8	234.2
6	236.1	234.9	234.7	233.9	233.2	232.8	234.7	234.5	234.7	234.4	234.2
7	236.1	235.0	235.0	234.4	233.8	233.4	232.8	233.5	234.0	234.1	233.2
8	235.7	235.0	235.2	235.5	235.3	235.8	232.5	232.8	236.7	234.2	234.0

RUN NUMBER 113

VOLTAGE DROP IN TUBE	= 13.5	VOLTS	
CURRENT TO TEST SECTION	= 330.0	AMPS	
CALCULATED HEAT GENERATION	= 14830.1	BTU/HOUR	(Q=I*I*R)
HEAT LOSS IN TEST SECTION	= 497.6	BTU/HOUR	(HEATED PART)
HEAT TRANSFERRED TO THE MIXTURE	= 14332.5	BTU/HOUR	(QIN=QGEN-QLOSS)
TOTAL MASS VELOCITY	= 40519.1	LBM/(HR-SQ.FT)	
AVERAGE HEAT FLUX	= 6508.4	BTU/(HR-SQ.FT)	

AXIAL STATION	QUALITY %	ENTHALPY BTU/HOUR	SAT TEMP DEGREE F	SAT PRESS PSIA
START	71.91	888.79	232.01	21.57
1	72.27	892.16	231.95	21.55
2	76.49	932.20	231.22	21.26
3	77.01	937.12	231.10	21.21
4	77.34	940.24	231.02	21.18
5	77.67	943.35	230.93	21.14
6	77.99	946.38	230.85	21.11
7	78.32	949.50	230.76	21.08
8	78.85	954.52	230.64	21.03
9	79.38	959.55	230.54	20.99
10	79.91	964.57	230.43	20.95
11	83.07	994.56	229.78	20.69
END	83.42	997.89	229.71	20.67

CORRECTED OUTSIDE WALL TEMPERATURES - DEGREES F

AXIAL STATION LOCATIONS

	1	2	3	4	5	6	7	8	9	10	11
1	236.8	236.6	236.7	238.0	237.9	238.4	233.4	233.4	295.6	262.4	234.2
2	236.6	236.3	236.3	236.9	236.4	236.9	233.3	235.7	255.9	236.4	234.2
3	236.8	236.2	236.0	235.2	234.6	234.7	233.9	234.8	235.3	235.0	234.8
4	236.8	235.9	236.1	234.8	234.0	233.7	236.0	235.7	235.6	235.6	235.2
5	237.4	236.3	236.1	234.7	233.9	233.6	237.5	236.4	236.2	236.1	235.5
6	237.6	236.1	236.1	235.1	234.2	233.8	236.1	235.9	235.8	235.6	235.5
7	237.5	236.4	236.4	235.7	234.8	234.4	233.7	234.8	235.3	235.1	234.5
8	237.2	236.5	236.3	237.0	236.7	237.5	233.3	235.7	258.7	235.7	235.3

RUN NUMBER 114

VOLTAGE DROP IN TUBE	= 5.3	VOLTS	
CURRENT TO TEST SECTION	= 130.0	AMPS	
CALCULATED HEAT GENERATION	= 2300.8	BTU/HOUR	(Q=I*I*R)
HEAT LOSS IN TEST SECTION	= 512.5	BTU/HOUR	(HEATED PART)
HEAT TRANSFERRED TO THE MIXTURE	= 1788.3	BTU/HOUR	(QIN=QGEN-QLOSS)
TOTAL MASS VELOCITY	= 41132.8	LBM/(HR-SQ.FT)	
AVERAGE HEAT FLUX	= 812.1	BTU/(HR-SQ.FT)	

AXIAL STATION	QUALITY %	ENTHALPY BTU/HOUR	SAT TEMP DEGREE F	SAT PRESS PSIA
START	86.32	1028.16	235.14	22.85
1	86.37	1028.56	235.08	22.83
2	86.92	1033.49	234.34	22.52
3	86.99	1034.10	234.21	22.47
4	87.03	1034.44	234.11	22.43
5	87.08	1034.87	234.00	22.38
6	87.12	1035.20	233.89	22.33
7	87.17	1035.64	233.79	22.29
8	87.24	1036.25	233.66	22.24
9	87.31	1036.88	233.56	22.20
10	87.38	1037.50	233.46	22.16
11	87.79	1041.16	232.86	21.91
END	87.84	1041.57	232.79	21.89

CORRECTED OUTSIDE WALL TEMPERATURES - DEGREES F

AXIAL STATION LOCATIONS

	1	2	3	4	5	6	7	8	9	10	11
1	235.7	235.2	235.1	235.2	235.4	235.5	234.6	234.5	234.4	234.1	234.0
2	235.6	235.4	235.0	235.2	235.0	235.2	234.6	234.5	234.5	234.4	233.9
3	235.9	235.2	235.1	234.8	234.9	235.0	234.7	234.5	234.5	234.4	234.3
4	235.7	234.9	235.0	234.9	234.7	234.8	234.8	234.8	234.7	234.6	234.4
5	236.0	235.4	235.2	235.0	234.9	234.9	235.1	234.8	235.0	234.9	234.6
6	236.0	235.1	235.1	234.9	235.0	234.9	234.8	234.9	234.8	234.5	234.8
7	236.0	235.1	234.9	235.2	234.8	234.8	234.5	234.5	234.5	234.6	234.2
8	235.8	235.1	235.1	235.0	235.0	235.3	234.5	234.6	234.5	234.3	235.0

RUN NUMBER 115

VOLTAGE DROP IN TUBE	= 8.4	VOLTS	
CURRENT TO TEST SECTION	= 205.0	AMPS	
CALCULATED HEAT GENERATION	= 5723.6	BTU/HOUR	(Q=I*I*R)
HEAT LOSS IN TEST SECTION	= 513.5	BTU/HOUR	(HEATED PART)
HEAT TRANSFERRED TO THE MIXTURE	= 5210.1	BTU/HOUR	(QIN=QGEN-QLOSS)
TOTAL MASS VELOCITY	= 42089.0	LBM/(HR-SQ.FT)	
AVERAGE HEAT FLUX	= 2365.9	BTU/(HR-SQ.FT)	

AXIAL STATION	QUALITY %	ENTHALPY BTU/HOUR	SAT TEMP DEGREE F	SAT PRESS PSIA
START	84.30	1009.28	236.22	23.31
1	84.42	1010.42	236.16	23.28
2	85.92	1024.42	235.43	22.98
3	86.11	1026.18	235.32	22.93
4	86.23	1027.29	235.22	22.89
5	86.35	1028.39	235.12	22.85
6	86.47	1029.49	235.02	22.80
7	86.58	1030.50	234.92	22.76
8	86.77	1032.25	234.79	22.71
9	86.96	1034.03	234.69	22.67
10	87.15	1035.80	234.60	22.63
11	88.27	1046.25	234.01	22.38
END	88.40	1047.46	233.95	22.36

CORRECTED OUTSIDE WALL TEMPERATURES - DEGREES F

AXIAL STATION LOCATIONS

	1	2	3	4	5	6	7	8	9	10	11
1	238.1	237.7	237.6	238.2	238.3	238.4	236.5	236.4	263.6	259.4	236.4
2	238.1	237.7	237.5	237.8	237.7	237.8	236.4	236.8	248.9	247.3	236.5
3	238.3	237.6	237.5	237.2	237.0	237.0	236.6	236.9	237.1	237.0	236.9
4	238.1	237.3	237.6	237.1	236.9	236.8	237.1	237.2	236.9	237.2	237.0
5	238.5	237.8	237.7	237.1	237.0	236.9	237.9	237.3	237.4	237.4	237.3
6	238.5	237.5	237.6	237.2	237.2	236.9	237.2	237.2	237.0	237.1	237.5
7	238.5	237.5	237.5	237.5	237.1	236.9	236.4	237.3	237.1	237.1	236.6
8	238.1	237.6	237.6	237.8	237.6	238.0	236.4	236.8	254.3	247.8	237.4

RUN NUMBER 116

VOLTAGE DROP IN TUBE	= 10.2	VOLTS	
CURRENT TO TEST SECTION	= 250.0	AMPS	
CALCULATED HEAT GENERATION	= 8515.3	BTU/HOUR	(Q=I*I*R)
HEAT LOSS IN TEST SECTION	= 511.9	BTU/HOUR	(HEATED PART)
HEAT TRANSFERRED TO THE MIXTURE	= 8003.3	BTU/HOUR	(QIN=QGEN-QLOSS)
TOTAL MASS VELOCITY	= 41718.9	LBM/(HR-SQ.FT)	
AVERAGE HEAT FLUX	= 3634.3	BTU/(HR-SQ.FT)	

AXIAL STATION	QUALITY %	ENTHALPY BTU/HOUR	SAT TEMP DEGREE F	SAT PRESS PSIA
START	83.63	1003.35	237.25	23.75
1	83.82	1005.17	237.20	23.73
2	86.12	1026.84	236.58	23.46
3	86.41	1029.55	236.44	23.40
4	86.60	1031.30	236.30	23.34
5	86.78	1032.95	236.16	23.28
6	86.96	1034.61	236.02	23.23
7	87.14	1036.27	235.88	23.17
8	87.43	1038.98	235.74	23.11
9	87.72	1041.71	235.66	23.07
10	88.01	1044.45	235.58	23.04
11	89.73	1060.67	235.09	22.83
END	89.93	1062.52	235.04	22.81

CORRECTED OUTSIDE WALL TEMPERATURES - DEGREES F

AXIAL STATION LOCATIONS

	1	2	3	4	5	6	7	8	9	10	11
1	240.0	239.6	239.6	240.4	240.4	240.4	237.8	287.6	293.6	287.4	242.5
2	240.0	239.7	239.4	239.7	239.4	239.4	238.2	284.4	277.8	269.4	237.8
3	240.3	239.6	239.5	238.8	238.5	238.3	239.9	259.2	246.2	239.3	238.3
4	240.0	239.4	239.3	238.5	238.2	238.0	239.2	239.5	239.1	239.0	238.5
5	240.5	239.7	239.5	238.7	238.3	238.0	240.2	239.4	239.5	239.2	238.7
6	240.6	239.5	239.3	238.8	238.6	238.3	239.6	239.6	239.2	238.9	238.9
7	240.5	239.6	239.5	239.1	238.4	239.0	240.9	266.3	246.0	239.4	238.0
8	240.1	239.5	239.4	239.6	239.4	239.9	238.7	288.7	282.3	271.4	239.1

RUN NUMBER 117

VOLTAGE DROP IN TUBE	= 8.1	VOLTS	
CURRENT TO TEST SECTION	= 200.0	AMPS	
CALCULATED HEAT GENERATION	= 5443.0	BTU/HOUR	(Q=I*I*R)
HEAT LOSS IN TEST SECTION	= 479.1	BTU/HOUR	(HEATED PART)
HEAT TRANSFERRED TO THE MIXTURE	= 4963.9	BTU/HOUR	(QIN=QGEN-QLOSS)
TOTAL MASS VELOCITY	= 44701.4	LBM/(HR-SQ.FT)	
AVERAGE HEAT FLUX	= 2254.1	BTU/(HR-SQ.FT)	

AXIAL STATION	QUALITY %	ENTHALPY BTU/HOUR	SAT TEMP DEGREE F	SAT PRESS PSIA
START	60.41	774.36	225.08	18.94
1	60.52	775.38	225.01	18.92
2	61.88	787.93	224.13	18.60
3	62.06	789.56	223.97	18.55
4	62.17	790.54	223.84	18.50
5	62.28	791.52	223.70	18.45
6	62.39	792.50	223.57	18.40
7	62.49	793.38	223.43	18.36
8	62.67	795.02	223.28	18.30
9	62.84	796.60	223.19	18.27
10	63.01	798.18	223.09	18.24
11	64.02	807.56	222.50	18.03
END	64.13	808.61	222.44	18.01

CORRECTED OUTSIDE WALL TEMPERATURES - DEGREES F

AXIAL STATION LOCATIONS

	1	2	3	4	5	6	7	8	9	10	11
1	227.0	226.3	226.3	226.8	226.7	226.8	225.0	224.9	224.7	224.7	224.1
2	226.9	226.3	226.2	226.8	226.4	226.3	225.0	225.0	224.8	224.7	224.1
3	226.9	226.2	226.0	226.2	226.0	225.8	225.2	225.4	225.0	224.7	224.2
4	227.0	226.2	226.2	226.1	225.6	225.5	225.7	225.4	225.2	224.9	224.3
5	227.3	226.3	226.2	225.7	225.4	225.4	226.2	225.7	225.4	225.2	224.5
6	227.2	226.1	226.2	225.5	225.6	225.6	225.6	225.4	225.3	225.0	224.3
7	227.2	226.3	226.4	225.5	225.8	225.9	225.2	225.0	225.0	224.9	224.1
8	226.9	226.3	226.3	225.7	226.3	226.6	224.9	224.8	224.8	224.7	224.1

RUN NUMBER 118

VOLTAGE DROP IN TUBE	= 16.3	VOLTS	
CURRENT TO TEST SECTION	= 400.0	AMPS	
CALCULATED HEAT GENERATION	= 21782.3	BTU/HOUR	(Q=I*I*R)
HEAT LOSS IN TEST SECTION	= 479.8	BTU/HOUR	(HEATED PART)
HEAT TRANSFERRED TO THE MIXTURE	= 21302.5	BTU/HOUR	(QIN=QGEN-QLOSS)
TOTAL MASS VELOCITY	= 45216.5	LBM/(HR-SQ.FT)	
AVERAGE HEAT FLUX	= 9673.4	BTU/(HR-SQ.FT)	

AXIAL STATION	QUALITY %	ENTHALPY BTU/HOUR	SAT TEMP DEGREE F	SAT PRESS PSIA
START	60.10	773.35	228.24	20.11
1	60.57	777.80	228.15	20.07
2	66.19	831.10	227.03	19.65
3	66.89	837.73	226.87	19.59
4	67.33	841.89	226.75	19.55
5	67.77	846.05	226.62	19.50
6	68.20	850.11	226.50	19.46
7	68.64	854.26	226.37	19.41
8	69.34	860.89	226.18	19.34
9	70.05	867.61	226.00	19.27
10	70.75	874.24	225.81	19.21
11	74.97	914.23	224.70	18.81
END	75.44	918.66	224.58	18.76

CORRECTED OUTSIDE WALL TEMPERATURES - DEGREES F

AXIAL STATION LOCATIONS

	1	2	3	4	5	6	7	8	9	10	11
1	235.2	234.1	234.4	236.2	236.0	236.5	230.3	230.4	230.9	231.8	230.7
2	234.8	233.6	232.9	234.4	234.1	234.4	230.4	230.7	231.5	231.8	230.9
3	234.9	233.4	233.2	232.3	232.2	231.9	231.3	232.1	232.1	232.2	231.2
4	234.9	233.3	233.5	231.3	231.0	230.6	233.6	232.9	233.0	232.7	231.6
5	235.4	233.6	233.0	230.8	230.7	230.3	235.5	234.1	233.7	233.4	231.9
6	235.7	233.8	233.5	231.7	231.3	230.9	233.8	233.4	233.3	233.0	231.7
7	236.0	233.9	234.3	232.7	232.7	232.1	231.4	232.3	232.5	232.7	231.2
8	235.5	234.2	234.0	234.6	234.4	235.6	230.3	230.8	231.6	232.2	230.8

RUN NUMBER 119

VOLTAGE DROP IN TUBE	= 20.4	VOLTS	
CURRENT TO TEST SECTION	= 500.0	AMPS	
CALCULATED HEAT GENERATION	= 34067.9	BTU/HOUR	(Q=I*I*R)
HEAT LOSS IN TEST SECTION	= 520.6	BTU/HOUR	(HEATED PART)
HEAT TRANSFERRED TO THE MIXTURE	= 33547.3	BTU/HOUR	(QIN=QGEN-QLOSS)
TOTAL MASS VELOCITY	= 46404.0	LBM/(HR-SQ.FT)	
AVERAGE HEAT FLUX	= 15233.8	BTU/(HR-SQ.FT)	

AXIAL STATION	QUALITY %	ENTHALPY BTU/HOUR	SAT TEMP DEGREE F	SAT PRESS PSIA
START	61.91	797.28	239.01	24.53
1	62.64	804.15	238.94	24.49
2	71.27	885.92	238.08	24.11
3	72.35	896.16	237.97	24.07
4	73.02	902.50	237.89	24.03
5	73.68	908.76	237.82	24.00
6	74.35	915.11	237.75	23.97
7	75.02	921.46	237.67	23.94
8	76.09	931.59	237.53	23.87
9	77.18	941.91	237.37	23.81
10	78.26	952.13	237.20	23.73
11	84.73	1013.41	236.23	23.31
END	85.45	1020.26	236.12	23.27

CORRECTED OUTSIDE WALL TEMPERATURES - DEGREES F

AXIAL STATION LOCATIONS

	1	2	3	4	5	6	7	8	9	10	11
1	249.5	248.8	249.3	252.1	251.8	252.8	243.2	243.4	256.4	245.2	245.3
2	248.9	248.1	248.3	249.2	248.8	249.4	243.2	243.8	245.3	245.6	245.2
3	249.0	247.6	247.4	245.8	245.6	245.5	244.7	245.9	246.3	246.4	245.8
4	249.1	247.3	247.7	244.5	243.8	243.3	248.6	247.4	247.3	247.3	246.3
5	249.9	247.9	247.0	243.8	243.2	242.9	251.6	249.3	248.7	248.3	246.9
6	250.5	248.2	247.7	244.8	244.0	243.7	248.9	248.3	248.0	247.8	246.6
7	250.6	248.7	249.1	246.7	246.3	245.6	244.7	246.3	246.9	247.0	246.0
8	250.0	248.8	248.5	249.6	249.5	251.1	243.3	244.1	246.4	246.1	245.5

RUN NUMBER 120

VOLTAGE DROP IN TUBE	= 20.9	VOLTS	
CURRENT TO TEST SECTION	= 515.0	AMPS	
CALCULATED HEAT GENERATION	= 36147.8	BTU/HOUR	(Q=I*I*R)
HEAT LOSS IN TEST SECTION	= 519.2	BTU/HOUR	(HEATED PART)
HEAT TRANSFERRED TO THE MIXTURE	= 35628.6	BTU/HOUR	(QIN=QGEN-QLOSS)
TOTAL MASS VELOCITY	= 48276.2	LBM/(HR-SQ.FT)	
AVERAGE HEAT FLUX	= 16179.0	BTU/(HR-SQ.FT)	

AXIAL STATION	QUALITY %	ENTHALPY BTU/HOUR	SAT TEMP DEGREE F	SAT PRESS PSIA
START	62.05	798.94	239.56	24.77
1	62.79	805.91	239.50	24.74
2	71.60	889.43	238.75	24.41
3	72.70	899.83	238.60	24.34
4	73.39	906.33	238.46	24.28
5	74.07	912.74	238.32	24.22
6	74.76	919.24	238.17	24.15
7	75.44	925.65	238.03	24.09
8	76.54	936.06	237.87	24.02
9	77.65	946.58	237.74	23.97
10	78.75	957.00	237.61	23.91
11	85.35	1019.62	236.86	23.58
END	86.08	1026.57	236.77	23.55

CORRECTED OUTSIDE WALL TEMPERATURES - DEGREES F

AXIAL STATION LOCATIONS

	1	2	3	4	5	6	7	8	9	10	11
1	251.0	250.4	250.4	253.7	253.2	254.1	244.1	244.3	295.6	245.5	246.1
2	250.3	249.6	249.7	250.6	250.1	250.7	244.0	244.4	248.2	246.7	246.1
3	250.6	249.2	248.8	247.1	246.7	246.4	245.5	246.9	247.4	247.3	247.0
4	250.6	248.7	248.8	245.9	244.9	244.3	249.6	248.5	248.6	248.5	247.6
5	251.7	249.5	248.4	245.4	244.6	244.1	252.9	250.3	250.0	249.6	248.2
6	252.0	249.7	248.8	246.6	245.5	244.6	249.9	249.5	249.4	248.8	248.1
7	252.1	250.1	250.2	248.2	247.5	246.4	245.5	247.2	247.9	248.1	246.8
8	251.6	250.3	249.8	251.0	250.7	252.3	244.1	245.1	251.7	247.1	247.1

RUN NUMBER 121

VOLTAGE DROP IN TUBE	= 8.2	VOLTS	
CURRENT TO TEST SECTION	= 200.0	AMPS	
CALCULATED HEAT GENERATION	= 5444.0	BTU/HOUR	(Q=I*I*R)
HEAT LOSS IN TEST SECTION	= 497.9	BTU/HOUR	(HEATED PART)
HEAT TRANSFERRED TO THE MIXTURE	= 4946.0	BTU/HOUR	(QIN=QGEN-QLOSS)
TOTAL MASS VELOCITY	= 46882.1	LBM/(HR-SQ.FT)	
AVERAGE HEAT FLUX	= 2246.0	BTU/(HR-SQ.FT)	

AXIAL STATION	QUALITY %	ENTHALPY BTU/HOUR	SAT TEMP DEGREE F	SAT PRESS PSIA
START	75.63	922.73	228.77	20.31
1	75.74	923.70	228.68	20.27
2	77.04	935.63	227.61	19.87
3	77.21	937.17	227.43	19.80
4	77.31	938.06	227.28	19.75
5	77.42	939.04	227.14	19.69
6	77.52	939.93	226.99	19.64
7	77.62	940.81	226.84	19.58
8	77.79	942.35	226.65	19.51
9	77.95	943.80	226.48	19.45
10	78.12	945.35	226.32	19.39
11	79.10	954.29	225.35	19.04
END	79.21	955.27	225.24	19.00

CORRECTED OUTSIDE WALL TEMPERATURES - DEGREES F

AXIAL STATION LOCATIONS

	1	2	3	4	5	6	7	8	9	10	11
1	231.0	230.3	230.1	230.7	230.7	230.5	228.8	228.7	228.6	228.6	227.9
2	231.0	230.3	230.1	230.4	230.0	230.0	228.9	228.8	229.0	228.7	227.9
3	231.1	230.2	230.1	229.8	229.6	229.5	229.1	229.1	228.8	228.7	228.3
4	230.9	230.0	230.0	229.8	229.2	229.1	229.5	229.4	229.2	229.2	228.4
5	231.3	230.3	230.2	229.8	229.5	229.2	230.0	229.5	229.6	229.3	228.7
6	231.3	230.1	230.0	229.9	229.7	229.2	229.5	229.4	229.3	229.0	228.9
7	231.3	230.1	230.0	230.0	229.6	229.3	229.0	229.1	229.0	228.8	228.1
8	231.1	230.2	230.1	230.3	230.1	230.2	228.8	228.9	228.9	228.8	228.9

RUN NUMBER 122

VOLTAGE DROP IN TUBE	= 14.4	VOLTS	
CURRENT TO TEST SECTION	= 350.0	AMPS	
CALCULATED HEAT GENERATION	= 16692.1	BTU/HOUR	(Q=I*I*R)
HEAT LOSS IN TEST SECTION	= 533.0	BTU/HOUR	(HEATED PART)
HEAT TRANSFERRED TO THE MIXTURE	= 16159.1	BTU/HOUR	(QIN=QGEN-QLOSS)
TOTAL MASS VELOCITY	= 49186.1	LBM/(HR-SQ.FT)	
AVERAGE HEAT FLUX	= 7337.8	BTU/(HR-SQ.FT)	

AXIAL STATION	QUALITY %	ENTHALPY BTU/HOUR	SAT TEMP DEGREE F	SAT PRESS PSIA
START	76.17	934.21	241.27	25.55
1	76.49	937.28	241.62	25.52
2	80.43	974.52	240.72	25.30
3	80.92	979.15	240.64	25.26
4	81.22	981.97	240.58	25.23
5	81.53	984.90	240.52	25.20
6	81.83	987.72	240.46	25.18
7	82.14	990.65	240.40	25.15
8	82.63	995.27	240.31	25.11
9	83.12	999.89	240.22	25.07
10	83.62	1004.61	240.13	25.03
11	86.57	1032.46	239.59	24.78
END	86.90	1035.54	239.53	24.76

CORRECTED OUTSIDE WALL TEMPERATURES - DEGREES F

AXIAL STATION LOCATIONS

	1	2	3	4	5	6	7	8	9	10	11
1	246.1	245.7	245.5	247.1	247.1	247.4	242.7	242.5	282.0	262.3	242.9
2	245.8	245.1	245.2	245.8	245.5	245.7	242.7	242.7	259.8	245.6	242.9
3	246.1	245.0	244.9	244.0	243.6	243.6	243.1	243.7	244.0	243.6	243.5
4	245.7	244.8	245.0	243.7	242.9	242.8	245.0	244.7	244.8	244.4	243.8
5	246.4	245.3	245.0	243.7	242.9	242.8	246.8	245.6	245.4	245.1	244.1
6	246.6	245.2	245.0	244.0	243.5	243.1	245.0	244.9	244.9	244.5	244.2
7	246.5	245.2	245.3	244.5	243.8	243.4	243.0	244.7	244.4	244.1	243.3
8	246.2	245.4	245.3	246.0	245.7	246.4	242.7	243.2	268.4	245.5	244.0

RUN NUMBER 123

VOLTAGE DROP IN TUBE	= 15.3	VOLTS	
CURRENT TO TEST SECTION	= 375.0	AMPS	
CALCULATED HEAT GENERATION	= 19163.8	BTU/HOUR	(Q=I*I*R)
HEAT LOSS IN TEST SECTION	= 530.3	BTU/HOUR	(HEATED PART)
HEAT TRANSFERRED TO THE MIXTURE	= 18633.5	BTU/HOUR	(QIN=QGEN-QLOSS)
TOTAL MASS VELOCITY	= 46931.4	LBM/(HR-SQ.FT)	
AVERAGE HEAT FLUX	= 8461.5	BTU/(HR-SQ.FT)	

AXIAL STATION	QUALITY %	ENTHALPY BTU/HOUR	SAT TEMP DEGREE F	SAT PRESS PSIA
START	80.89	979.78	242.54	26.14
1	81.29	983.55	242.51	26.12
2	86.03	1028.44	242.14	25.95
3	86.62	1034.03	242.08	25.92
4	86.99	1037.52	242.02	25.89
5	87.36	1041.01	241.97	25.87
6	87.73	1044.51	241.91	25.84
7	88.09	1047.90	241.85	25.81
8	88.69	1053.58	241.79	25.79
9	89.28	1059.17	241.74	25.76
10	89.87	1064.76	241.69	25.74
11	93.43	1098.51	241.41	25.61
END	93.82	1102.24	241.38	25.60

CORRECTED OUTSIDE WALL TEMPERATURES - DEGREES F

AXIAL STATION LOCATIONS

	1	2	3	4	5	6	7	8	9	10	11
1	247.3	247.0	247.0	248.8	248.6	249.1	244.2	244.3	318.7	288.8	244.8
2	247.0	246.5	246.7	247.2	246.8	247.1	244.2	249.1	275.5	249.4	244.6
3	247.3	246.5	246.3	245.3	244.9	244.6	244.2	246.0	245.7	245.4	245.2
4	247.2	246.1	246.3	244.8	244.4	244.0	246.2	245.9	246.0	245.9	245.5
5	247.8	246.6	246.2	244.7	244.2	243.8	248.3	246.8	246.7	246.5	245.8
6	247.7	246.5	246.3	245.3	244.6	244.2	246.5	246.3	246.3	246.0	245.8
7	247.9	246.6	246.9	245.8	245.0	244.6	244.2	249.3	245.9	245.6	244.8
8	247.6	246.8	246.6	247.4	247.1	248.0	244.4	253.7	280.4	248.9	245.5

RUN NUMBER 124

VOLTAGE DROP IN TUBE	= 22.3	VOLTS	
CURRENT TO TEST SECTION	= 550.0	AMPS	
CALCULATED HEAT GENERATION	= 41248.8	BTU/HOUR	(Q=I*I*R)
HEAT LOSS IN TEST SECTION	= 538.9	BTU/HOUR	(HEATED PART)
HEAT TRANSFERRED TO THE MIXTURE	= 40709.9	BTU/HOUR	(QIN=QGEN-QLOSS)
TOTAL MASS VELOCITY	= 53504.2	LBM/(HR-SQ.FT)	
AVERAGE HEAT FLUX	= 18486.4	BTU/(HR-SQ.FT)	

AXIAL STATION	QUALITY %	ENTHALPY BTU/HOUR	SAT TEMP DEGREE F	SAT PRESS PSIA
START	64.49	826.17	246.47	28.03
1	65.25	833.33	246.39	27.99
2	74.39	919.47	245.42	27.51
3	75.53	930.21	245.27	27.44
4	76.24	936.88	245.14	27.38
5	76.95	943.55	245.02	27.32
6	77.65	950.13	244.89	27.26
7	78.36	956.81	244.76	27.19
8	79.50	967.54	244.58	27.11
9	80.65	978.37	244.41	27.02
10	81.79	989.11	244.24	26.94
11	88.64	1053.72	243.23	26.46
END	89.40	1060.85	243.12	26.41

CORRECTED OUTSIDE WALL TEMPERATURES - DEGREES F

AXIAL STATION LOCATIONS

	1	2	3	4	5	6	7	8	9	10	11
1	257.9	257.7	258.1	262.0	261.3	262.2	251.6	251.9	276.0	276.2	253.3
2	257.4	257.0	257.5	258.5	258.0	258.4	251.6	252.0	257.1	254.3	253.5
3	257.5	256.3	256.3	254.8	254.4	253.6	252.8	254.7	254.9	254.7	254.3
4	257.8	256.1	256.4	253.3	252.6	251.9	257.2	256.3	256.1	255.9	255.1
5	258.9	256.6	255.9	252.7	252.2	251.6	260.7	257.9	257.4	257.0	255.6
6	259.1	256.8	256.4	254.2	253.3	252.4	257.6	257.0	256.8	256.3	255.5
7	259.1	257.5	258.2	255.9	255.3	253.9	253.0	255.1	255.5	255.6	254.1
8	258.6	257.8	257.4	259.0	258.5	260.2	252.0	252.6	258.2	254.5	254.5

RUN NUMBER 125

VOLTAGE DROP IN TUBE	= 16.4	VOLTS	
CURRENT TO TEST SECTION	= 400.0	AMPS	
CALCULATED HEAT GENERATION	= 21792.6	BTU/HOUR	(Q=I*I*R)
HEAT LOSS IN TEST SECTION	= 513.8	BTU/HOUR	(HEATED PART)
HEAT TRANSFERRED TO THE MIXTURE	= 21278.8	BTU/HOUR	(QIN=QGEN-QLOSS)
TOTAL MASS VELOCITY	= 55277.7	LBM/(HR-SQ.FT)	
AVERAGE HEAT FLUX	= 9662.7	BTU/(HR-SQ.FT)	

AXIAL STATION	QUALITY %	ENTHALPY BTU/HOUR	SAT TEMP DEGREE F	SAT PRESS PSIA
START	68.37	856.85	235.48	23.00
1	68.76	860.49	235.40	22.96
2	73.37	904.05	234.51	22.59
3	73.95	909.51	234.35	22.52
4	74.31	912.88	234.21	22.47
5	74.67	916.25	234.07	22.41
6	75.03	919.62	233.93	22.35
7	75.39	922.99	233.79	22.29
8	75.96	928.35	233.61	22.22
9	76.54	933.82	233.47	22.16
10	77.12	939.29	233.32	22.10
11	80.58	971.97	232.45	21.75
END	80.96	975.58	232.36	21.71

CORRECTED OUTSIDE WALL TEMPERATURES - DEGREES F

AXIAL STATION LOCATIONS

	1	2	3	4	5	6	7	8	9	10	11
1	241.5	240.9	241.0	242.8	242.6	242.8	237.5	237.7	238.1	238.2	237.4
2	241.1	240.5	240.8	241.2	240.8	240.8	237.5	237.9	236.9	238.3	237.5
3	241.1	240.2	240.2	239.2	239.3	238.8	238.3	238.8	238.8	238.4	238.0
4	241.0	240.0	240.1	238.5	238.2	237.8	240.2	239.7	239.4	239.2	238.3
5	241.8	240.3	239.9	238.1	238.0	237.5	241.9	240.3	240.2	239.8	238.6
6	242.0	240.2	240.1	238.9	238.6	238.0	240.4	240.0	239.8	239.2	238.7
7	242.1	240.6	240.9	239.9	239.6	239.0	238.4	239.2	239.0	238.9	237.6
8	241.7	240.6	240.6	241.4	241.0	241.8	237.6	238.3	238.5	238.4	238.2

RUN NUMBER 126

VOLTAGE DROP IN TUBE	= 26.1	VOLTS	
CURRENT TO TEST SECTION	= 650.0	AMPS	
CALCULATED HEAT GENERATION	= 57596.9	BTU/HOUR	(Q=I*I*R)
HEAT LOSS IN TEST SECTION	= 515.7	BTU/HOUR	(HEATED PART)
HEAT TRANSFERRED TO THE MIXTURE	= 57081.1	BTU/HOUR	(QIN=QGEN-QLOSS)
TOTAL MASS VELOCITY	= 60619.7	LBM/(HR-SQ.FT)	
AVERAGE HEAT FLUX	= 25920.6	BTU/(HR-SQ.FT)	

AXIAL STATION	QUALITY %	ENTHALPY BTU/HOUR	SAT TEMP DEGREE F	SAT PRESS PSIA
START	60.25	783.01	241.56	25.68
1	61.19	791.85	241.44	25.63
2	72.48	898.45	239.94	24.94
3	73.89	911.75	239.70	24.83
4	74.77	920.03	239.51	24.75
5	75.64	928.22	239.32	24.66
6	76.51	936.41	239.13	24.58
7	77.39	944.70	238.94	24.49
8	78.80	958.00	238.67	24.37
9	80.21	971.32	238.43	24.27
10	81.62	984.65	238.18	24.16
11	90.07	1064.60	236.73	23.53
END	91.00	1073.44	236.57	23.46

CORRECTED OUTSIDE WALL TEMPERATURES - DEGREES F

AXIAL STATION LOCATIONS

	1	2	3	4	5	6	7	8	9	10	11
1	256.6	255.8	256.3	260.7	259.8	260.9	248.0	249.1	248.8	250.7	249.4
2	255.7	254.8	255.5	256.2	255.5	256.1	248.1	249.3	248.9	250.6	249.7
3	255.7	254.0	253.8	251.3	251.7	251.0	249.7	251.3	251.7	251.3	250.6
4	256.1	253.6	253.7	249.3	249.3	248.4	254.5	253.1	253.0	252.8	251.5
5	257.4	254.1	252.7	248.2	248.7	247.9	258.6	255.0	254.8	254.4	252.1
6	258.0	254.7	253.7	250.3	250.2	249.0	255.1	254.2	254.0	253.4	252.0
7	258.0	255.4	256.4	252.5	252.9	251.5	250.2	252.3	252.4	252.6	250.1
8	257.0	255.9	255.3	256.8	256.4	258.3	248.5	249.9	251.1	251.4	250.6

RUN NUMBER 204

VOLTAGE DROP IN TUBE	= 10.0	VOLTS	
CURRENT TO TEST SECTION	= 250.0	AMPS	
CALCULATED HEAT GENERATION	= 7862.4	BTU/HOUR	(Q=I*I*R)
HEAT LOSS IN TEST SECTION	= 323.9	BTU/HOUR	(HEATED PART)
HEAT TRANSFERRED TO THE MIXTURE	= 7538.6	BTU/HOUR	(QIN=QGEN-QLOSS)
TOTAL MASS VELOCITY	= 31429.5	LBM/(HR-SQ.FT)	
AVERAGE HEAT FLUX	= 3703.3	BTU/(HR-SQ.FT)	

AXIAL STATION	QUALITY %	ENTHALPY BTU/HOUR	SAT TEMP DEGREE F	SAT PRESS PSIA
START	68.09	845.85	220.94	17.50
1	68.34	848.28	220.91	17.49
2	70.57	869.67	220.69	17.42
3	70.96	873.41	220.65	17.40
4	71.45	878.09	220.57	17.38
5	71.95	882.87	220.49	17.35
6	72.44	887.56	220.41	17.32
7	72.94	892.34	220.33	17.30
8	73.32	895.98	220.28	17.28
9	73.70	899.62	220.22	17.26
10	74.09	903.35	220.17	17.24
11	75.55	917.34	219.97	17.18
END	75.81	919.83	219.94	17.17

CORRECTED OUTSIDE WALL TEMPERATURES - DEGREES F

AXIAL STATION LOCATIONS

	1	2	3	4	5	6	7	8	9	10	11
1	222.1	236.4	241.4	224.3	224.4	224.4	221.3	221.3	262.8	255.4	222.7
2	222.1	224.2	224.3	223.3	223.8	223.8	221.4	221.8	238.7	233.1	222.1
3	222.6	222.7	222.9	222.7	222.7	222.2	221.8	222.3	222.7	222.8	222.2
4	222.6	223.1	222.8	222.2	221.7	221.5	223.6	223.2	223.0	223.0	222.6
5	223.0	222.7	222.7	222.0	221.5	221.4	224.4	223.7	223.3	223.0	222.3
6	223.1	222.8	222.9	222.1	221.6	221.7	223.4	223.0	222.7	222.5	222.0
7	223.2	222.7	222.9	223.6	222.6	222.2	221.6	221.9	222.4	222.7	221.5
8	222.6	224.0	225.0	223.4	223.8	223.7	221.4	221.5	243.2	231.7	221.5

RUN NUMBER 205

VOLTAGE DROP IN TUBE	= 7.6	VOLTS	
CURRENT TO TEST SECTION	= 190.0	AMPS	
CALCULATED HEAT GENERATION	= 4543.9	BTU/HOUR	(Q=I*I*R)
HEAT LOSS IN TEST SECTION	= 345.9	BTU/HOUR	(HEATED PART)
HEAT TRANSFERRED TO THE MIXTURE	= 4198.1	BTU/HOUR	(QIN=QGEN-QLOSS)
TOTAL MASS VELOCITY	= 33209.2	LBM/(HR-SQ.FT)	
AVERAGE HEAT FLUX	= 2062.3	BTU/(HR-SQ.FT)	

AXIAL STATION	QUALITY %	ENTHALPY BTU/HOUR	SAT TEMP DEGREE F	SAT PRESS PSIA
START	80.13	965.63	228.22	20.10
1	80.27	966.93	228.18	20.08
2	81.46	978.20	227.86	19.96
3	81.67	980.17	227.78	19.93
4	81.93	982.60	227.64	19.88
5	82.20	985.13	227.50	19.83
6	82.47	987.66	227.36	19.78
7	82.73	990.09	227.22	19.72
8	82.94	992.06	227.13	19.69
9	83.14	993.94	227.03	19.65
10	83.35	995.91	226.94	19.62
11	84.14	1003.34	226.59	19.49
END	84.28	1004.62	226.53	19.47

CORRECTED OUTSIDE WALL TEMPERATURES - DEGREES F

AXIAL STATION LOCATIONS

	1	2	3	4	5	6	7	8	9	10	11
1	229.7	232.1	239.5	230.2	230.1	230.1	231.1	265.0	262.8	257.2	248.1
2	229.6	229.8	230.7	229.6	229.7	229.9	239.8	259.1	252.1	246.3	234.8
3	229.8	229.7	229.8	229.3	228.7	240.5	237.7	235.9	229.7	229.3	228.8
4	229.7	230.0	229.8	229.0	228.4	243.4	229.5	229.3	229.3	229.2	228.9
5	230.1	229.8	229.8	228.9	228.3	238.2	229.0	229.6	229.5	229.3	228.9
6	229.9	229.9	230.0	229.0	228.4	241.0	229.4	229.2	229.0	229.2	228.7
7	230.1	229.7	229.9	229.2	228.8	238.2	238.5	236.5	229.9	229.2	228.8
8	229.8	232.5	234.4	229.6	229.7	229.6	237.4	259.7	254.2	248.0	232.9

RUN NUMBER 206

VOLTAGE DROP IN TUBE	= 3.8	VOLTS	
CURRENT TO TEST SECTION	= 95.0	AMPS	
CALCULATED HEAT GENERATION	= 1135.6	BTU/HOUR	(Q=I*I*R)
HEAT LOSS IN TEST SECTION	= 373.0	BTU/HOUR	(HEATED PART)
HEAT TRANSFERRED TO THE MIXTURE	= 762.6	BTU/HOUR	(QIN=QGEN-QLOSS)
TOTAL MASS VELOCITY	= 34846.9	LBM/(HR-SQ.FT)	
AVERAGE HEAT FLUX	= 374.6	BTU/(HR-SQ.FT)	

AXIAL STATION	QUALITY %	ENTHALPY BTU/HOUR	SAT TEMP DEGREE F	SAT PRESS PSIA
START	97.12	1130.92	234.13	22.43
1	97.15	1131.18	234.08	22.41
2	97.37	1133.12	233.64	22.23
3	97.41	1133.48	233.56	22.20
4	97.45	1133.82	233.45	22.15
5	97.50	1134.25	233.34	22.11
6	97.55	1134.69	233.23	22.06
7	97.60	1135.13	233.13	22.02
8	97.64	1135.48	233.03	21.98
9	97.68	1135.83	232.94	21.95
10	97.72	1136.17	232.84	21.91
11	97.87	1137.47	232.46	21.75
END	97.89	1137.67	232.40	21.73

CORRECTED OUTSIDE WALL TEMPERATURES - DEGREES F

AXIAL STATION LOCATIONS

	1	2	3	4	5	6	7	8	9	10	11
1	234.8	238.4	239.7	234.7	234.7	234.9	242.1	243.8	244.7	245.9	247.4
2	234.6	238.2	240.2	234.4	234.5	236.9	242.3	243.7	244.4	245.6	246.9
3	234.8	234.8	237.1	234.5	234.5	241.0	241.3	241.8	241.8	242.4	243.6
4	234.6	234.8	234.6	234.3	234.3	241.2	236.3	235.0	235.1	235.1	234.9
5	234.5	234.7	234.6	234.4	234.3	240.8	234.8	234.5	234.4	234.4	234.1
6	234.7	234.7	234.7	234.4	234.3	240.7	236.1	235.8	234.9	234.8	234.3
7	234.9	234.6	235.2	234.4	234.4	240.7	241.1	241.2	241.2	241.9	242.0
8	234.7	235.5	236.0	234.4	234.6	236.0	242.1	243.4	244.0	244.8	246.2

RUN NUMBER 207

VOLTAGE DROP IN TUBE	= 12.7	VOLTS	
CURRENT TO TEST SECTION	= 315.0	AMPS	
CALCULATED HEAT GENERATION	= 12486.7	BTU/HOUR	(Q=I*I*R)
HEAT LOSS IN TEST SECTION	= 332.5	BTU/HOUR	(HEATED PART)
HEAT TRANSFERRED TO THE MIXTURE	= 12154.3	BTU/HOUR	(QIN=QGEN-QLOSS)
TOTAL MASS VELOCITY	= 39180.4	LBM/(HR-SQ.FT)	
AVERAGE HEAT FLUX	= 5970.7	BTU/(HR-SQ.FT)	

AXIAL STATION	QUALITY %	ENTHALPY BTU/HOUR	SAT TEMP DEGREE F	SAT PRESS PSIA
START	72.30	888.30	224.27	18.65
1	72.63	891.45	224.22	18.63
2	75.53	919.12	223.74	18.46
3	76.03	923.87	223.62	18.42
4	76.68	930.02	223.42	18.35
5	77.33	936.18	223.21	18.28
6	77.97	942.24	223.01	18.21
7	78.62	948.40	222.80	18.14
8	79.12	953.14	222.65	18.08
9	79.62	957.89	222.51	18.04
10	80.12	962.64	222.37	17.99
11	82.03	980.78	221.82	17.80
END	82.37	983.98	221.72	17.76

CORRECTED OUTSIDE WALL TEMPERATURES - DEGREES F

AXIAL STATION LOCATIONS

	1	2	3	4	5	6	7	8	9	10	11
1	229.8	229.9	230.1	231.1	231.3	231.0	226.5	226.5	276.8	237.8	227.7
2	229.3	229.8	229.9	229.9	230.3	230.0	226.6	228.1	235.2	228.0	228.1
3	229.2	229.2	229.4	228.9	228.4	227.6	227.6	228.3	228.8	228.5	228.2
4	229.3	229.5	229.2	228.1	227.2	226.5	229.7	229.5	229.1	229.0	228.2
5	229.5	229.0	229.0	227.9	227.0	226.4	230.5	229.9	229.4	229.0	228.2
6	229.6	229.2	229.4	228.1	227.2	226.2	229.2	228.9	228.6	228.2	227.6
7	229.9	229.2	229.6	228.7	228.4	227.2	226.8	227.8	228.3	227.4	227.2
8	230.0	229.7	230.1	230.0	230.2	229.6	226.5	227.9	236.2	227.5	227.2

RUN NUMBER 208

VOLTAGE DROP IN TUBE	= 9.6	VOLTS	
CURRENT TC TEST SECTION	= 240.0	AMPS	
CALCULATED HEAT GENERATION	= 7256.5	BTU/HOUR	(Q=I*I*R)
HEAT LOSS IN TEST SECTION	= 364.9	BTU/HOUR	(HEATED PART)
HEAT TRANSFERRED TO THE MIXTURE	= 6891.5	BTU/HOUR	(QIN=QGEN-QLOSS)
TOTAL MASS VELOCITY	= 41450.5	LBM/(HR-SQ.FT)	
AVERAGE HEAT FLUX	= 3385.4	BTU/(HR-SQ.FT)	

AXIAL STATION	QUALITY %	ENTHALPY BTU/HOUR	SAT TEMP DEGREE F	SAT PRESS PSIA
START	83.96	1006.33	236.87	23.59
1	84.14	1008.05	236.82	23.57
2	85.71	1022.86	236.44	23.40
3	85.98	1025.40	236.35	23.37
4	86.33	1028.66	236.16	23.28
5	86.68	1031.92	235.97	23.20
6	87.04	1035.27	235.79	23.13
7	87.39	1038.53	235.60	23.05
8	87.66	1041.06	235.49	23.00
9	87.93	1043.60	235.39	22.96
10	88.20	1046.14	235.29	22.92
11	89.24	1055.91	234.91	22.76
END	89.42	1057.61	234.85	22.73

CORRECTED OUTSIDE WALL TEMPERATURES - DEGREES F

AXIAL STATION LOCATIONS

	1	2	3	4	5	6	7	8	9	10	11
1	239.5	239.0	239.2	239.9	240.0	240.1	249.1	290.0	287.8	281.2	251.2
2	239.3	239.2	239.1	239.0	239.4	240.3	258.8	286.1	273.7	263.0	239.1
3	239.4	239.0	239.0	238.4	240.2	262.7	257.0	250.8	239.6	238.6	238.2
4	239.2	239.3	239.0	238.0	238.3	263.4	239.7	239.0	238.7	238.6	238.2
5	239.6	239.1	238.9	238.0	237.6	254.2	239.9	239.4	238.9	238.8	238.2
6	239.5	239.1	239.1	238.1	237.6	261.0	239.5	238.9	238.4	238.1	237.8
7	239.9	239.0	239.0	238.4	239.0	260.8	263.0	253.7	240.2	238.1	237.5
8	239.6	239.4	239.3	239.1	239.4	239.6	263.4	286.0	277.0	265.0	238.1

RUN NUMBER 209

VOLTAGE DROP IN TUBE	= 19.9	VOLTS	
CURRENT TO TEST SECTION	= 500.0	AMPS	
CALCULATED HEAT GENERATION	= 31481.9	BTU/HOUR	(Q=I*I*R)
HEAT LOSS IN TEST SECTION	= 340.5	BTU/HOUR	(HEATED PART)
HEAT TRANSFERRED TO THE MIXTURE	= 31141.3	BTU/HOUR	(QIN=QGEN-QLOSS)
TOTAL MASS VELOCITY	= 47946.2	LBM/(HR-SQ.FT)	
AVERAGE HEAT FLUX	= 15298.1	BTU/(HR-SQ.FT)	

AXIAL STATION	QUALITY %	ENTHALPY BTU/HOUR	SAT TEMP DEGREE F	SAT PRESS PSIA
START	62.97	801.76	229.67	20.65
1	63.66	808.34	229.62	20.63
2	69.74	866.40	229.17	20.46
3	70.78	876.31	229.06	20.42
4	72.13	889.15	228.85	20.34
5	73.47	901.90	228.64	20.26
6	74.82	914.74	228.43	20.18
7	76.17	927.59	228.22	20.10
8	77.21	937.48	228.04	20.03
9	78.26	947.47	227.86	19.96
10	79.30	957.36	227.67	19.89
11	83.30	995.44	226.96	19.63
END	84.00	1002.09	226.84	19.58

CORRECTED OUTSIDE WALL TEMPERATURES - DEGREES F

AXIAL STATION LOCATIONS

	1	2	3	4	5	6	7	8	9	10	11
1	241.6	240.8	241.1	242.9	243.2	243.3	234.1	233.8	283.0	236.4	236.6
2	240.7	240.5	240.5	240.3	241.3	241.3	234.4	234.8	237.7	237.2	237.4
3	239.9	239.3	239.7	238.0	237.6	236.6	236.8	238.2	238.6	238.6	237.9
4	239.7	239.1	238.4	236.5	235.0	234.2	240.7	239.9	239.5	239.3	238.0
5	240.5	238.8	238.1	236.2	234.4	233.8	242.3	240.6	239.8	239.4	237.5
6	240.9	239.2	238.8	236.4	234.6	233.7	239.9	238.6	238.3	237.9	236.5
7	241.9	239.7	239.5	237.7	237.4	235.9	234.8	236.6	237.0	236.4	235.6
8	242.1	240.6	240.8	240.2	241.0	240.6	234.0	234.1	237.5	235.9	235.8

RUN NUMBER 210

VOLTAGE DROP IN TUBE	= 14.0	VOLTS	
CURRENT TO TEST SECTION	= 350.0	AMPS	
CALCULATED HEAT GENERATION	= 15433.8	BTU/HOUR	(Q=I*I*R)
HEAT LOSS IN TEST SECTION	= 389.1	BTU/HOUR	(HEATED PART)
HEAT TRANSFERRED TO THE MIXTURE	= 15044.8	BTU/HOUR	(QIN=QGEN-QLOSS)
TOTAL MASS VELOCITY	= 48948.6	LBM/(HR-SQ.FT)	
AVERAGE HEAT FLUX	= 7390.7	BTU/(HR-SQ.FT)	

AXIAL STATION	QUALITY %	ENTHALPY BTU/HOUR	SAT TEMP DEGREE F	SAT PRESS PSIA
START	77.31	944.79	240.57	25.23
1	77.65	947.95	240.50	25.19
2	80.56	975.36	239.88	24.91
3	81.06	980.07	239.77	24.87
4	81.70	986.07	239.59	24.78
5	82.35	992.19	239.42	24.71
6	83.00	998.29	239.24	24.63
7	83.64	1004.31	239.07	24.55
8	84.14	1009.01	238.93	24.49
9	84.64	1013.71	238.78	24.42
10	85.14	1018.41	238.63	24.36
11	87.06	1036.46	238.06	24.11
END	87.39	1039.59	237.96	24.06

CORRECTED OUTSIDE WALL TEMPERATURES - DEGREES F

AXIAL STATION LOCATIONS

	1	2	3	4	5	6	7	8	9	10	11
1	245.9	245.5	245.9	247.1	247.3	247.1	242.3	242.3	291.8	256.2	243.6
2	245.4	245.6	245.6	245.8	246.2	246.1	242.5	243.0	253.2	244.2	244.1
3	245.3	245.1	245.1	244.5	244.1	243.4	243.5	244.2	244.8	244.7	244.2
4	245.0	245.2	244.8	243.7	243.0	242.8	245.8	245.2	245.0	245.2	244.4
5	245.5	244.9	244.6	243.5	242.8	242.6	246.6	245.7	245.4	245.2	244.2
6	245.6	245.1	245.1	243.7	242.9	242.6	245.2	244.6	244.5	244.3	243.7
7	246.2	245.2	245.3	244.3	244.0	243.2	242.7	243.6	244.1	243.5	243.1
8	246.1	245.8	245.9	245.7	246.2	245.8	242.6	243.0	253.2	243.5	243.2

RUN NUMBER 211

VOLTAGE DROP IN TUBE	= 21.0	VOLTS	
CURRENT TO TEST SECTION	= 530.0	AMPS	
CALCULATED HEAT GENERATION	= 35385.4	BTU/HOUR	(Q=I*I*R)
HEAT LOSS IN TEST SECTION	= 359.0	BTU/HOUR	(HEATED PART)
HEAT TRANSFERRED TO THE MIXTURE	= 35026.4	BTU/HOUR	(QIN=QGEN-QLOSS)
TOTAL MASS VELOCITY	= 53053.8	LBM/(HR-SQ.FT)	
AVERAGE HEAT FLUX	= 17206.6	BTU/(HR-SQ.FT)	

AXIAL STATION	QUALITY %	ENTHALPY BTU/HOUR	SAT TEMP DEGREE F	SAT PRESS PSIA
START	67.34	846.83	235.18	22.87
1	68.05	853.53	235.09	22.83
2	74.27	912.53	234.27	22.49
3	75.33	922.57	234.09	22.42
4	76.71	935.62	233.80	22.30
5	78.09	948.67	233.51	22.18
6	79.47	961.73	233.22	22.06
7	80.84	974.69	232.93	21.94
8	81.91	984.82	232.70	21.85
9	82.98	994.96	232.48	21.76
10	84.04	1005.00	232.25	21.67
11	88.13	1043.77	231.37	21.32
END	88.84	1050.46	231.22	21.26

CORRECTED OUTSIDE WALL TEMPERATURES - DEGREES F

AXIAL STATION LOCATIONS

	1	2	3	4	5	6	7	8	9	10	11
1	247.3	246.1	246.6	248.3	248.8	248.8	239.3	239.2	283.0	241.5	241.9
2	246.3	245.9	245.9	245.5	246.8	246.6	239.8	240.2	242.7	242.6	242.7
3	245.5	244.6	244.6	243.3	242.9	241.9	241.9	243.5	243.8	243.8	243.2
4	245.1	244.5	243.6	241.9	240.3	239.8	246.1	245.1	244.7	244.4	243.3
5	245.8	243.8	243.2	241.2	239.6	239.3	247.7	245.7	245.1	244.6	242.9
6	246.3	244.4	244.1	241.6	239.8	239.3	245.1	243.7	243.4	243.0	241.7
7	247.5	245.1	244.8	243.1	242.6	241.1	240.0	241.7	242.1	241.4	240.7
8	247.6	246.1	246.2	245.6	246.6	246.1	239.4	239.2	241.4	241.2	241.0

RUN NUMBER 212

VOLTAGE DROP IN TUBE	= 25.5	VOLTS	
CURRENT TC TEST SECTION	= 650.0	AMPS	
CALCULATED HEAT GENERATION	= 53258.6	BTU/HOUR	(Q=I*I*R)
HEAT LOSS IN TEST SECTION	= 389.7	BTU/HOUR	(HEATED PART)
HEAT TRANSFERRED TO THE MIXTURE	= 52868.9	BTU/HOUR	(QIN=QGEN-QLOSS)
TOTAL MASS VELOCITY	= 61181.1	LBM/(HR-SQ.FT)	
AVERAGE HEAT FLUX	= 25971.7	BTU/(HR-SQ.FT)	

AXIAL STATION	QUALITY %	ENTHALPY BTU/HOUR	SAT TEMP DEGREE F	SAT PRESS PSIA
START	61.15	791.11	240.92	25.39
1	62.08	799.96	240.84	25.35
2	70.22	877.02	240.12	25.02
3	71.62	890.25	239.93	24.94
4	73.43	907.29	239.56	24.77
5	75.25	924.44	239.20	24.61
6	77.05	941.40	238.83	24.45
7	78.86	958.47	238.46	24.28
8	80.26	971.68	238.18	24.16
9	81.66	984.90	237.91	24.04
10	83.06	998.13	237.64	23.92
11	88.42	1048.80	236.59	23.47
END	89.35	1057.64	236.41	23.39

CORRECTED OUTSIDE WALL TEMPERATURES - DEGREES F

AXIAL STATION LOCATIONS

	1	2	3	4	5	6	7	8	9	10	11
1	258.4	257.2	257.8	260.0	260.3	259.9	248.3	248.5	249.0	251.0	250.8
2	256.9	256.7	257.0	256.1	257.4	257.2	248.8	250.1	251.9	252.0	252.0
3	255.7	254.9	254.9	253.2	252.7	251.6	251.6	253.4	253.7	253.6	252.6
4	255.1	254.6	253.4	251.2	249.6	248.6	256.6	255.5	254.9	254.5	252.9
5	256.1	253.7	252.8	250.1	248.4	247.7	258.7	256.0	255.4	254.6	252.0
6	257.1	254.4	254.0	250.8	249.0	247.7	255.2	253.3	253.1	252.5	250.5
7	258.5	255.5	255.3	252.8	252.0	250.4	249.0	250.9	251.4	250.6	249.4
8	258.7	257.0	257.0	256.1	257.1	256.4	248.1	248.1	250.2	250.1	249.6

APPENDIX F

EXPERIMENTAL DATA FROM AIR-WATER TESTS

********** **********
SMALL BEND (10 INCH DIAMETER) UPWARD FLOW
********** **********

RUN NO.	AIR SUPF VELOCITY FT/SEC	H2O SUPF VELOCITY FT/SEC	MODIFIED BAKER'S ORDINATE	MODIFIED BAKER'S ABSCISSA	MASS VELOCITY #M/HRSQFT	GAS QUALITY %	FLOW PATTERN
USP 1,M	21.432	0.044	2679.4	11.6	15647.133	37.06	STRTFIED
USP 2	41.577	0.044	5290.1	11.6	21503.652	54.20	WAVY
USP 3,M	61.270	0.044	7866.8	11.6	27340.762	63.97	WAVY
USP 4	80.347	0.044	10399.3	11.6	33157.754	70.29	WAVY
USP 5	108.329	0.044	14286.4	11.6	42475.836	76.81	WAVY
USP 6	21.697	0.070	2712.5	18.3	21480.941	27.33	STRTFIED
USP 7	46.857	0.070	5967.3	18.4	28773.504	45.74	WAVY
USP 8	60.587	0.070	7841.8	18.4	33189.309	52.96	WAVY
USP 9	85.867	0.070	11344.4	18.6	41576.738	62.44	WAVYSMAN
USP 10	93.263	0.070	12471.8	18.6	44504.492	64.91	WAVYSMAN
USP 11	113.956	0.070	15701.0	18.9	53109.301	70.58	ANNULAR
USP 12,M	20.286	0.150	2565.1	39.5	39465.012	14.45	STRTFIED
USP 13	39.331	0.150	5081.6	39.6	45132.895	25.18	WAVYSLUG
USP 14,M	57.271	0.150	7536.5	40.1	50953.613	33.71	WAVY-ANN
USP 15	74.210	0.150	9944.6	40.1	56857.645	40.59	WAVY-ANN
USP 16	103.980	0.150	15000.4	40.3	71271.000	52.60	ANNULAR
USP 17	20.002	0.317	2566.3	84.4	76851.000	7.42	WAVY
USP 18	37.901	0.317	4987.5	84.4	82514.875	13.77	WAVYSLUG
USP 19	54.986	0.317	7392.4	83.5	88330.063	19.48	WAVY-ANN
USP 20	68.747	0.317	9545.4	83.8	94080.000	24.39	WAVY-ANN
USP 21	93.807	0.317	14154.6	84.4	108137.313	34.21	ANNULAR
USP 22,M	19.732	0.526	2549.4	138.6	123797.000	4.61	WAVY
USP 23	37.743	0.526	4999.1	138.6	129557.750	8.85	WAVYSLUG
USP 24	53.017	0.526	7252.4	138.6	135270.000	12.70	WAVY-ANN
USP 25	87.948	0.526	13872.2	138.6	155975.563	24.29	WAVY-ANN
USP 26	1.905	0.951	237.8	248.8	213856.563	0.24	PLUG
USP SPCL	5.542	0.951	701.4	246.4	214800.500	0.72	SLUG
USP 27	12.010	0.951	1573.4	248.8	216910.625	1.64	SLUG
USP 28,M	18.621	0.951	2476.8	248.8	219045.375	2.60	WAVY
USP 29	35.218	0.951	4809.1	248.8	224709.250	5.06	WAVYSLUG
USP 30,M	48.783	0.951	6957.6	248.8	230518.375	7.45	WAVYSLUG
USP 31	71.756	0.909	11298.1	237.7	234593.813	13.12	WAVY-ANN
USP 32	1.819	1.378	232.3	360.4	309583.750	0.17	SLUG
USP 33	11.863	1.378	1563.7	360.4	312637.813	1.14	SLUG
USP 34	18.292	1.378	2454.9	360.4	314772.563	1.81	WAVY
USP 35	33.687	1.334	4703.4	349.1	310679.938	3.66	WAVYSLUG
USP 36	66.656	1.292	10891.4	337.9	320553.000	9.61	WAVY-ANN
USP 37	0.223	1.806	27.9	472.5	405213.688	0.01	BUBBLE
USP 38	1.784	1.806	230.1	472.5	405667.000	0.13	PLUG
USP 39	11.720	1.806	1554.3	472.5	408721.063	0.87	SLUG
USP 40	17.872	1.806	2426.5	472.5	410855.813	1.39	WAVY
USP 41	31.951	1.806	4580.6	472.5	416519.688	2.73	WAVYSLUG
USP 42	42.602	1.761	6474.3	460.7	412113.000	4.13	WAVYSLUG
USP 43	60.581	1.676	10131.6	438.4	405235.750	7.24	WAVY-ANN
USP 45	1.687	3.524	223.7	921.8	790958.688	0.06	PLUG
USP 46	10.133	3.437	1445.2	899.2	774625.750	0.46	SLUG
USP 47	15.023	3.394	2224.7	887.9	767070.938	0.74	WAVY
USP 48	36.654	3.157	6130.0	825.8	725866.125	2.44	WAVYSLUG

LARGE BEND (22 INCH DIAMETER) — UPWARD FLOW

RUN NO.	AIR SUPF VELOCITY FT/SEC	H2O SUPF VELOCITY FT/SEC	MODIFIED BAKER'S ORDINATE	MODIFIED BAKER'S ABSCISSA	MASS VELOCITY #M/HR SQFT	GAS QUALITY %	FLOW PATTERN
ULP 1,M	21.619	0.044	2714.8	11.8	15759.020	37.47	STRTFIED
ULP 2	42.533	0.044	5376.7	11.7	21622.523	54.44	WAVY
ULP 3,M	51.342	0.044	6574.0	11.9	24442.402	59.67	WAVY
ULP 4	62.751	0.044	8051.1	11.7	27740.773	64.49	WAVY
ULP 5,M	106.735	0.044	14303.2	11.7	43045.914	77.11	SEMI-ANN
ULP 6,M	21.990	0.065	2737.1	16.8	20473.379	28.79	STRTFIED
ULP 7,M	47.672	0.065	6033.6	16.8	27791.715	47.54	WAVY
ULP 8	51.180	0.065	6562.3	16.8	29137.301	49.96	WAVY
ULP 9,M	59.454	0.065	7757.8	17.4	32127.520	54.57	WAVY
ULP 10,M	83.249	0.065	11173.0	17.6	40584.531	64.02	WAVYSMAN
ULP 11	91.722	0.065	12402.0	17.6	43657.824	66.56	WAVY-ANN
ULP 12	111.999	0.065	15634.2	17.8	52427.762	72.14	ANNULAR
ULP 13,M	20.394	0.161	2594.3	42.1	41922.707	13.62	STRTFIED
ULP 14,M	39.406	0.161	5082.3	42.2	47560.945	23.85	WAVYSLUG
ULP 15	47.739	0.161	6245.9	42.5	50371.910	28.09	WAVYSMAN
ULP 16,M	56.550	0.161	7467.3	42.5	53295.469	32.03	WAVY-ANN
ULP 17	72.186	0.161	9779.1	42.8	59173.598	38.77	WAVY-ANN
ULP 18,M	108.514	0.161	15852.0	42.8	76332.688	52.53	ANNULAR
ULP 19,M	20.442	0.328	2606.5	85.3	79367.375	7.25	WAVY
ULP 20,M	38.366	0.328	5032.9	85.3	85040.938	13.43	WAVYSLUG
ULP 21,M	54.345	0.328	7344.4	85.3	90791.813	18.92	WAVYSLUG
ULP 22	68.774	0.328	9585.3	85.3	96734.000	23.90	WAVY-ANN
ULP 23,M	93.650	0.328	14113.7	86.2	110462.875	33.33	ANNULAR
ULP 24	19.911	0.526	2545.1	137.2	123682.563	4.55	SLUG
ULP 25	36.890	0.526	4933.2	138.1	129500.625	8.82	WAVYSLUG
ULP 26	53.588	0.526	7271.7	138.1	135162.000	12.64	WAVYSLUG
ULP 27	85.396	0.526	13543.7	138.1	155263.625	23.95	WAVY-ANN
ULP 33	1.853	0.954	234.7	248.1	214568.625	0.24	PLUG
ULP 32	12.078	0.954	1579.5	248.1	217628.438	1.64	SLUG
ULP 31	18.677	0.954	2472.5	248.1	219718.000	2.58	SLUG
ULP 30	35.157	0.954	4805.9	248.1	225422.188	5.04	WAVYSLUG
ULP 29	47.410	0.954	6837.2	248.1	231116.250	7.38	WAVYSLUG
ULP 28	66.585	0.954	10532.4	248.1	242882.750	11.87	WAVY-ANN
ULP 34	11.716	1.377	1555.7	357.9	312377.938	1.14	SLUG
ULP 35	18.182	1.377	2450.1	357.9	314516.625	1.82	WAVY
ULP 36	32.466	1.377	4622.3	357.9	320191.188	3.56	WAVYSLUG
ULP 37	65.956	1.377	10883.3	360.2	339962.063	9.14	WAVY-ANN
ULP 44	0.290	1.804	36.9	471.9	404755.000	0.02	BUBBLE
ULP 43	1.774	1.804	229.5	471.9	405188.063	0.13	PLUG
ULP 42	11.322	1.804	1528.4	471.9	408245.000	0.87	SLUG
ULP 41	17.102	1.793	2374.8	469.1	407983.438	1.40	WAVY
ULP 40	30.714	1.772	4493.2	463.5	408857.313	2.78	WAVYSLUG
ULP 39	42.265	1.761	6437.9	460.7	412055.875	4.12	WAVYSLUG
ULP 38	58.821	1.676	9818.6	438.4	404275.938	7.02	WAVYSLUG
ULP 45	1.669	3.524	222.6	921.8	790959.188	0.06	PLUG
ULP 46	9.843	3.394	1422.0	887.9	764924.250	0.46	SLUG
ULP 47	14.869	3.265	2228.4	854.0	738095.313	0.78	WAVY
ULP 48	35.918	3.092	6153.1	808.9	711858.063	2.56	WAVYSLUG

****
SMALL BEND (10 INCH DIAMETER)
****

****
DOWNWARD FLOW
****

RUN NO.	AIR SUPF VELOCITY FT/SEC	H2O SUPF VELOCITY FT/SEC	MODIFIED BAKER'S ORDINATE	MODIFIED BAKER'S ABSCISSA	MASS VELOCITY #M/HRSQFT	GAS QUALITY %	FLOW PATTERN
DSP 1	58.038	0.044	7552.5	11.9	26886.852	63.34	WAVY
DSP 2	75.890	0.044	9969.6	11.9	32550.750	69.72	WAVY
DSP 3	94.477	0.044	12565.5	11.9	38815.285	74.61	WAVY
DSP 4	111.011	0.044	15010.1	11.9	45024.398	78.11	WAVY
DSP 5	115.569	0.044	15820.6	11.7	47363.633	79.20	SEMI-ANN
DSP 6	39.946	0.058	5120.5	15.5	24488.988	46.41	WAVY
DSP 7	58.833	0.058	7639.0	15.5	30298.078	56.69	WAVY
DSP 8	84.637	0.058	11264.1	15.5	39082.145	66.42	SEMI-ANN
DSP 9	112.881	0.058	15512.8	15.5	50039.133	73.77	ANNULAR
DSP 10	20.458	0.150	2596.2	39.4	39460.969	14.45	STRTFIED
DSP 11	39.480	0.150	5091.8	39.4	45124.879	25.19	WAVYSLUG
DSP 12	57.462	0.150	7551.2	39.4	50933.969	33.72	WAVY-ANN
DSP 13	73.616	0.150	9905.9	39.8	56849.945	40.60	WAVY-ANN
DSP 14	102.048	0.150	14631.2	39.8	70092.188	51.82	ANNULAR
DSP 15	19.873	0.331	2558.0	88.1	80012.500	7.13	WAVY
DSP 16	37.884	0.331	4987.2	87.2	85650.813	13.27	WAVYSLUG
DSP 17	54.093	0.331	7325.6	87.2	91459.938	18.78	WAVY-ANN
DSP 18	68.023	0.331	9527.2	87.2	97385.625	23.72	WAVY-ANN
DSP 19	91.499	0.331	14057.3	87.2	111673.750	33.48	ANNULAR
DSP 20	19.441	0.526	2531.7	138.6	123802.313	4.61	WAVY
DSP 21	37.291	0.526	4969.1	138.6	129557.750	8.85	WAVYSLUG
DSP 22	52.717	0.526	7231.9	138.6	135270.000	12.70	WAVYSLUG
DSP 23	87.433	0.505	13879.0	133.0	151478.125	25.18	WAVY-ANN
DSP 24	18.961	0.951	2499.4	248.8	219045.375	2.60	WAVY
DSP 25	35.623	0.951	4836.7	248.8	224709.250	5.06	WAVYSLUG
DSP 26	47.872	0.930	6863.1	243.2	225603.313	7.55	WAVYSLUG
DSP 27	70.708	0.909	11321.8	237.7	235181.313	13.34	WAVY-ANN
DSP 28	17.941	1.377	2433.2	362.6	314665.438	1.82	WAVY
DSP 29	33.623	1.334	4702.8	351.4	310772.438	3.66	WAVYSLUG
DSP 30	64.437	1.292	10775.2	340.2	321013.813	9.72	WAVY-ANN
DSP 31	17.243	1.806	2385.4	475.7	410962.875	1.39	WAVY
DSP 32	31.404	1.761	4545.0	463.8	406564.188	2.80	WAVYSLUG
DSP 33	42.134	1.740	6444.0	458.2	407443.125	4.19	WAVYSLUG
DSP 34	58.951	1.676	9932.5	441.3	404969.688	7.15	WAVY-ANN
DSP 35	36.611	3.222	6225.9	848.4	741137.438	2.47	WAVYSLUG

****
LARGE BEND (22 INCH DIAMETER)
****

****
DOWNWARD FLOW
****

RUN NO.	AIR SUPF VELOCITY FT/SEC	H2O SUPF VELOCITY FT/SEC	MODIFIED BAKER'S ORDINATE	MODIFIED BAKER'S ABSCISSA	MASS VELOCITY #M/HRSQFT	GAS QUALITY %	FLOW PATTERN
DLP 1	97.338	0.044	13040.2	11.8	40119.492	75.44	WAVYSMAN
DLP 5,M	60.838	0.066	7816.5	17.0	32262.578	53.82	WAVYSMAN
DLP 2,BM	59.016	0.161	7789.1	42.0	53996.324	32.95	WAVY-ANN
DLP 6	53.786	0.323	7256.2	83.3	89269.563	18.97	WAVY-ANN
DLP 3	28.950	0.526	3766.3	134.3	126418.938	6.70	WAVYSLUG
DLP 14M	52.090	0.526	7220.5	136.8	135357.125	12.80	WAVY-ANN
DLP 4	64.151	0.526	9273.2	134.3	141124.250	16.42	WAVY-ANN
DLP 8	47.568	0.951	6958.7	248.8	230962.750	7.63	WAVYSLUG
DLP 7	18.594	1.377	2490.5	350.3	314291.125	1.83	WAVY
DLP 11	1.782	1.804	229.4	468.9	405086.500	0.13	PLUG
DLP 13	1.015	2.018	128.9	522.8	452785.063	0.06	PLUG
DLP 10	16.863	2.018	2405.0	527.9	458605.500	1.29	WAVY
DLP 9	40.730	2.018	6521.8	527.9	470743.063	3.84	WAVYSLUG
DLP 12	1.657	3.524	220.3	910.1	790561.375	0.06	PLUG

APPENDIX G

DISCUSSION ON EXPERIMENTAL ERRORS

A general discussion of the experimental errors associated with the various measurements is given in this appendix.

Temperature Measurements

The errors in thermocouple calibration would arise from the fact that the reference used for calibrating the thermocouples could be inaccurate and the instrument used for indicating the temperature could be inaccurate. For this study, the Numatron was calibrated against a null-balance potentiometer and it registered inaccuracies of $\pm$0.2°F for a temperature range from 200°F to 275°F. Since the temperatures recorded for the steam-water runs were in this range, except for the case where a dry patch existed, the instrument inaccuracy can be assumed to be $\pm$0.2°F. All thermocouples were calibrated in situ and with dry saturated steam at atmospheric pressures used as a reference. The steam temperature was read on a mercury thermometer with reading inaccuracies of $\pm$0.1°F and the thermocouples were read on the Numatron. Therefore, for the worst case the combined inaccuracy could be $\pm$0.5°F.

Flow Measurement

All flow rates were read on calibrated rotameters and the readings were checked by taking timed volume samples. It is estimated that the

inaccuracies associated with measuring flow rates were ±1 lbm/hour for flow rates greater than 90 lbm/hour and slightly less for lower flow rates.

Heat Transfer Coefficients

In general, the heat transfer coefficients determined for single-phase runs (in the inlet leg) compared to within ±10 percent of the Dittus-Boelter (22) and the Sieder-Tate (23) correlations. There were no known established two phase heat transfer correlations available (for the operating conditions encountered here) to use as a reference for the calculated two phase heat transfer coefficients. Therefore, a summary of the maximum estimated errors is given below.

The inaccuracies associated with the calculated two phase heat transfer coefficients, for a wet wall, varied with the heat flux since the film temperature drop is directly proportional to the heat flux for a constant heat transfer coefficient (see Table VIII).

The maximum errors possible for dry wall conditions were 2 percent while those prior to the onset of dryout were 50 percent.

TABLE VIII

Heat Flux (Btu/hr-sq ft)	Percent Maximum Error
1,000	50
2,000	33
3,000	20
9,000	10
15,000	8
25,000	5

VITA η

M. Nayeem Farukhi

Candidate for the Degree of

Doctor of Philosophy

Thesis: AN EXPERIMENTAL INVESTIGATION OF FORCED CONVECTIVE BOILING AT HIGH QUALITIES INSIDE TUBES PRECEDED BY 180 DEGREE BENDS

Major Field: Mechanical Engineering

Biographical:

Personal Data: Born in Bangalore, British India, November 3, 1946, the son of Mr. and Mrs. M. Himayathullah Farukhi. Citizen of Pakistan.

Education: Graduated with a School Leaving Certificate, ordinary level, from University of Cambridge, England, by correspondence through St. Patrick's High School, Karachi, Pakistan; received a Bachelor of Science degree in Mechanical Engineering in May, 1965, and a Master of Science degree in May, 1967, from Oklahoma State University, Stillwater, Oklahoma; completed requirements for degree of Doctor of Philosophy at Oklahoma State University in December, 1973.

Professional Experience: Graduate teaching assistant, Mechanical Engineering Department, Oklahoma State University, 1965-67; Engineer, Westinghouse Electric Corp., Philadelphia, Pennsylvania and Tampa, Florida, 1967-69 and summers of 1970, 1971; graduate teaching assistant, Mechanical Engineering Department, Oklahoma State University, 1969-71, graduate research assistant, 1972-73; Heat Transfer Consultant (part-time) to Westinghouse Electric Corporation, 1969-73; Staff Research Assistant, Mechanical Engineering Department, Oklahoma State University, June to September, 1973; Senior Research Engineer, Babcock and Wilcox Co., Research Center, Alliance, Ohio, October, 1973 to present.

Professional Affiliations: American Society of Mechanical Engineers, American Society of Chemical Engineers, American Institute of Aeronautics and Astronautics, Registered Engineer-In-Training, Oklahoma.